Copyright

by

Dae Seok Eom

2010

The Dissertation Committee for Dae Seok Eom Certifies that this is the approved version of the following dissertation:

THE ROLE OF BONE MORPHOGENETIC PROTEINS IN THE DEVELOPMENT OF THE VERTEBRATE MIDBRAIN

Committee:

Seema Agarwala, Supervisor

John Wallingford

Jeffrey Gross

Wesley Thompson

Arturo De Lozanne

THE ROLE OF BONE MORPHOGENETIC PROTEINS IN THE DEVELOPMENT OF THE VERTEBRATE MIDBRAIN

by

Dae Seok Eom, B.S.; M.S.

Dissertation

Presented to the Faculty of the Graduate School of

The University of Texas at Austin

in Partial Fulfillment

of the Requirements

for the Degree of

Doctor of Philosophy

The University of Texas at Austin

December, 2010

Dedication

To my family, my wife Jiae, and the Lord Jesus Christ who saved my life, shows His love and makes everything possible.

Acknowledgements

I am heartily thankful to my advisor, Seema Agarwala, whose patient encouragement, guidance, sage advice and support from the initial to the final step enabled me to finish my Ph.D. course. I also would like to thank my committee members for their insightful criticisms, warm concerns and support.

I also would like to acknowledge the past and present Agarwala lab members throughout the years for providing a lab environment that was fun to work as well as provided with a platform where we could have scientific discussions. I also would like to give special thanks to former lab member, Jennifer Fogel who did the gene expression pattern experiments and current lab postdoc, Smita Amarnath who helped with the co-immunoprecipitation experiments for the project.

I am also very thankful to all the Korean students in the biological science department who provided a great support group helping us overcome every difficulty. Finally, I would like to thank my family and my wife Jiae for their endless love and support.

THE ROLE OF BONE MORPHOGENETIC PROTEINS IN THE DEVELOPMENT OF THE VERTEBRATE MIDBRAIN

Publication No._____

Dae Seok Eom, Ph.D.

The University of Texas at Austin, 2010

Supervisor: Seema Agarwala

The purpose of the thesis is to explore the role of BMP signaling in developing vertebrate midbrain. BMP signaling plays important roles in various tissues and stages of neural development to regulate cell fate, proliferation, differentiation, morphogenesis and more. We observed that several major BMPs are expressed not only at the roof plate but also the floor plate of the midbrain. This has led us to ask the role of BMP signaling in dorsal and ventral midbrain patterning. Despite ventral experiments, we found that BMP signaling does not regulate ventral cell fate specification in the midbrain. Instead BMPs profoundly influence the shape and early morphogenesis of the midbrain neural plate as it closes into a neural tube.

During neural tube closure, one of the early events occurring at the ventral midline is median hinge point (MHP) formation. Failure to form MHP leads to neural tube closure defects, the 2nd most common birth defects in

humans. However, the molecular mechanisms underlying MHP formation are not well known. We found that the lowest BMP signaling occurs at the MHP during early neurulation and BMP blockade is necessary and sufficient for MHP formation. Interestingly, we also demonstrated that BMP blockade directs MHP formation by regulating the apicobasal polarity pathway and this regulation may be mediated by biochemical interactions between pSMAD5 and the apical protein, PAR3. Additionally, our time-lapse data suggest that BMP blockade slows cell cycle progression by increasing duration of G1 to S transition and S phase which leads cell nuclei stay at the basal location longer. This mimics basal nuclear migration seen at the MHP where low BMP signaling occurs. Thus, we conclude that BMP signaling regulates neural tube closure via the apicobasal polarity pathway and in a cell cycle dependent manner at the ventral midline.

We observed that BMP signaling is necessary and sufficient for the dorsal cell fate specification in a context-dependent manner and ventral BMP signaling affects dorsal cell fates.

Taken together, we propose the idea that BMP signaling has distinct roles in different contexts. BMPs regulate tissue morphogenesis in the ventral midbrain and dorsally cell fate specification.

Table of Contents

List of Figures

List of Tables

CHAPTER 1 : GENERAL INTRODUCTION

The main goal of this thesis is to understand the role of Bone Morphogenetic Proteins (BMPs) in the ventral and dorsal midbrain development. We found several lines of evidence that show BMPs regulate neural progenitor fate determination dorsally and cell/tissue morphogenesis which lead to the formation of median hinge point during neurulation ventrally. For the better understanding of these issues, I will first describe the canonical BMP signaling cascade, the known roles of BMP signaling in neural patterning in the spinal cord, neurulation and neural tube closure defects, interkinetic nuclear migration and apicobasal polarity pathway and its role in cell shape change.

1.1 Bone Morphogenetic Protein (BMP) signaling pathway

1.1.1 BMP signaling cascade

BMPs are Transforming Growth Factor (TGF) β superfamily member and evolutionarily conserved among species (Liu and Niswander, 2005). They were first identified as bone forming proteins and hence the name. However, BMPs are now known to have important roles in non-skeletal development during development including cell division, apoptosis, cell migration, cell differentiation, axon guidance and morphogenesis (Liu and Niswander, 2005). The BMP signaling transduction begins with the binding of a BMP ligand to the single transmembrane serine/threonine receptors, type I (ALK2, BMPRIA, and

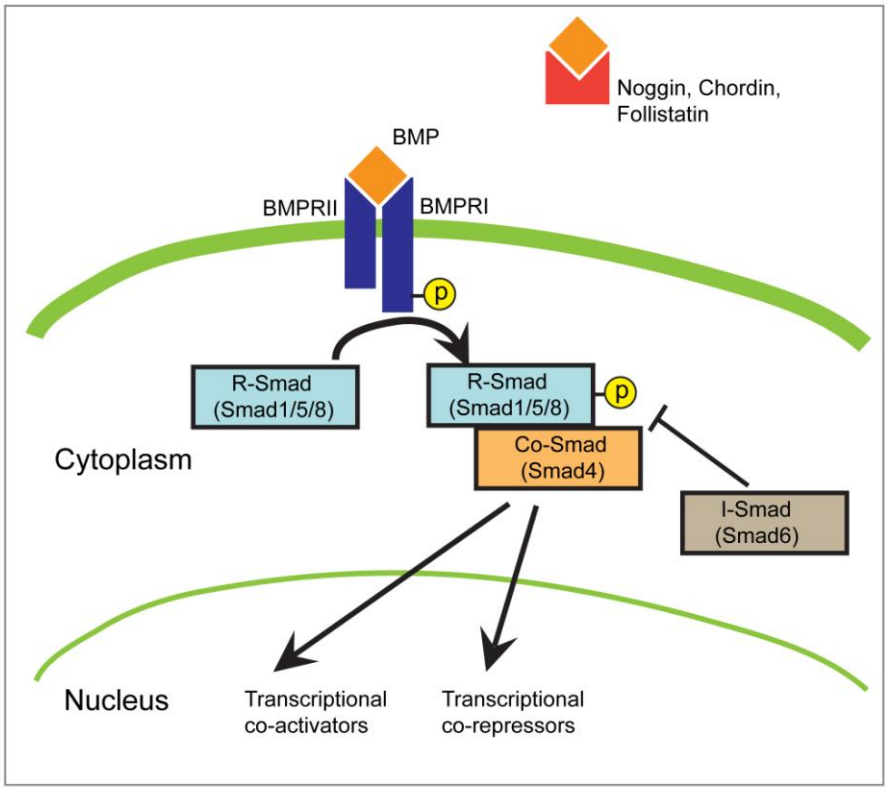

Figure 1.1 Bone morphogenetic protein (BMP) receptors mediate BMP signaling by activating Smads.

BMP ligands bind to the BMP receptors BMPRI and BMPRII, and BMPRI is phosphorylated. Phosphorylated BMPRI in turn phosphorylates receptor-Smads (R-Smads), which make complex with common-Smad (Co-Smad) and this complex enter the nucleus, where they regulate gene expression. Modified from Liu et al., 2005.

BMPRIB) and type II (BMPRIIB, ACTRIIA and ACTRIIB). Upon binding, type I and type II receptors dimerize and cross phosphorylate each other as a result of which type I BMP receptor gets phosphorylated. Phosphorylated type I BMP receptor, in turn phosphorylates its down stream effector Receptor-Smad (Smad 1, 5 or 8). Phosphorylated Smad1/5/8 associates with a second class of Smads called Common-Smads (Smad 4), forming a protein complex that translocates into the nucleus to activate or repress target gene expression (Liu and Niswander, 2005) (Fig. 1.1).

BMP signaling can be altered by extracellular antagonists, Noggin, Chordin, and Follistatin which bind to BMP ligands and inhibit the ability of the ligand to bind to receptors (Iemura et al., 1998; Nakamura et al., 1990). Intracellularly, inhibitory Smads (Smad 6) can inhibit the phosphorylation of Receptor-Smads or prevent their binding to the Common-Smads (Hata et al., 1998; Imamura et al., 1997) (Fig. 1.1).

Recently, it has been found that type II BMP receptor could have a distinct, Smad-independent, non-canonical role. In this cascade, the C-terminus of the type II BMP receptor binds to LIM Kinase 1 (LIMK1) to regulate cytoskeleton via Cofilin. LIMK1 can interact with Rho GTPase, Cdc42 which are well known to regulate actin dynamics (Foletta et al., 2003).

1.1.2 BMP signaling in neural tube patterning

As the neural tube closes, in avian midbrain, BMP proteins are secreted

from the surface ectoderm and roof plate and induce dorsal cell-fates. In the spinal cord, SHH, another powerful signaling molecule is released from the notochord and the floor plate, a signaling center in the ventral midline. These two potent morphogens establish opposing gradients which pattern the neural tube along the dorsoventral axis. Neural crest, commissural neurons and sensory interneurons are formed dorsally and floor plate, motor neurons and multiple interneurons are formed ventrally (Liu and Niswander, 2005). Repression of BMP signaling is also important for the normal ventral patterning in the spinal cord. In the chick spinal cord, addition of BMP attenuates the effect of SHH such that cells adopt a more dorsal fate, whereas BMP blockade enhances the effect of SHH so that cells adopt a more ventral fate (Liem et al., 1997). Thus BMP signaling is crucial in dorsoventral patterning in the spinal cord. However, there are substantial controversies concerning the role of BMPs in dorsal cell fate specification. For example, a BMP loss-of-function mutant caused defective neural tube closure (spina bifida) thus it is not clear whether the loss of dorsal cell fates are due to the loss of BMP signaling or secondary effect of neural tube closure defects (Lee et al., 2000). Also BMP loss-of or gain-of-function studies have shown only a subset of cell fates are affected; these manipulations do not support gradient model generally proposed as the mechanism for the DV patterning in the neural tube (Lee et al., 2000; Timmer et al., 2002). Also, it has been suggested that BMP signaling does not affect dorsal cell fate specification in the avian midbrain (Bobak et al., 2009). We will clarify

the controversies in Chapter 4 by taking advantage of electroporation to alter temporospatial BMP signaling without causing neural tube closure defects.

1.2 Vertebrate neurulation

Neurulation is a morphological event that converts a flat neural plate into the neural tube that is the precursor of the brain and spinal cord (Smith and Schoenwolf, 1997). There are two distinct modes of neurulation : primary and secondary neurulation. In general, the anterior part of the neural tube is formed by primary neurulation, while the posterior part is made by secondary neurulation. In avians, mammalians and amphibians, the neural tube is formed by both but in fish the neural tube is thought to be formed solely by secondary neurulation (Lowery and Sive, 2004).

In primary neurulation, the neural tube is formed by the shaping, folding and dorsal midline fusion of the neural plate (Smith and Schoenwolf, 1997). The neural tube is concurrently pinched off from the surface ectoderm. In secondary neurulation, the neural tube is formed from migratory mesenchyme cells which make a solid cord ; the center of the cord is eliminated by cell death to create a hollow tube by a process called cavitation. Thus no neural folding is associated with secondary neurulation (Copp et al., 2003; Lowery and Sive, 2004).

1.2.1 The sequence of neurulation

Primary neurulation is often divided into several distinct stages, although

these stages are continuous events that overlap each other. Neurulation begins with the formation of neural plate which is induced by the signals from underlying dorsal mesoderm. With this signal, ectodermal cells above it elongate into the columnar shape of neural plate cells (Smith and Schoenwolf, 1987; Smith and Schoenwolf, 1997). The neural plate is shaped by both intrinsic and extrinsic forces actions on the surface ectoderm and neural plate area. Intrinsically, it is thought that convergent extension is the main force for shaping the neural tube whereby medially directed cell intercalation and movement results in narrowing and lengthening of the neural plate (Keller, 2002). Recently, it has been shown that convergent extension is required for the initiation of neural tube closure by the study of various mutants that lack convergent extension. *Loop-tail, crash, circletail* and *dishevelled-1;dishevelled-2* double mutants fail to close the neural tube which leads to neural tube closure defects in mouse (Copp et al., 2003). Interestingly, all of these genes encode for proteins that function in the non-canonical Wnt signaling pathway called the planar cell-polarity pathway. After the neural plate has been shaped, bending of the neural plate follows. In chicken embryos, the ventral midline starts to bend at HH5 and the region that bends is called median hinge point (MHP). Cells in MHP are derived from the portion of the neural plate just anterior to Hensen's node (Schoenwolf, 1985; Schoenwolf and Smith, 2000a; Schoenwolf and Smith, 2000b). The MHP overlies the notochord and is induced by signals from it (Smith and Schoenwolf, 1997). MHP cells show characteristic polarized cell

behaviors such as apical constriction, basal nuclear migration and apicobasal shortening (Smith and Schoenwolf, 1997). However, the signaling mechanisms involved in the MHP formation are not fully understood. In chapter 2 of this thesis, I deal with the molecular mechanisms underlying MHP formation. Two other hinge points are formed after MHP formation. These paired dorsolateral hinge points (DLHPs) are located at the point of attachment of the surface ectoderm to the each side of neural folds. DLHPs help both neural folds to meet at the midline and finally fuse. It is known that SHH negatively regulates DLHP formation in mouse (Ybot-Gonzalez et al., 2002; Ybot-Gonzalez et al., 2007) and intrinsic forces are generated by cell shape changes mediated by SHH-related signaling (Ybot-Gonzalez et al., 2002). However, extrinsic forces are also at work. The surface ectoderm of the chick embryos pushes neural folds toward the midline of the embryo provides an extrinsic force for the bending at the DLHPs (Schoenwolf and Smith, 2000b). The pushing of the paired neural folds towards each other at the dorsal midline culminates in neural tube fusion. At the dorsal midline the two neural folds fuse with each other. Midline cell death and epithelial remodeling are important to ensure proper dorsal midline fusion of the neural tube (Copp et al., 2003).

1.2.2 Neural tube closure defects

Neural tube closure defects are a group of congenital malformations caused when the neural tube fails to close during neurulation (Copp et al.,

2003). Neural tube closure defects occur in 1 out of 1000 pregnancies and are the second most common malformations among humans. Neural tube closure defects vary depending on the axial level of the neuroaxis. If the neural tube closure defects occur at the posterior region, it is called *spina bifida* which results in exposure of the spinal cord. Failure of anterior neural tube closure causes *anencephaly* which is usually lethal. In some cases, the entire neural tube caudal to the midbrain fails to close resulting in *craniorachischisis* (Copp et al., 2003). As mentioned earlier, shaping of the neural plate by convergent extension, elevation and apposition of the neural folds by hinge point formation and fusion of the neural folds at the dorsal midline by apoptosis are required for proper neural tube closure. Misregulation in any of these steps of neurulation can cause neural tube closure defects (Copp et al., 2003). Although, more than 200 genes are known to be involved in neural tube closure, the molecular mechanisms underlying neurulation are not well understood. In Chapter 2 and 3, I show evidence that BMP signaling might be involved in ventral midline hinge point formation during chick midbrain neural tube closure.

1.2.3 Molecular mechanisms underlying neural tube closure

Despite extensive studies carried out on the cell behaviors or shape changes, molecular mechanisms of neural tube closure are not well known (Jacobson et al., 1986; Keller, 2002; Schoenwolf and Smith, 2000b). As mentioned earlier, planar cell polarity (PCP) related gene mutants caused

neural tube closure defects by defective convergent extension (Wallingford and Harland, 2002). Additionally, it has been shown that actin binding protein, Shroom3, is required for apical constriction at the MHP in *Xenopus* neurulation (Lee et al., 2007; Lee and Harland, 2007). Copp and colleagues have shown that BMP inhibition is required for dorsolateral hinge point (DLHP) formation in mice (Ybot-Gonzalez et al., 2007). In humans, genetic studies have suggested that mutants in BMP or its antagonist are highly correlated with neural tube closure defects (Felder et al., 2002). However, how precisely these signaling molecules regulate cell shape changes at the subcellular level and at the HP is not well characterized. It is very important to understand the precise regulation of neural tube closure since neural tube closure defects are one of the most frequent birth defects in humans.

1.3 Regulation of epithelial cell shape by apicobasal polarity and cell-cell adhesion

In metazoans, adhesion is involved in most processes during development. In particular, cell–cell adhesion is required for generation of coherent sheets or tubes of epithelial cells with distinct apical–basal polarity (Carthew, 2005). Each epithelial cell is subdivided into an apical and a basolateral membrane compartment each associated with different membrane proteins (Nelson, 2003). The apical domain faces toward either the exterior environment or the ventricular space. The basolateral domain is subdivided into different compartments, including the adherens junction, which is involved in

cell–cell adhesion. (Carthew, 2005). In *Drosophila*, adherens junction form an apically localized cell–cell adhesive belt known as the zonula adherens (ZA), and a more basal junctional complex known as the septate junction (SJ). Just apical to the *Drosophila* ZA lies the subapical region (SAR), which has an organizing role in epithelial polarization (Knust, 2002; Knust and Bossinger, 2002). In contrast to *Drosophila*, vertebrate epithelial cells have tight junctions (TJ) instead of SJs located apical to the vertebrate ZAs in a position analogous to the *Drosophila* SAR (Knust, 2002; Knust and Bossinger, 2002) (Fig. 1.2). The apical tight junction complexes between vertebrate epithelial cells serve an organizing role in epithelial polarization and establish a paracellular diffusion barrier that restricts the movement of solutes across the cell layer (Tsukita et al., 2001). This barrier effectively segregates the epithelium and surrounding media into unmixed apical and basolateral compartments. In *Drosophila*, septate junctions appear to have similar functions to the vertebrate tight junctions and localize basal to the zonula adherens (Gibson and Perrimon, 2003).

Polarity proteins which regulate apicobasal polarization are conserved in both *Drosophila* and vertebrates. Studies have shown that three groups of epithelial polarity protein complexes exist. Par3(Partitioning defective 3)/Par6 (Partitioning defective 6)/aPKC (atypical Protein Kinase C) (the Par complex) and Crumbs/Discs lost/Stardust (the Crb complex) are associated with apical domains of epithelial cells and regulate junctional assembly, whereas the Lethal giant larvae (Lgl)/Discs large/Scribble (the Lgl complex) is associated with

basolateral membrane domain and involved in zonula adherence formation (Gibson and Perrimon, 2003) (Fig. 1.2).

It has been shown that basolateral Lgl complex proteins antagonize the apical polarization activity of the Crb complex through interactions with Par complex directly or indirectly in *Drosophila* (Bilder et al., 2003). This mechanism is conserved in vertebrates. Members of the vertebrate Par3/Par6/aPKC complex localize to the tight junction and members of both the Par and Crb complexes are involved in tight junction formation (Hurd and Margolis, 2005) (Fig. 1.2). Several studies have shown that direct interactions exist between the Crb and Par3/Par6/aPKC complexes during cell polarization and tight junction formation (Gibson and Perrimon, 2003; Hurd and Margolis, 2005). Crb acts through PALS1 (the homologue of *Drosophila* Stardust) to recruit the Par3/Par6/aPKC complex to the apical tight junction complex of vertebrate epithelia (Gibson and Perrimon, 2003) (Fig. 1.2). Vertebrate homologues of the *Drosophila* Lgl group are localized to the basolateral plasma membrane in polarized epithelial cells. Interestingly, recent studies have shown that mammalian Lgl (mLgl) can bind Par6b and aPKC without Par3 in several different types of tissue culture cells (Yamanaka et al., 2006). These results suggest the existence of at least two distinct Par6/aPKC complexes in epithelial cells. Active state complex composed of Par3/Par6/aPKC and an inactive one where Lgl binds with Par6b/aPKC instead of Par3 in MDCK cells (Margolis and Borg, 2005). During polarization, Lgl phosphorylation by aPKC dissociates Lgl

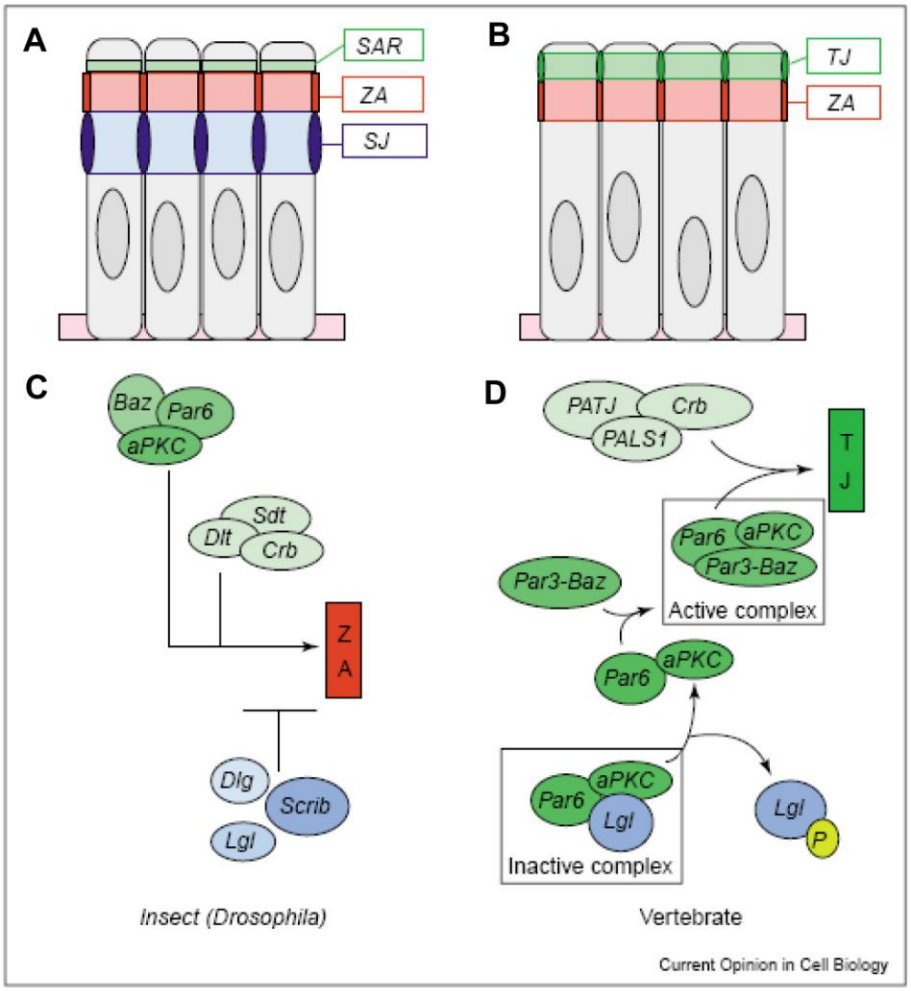

Figure 1.2 Distribution and activity of polarity complexes in Drosophila and vertebrate epithelia

(A) Drosophila epithelial cells exhibit two major junctions : zonula adherens (ZA) and saptate junctions (SJ). Basolateral proteins (Lgl complex) localize at or below the SJ. The subapical marginal zone (SAR) lies apical to the ZA in a position analogous to the vertebrate tight junction (TJ). Drosophila Crb and Baz-Par3 complexes proteins are localized to the SAR. (B) Vertebrate epithelia exhibit a ZA and more apical TJ complex. Both the vertebrate Crb and Baz-Par3 complexes localize to the TJ. (C) Model for the activity of polarity protein complexes in Drosophila epithelial polarization. (D) Model for vertebrate epithelia. Lgl binds and inactivates Par6/aPKC in the lateral membrane domain. Par6/aPKC is then free to bind Par3 and form an active complex that mediates TJ formation through interactions between Par6 and Crb complex. Taken from Gibson and Perrimon (2003).

from the complex which in turn allows for the formation of active complex (Yamanaka et al., 2006). These findings suggest a general model for polarity control applicable in both *Drosophila* and vertebrate which suggests that opposing apical and basolateral protein complexes position cell–cell junctions at the boundary between apical and basolateral plasma membrane domains (Gibson and Perrimon, 2003) (Fig. 1.2).

It has been described above that there are differences and similarities in cell-cell adhesion and apicobasal polarity formation between *Drosophila* and vertebrates. However, proteins involved in adhesion and apicobasal polarity are tightly associated each other (Carthew, 2005). Thus, loss of any of related gene function caused disruption of both polarity and cell-cell adhesion leading to cell shape change, migration defects and disintegration of cell and tissue architecture (Afonso and Henrique, 2006; Betschinger et al., 2003; Bilder et al., 2003; Chalmers et al., 2005; Doudney and Stanier, 2005; Ganzler-Odenthal and Redies, 1998; Georgiou et al., 2008; Ghosh et al., 2008; Hong and Brewster, 2006). Again, proteins involved in cell-cell adhesion and polarity are structurally related each other. Although there is a close relationship between adhesion and polarity, they are frequently studied separately.

Thus, it will be explained how these closely related cell-cell adhesion and apicobasal polarity proteins regulate cell shape in epithelial cells and how they are regulated by extracellular signals.

1.3.1 Cell shape changes associated with apicobasal polarity

In the *Drosophila* embryo, loss of function mutants for any component of the SAR complex (Crumbs, Stardust and Baz/Par3) shows the loss of cell adhesion and polarity. This indicates that the SAR complex has an essential function in the control of adhesion and polarity. In fact, one of the known functions of the protein complex in the SAR is to stabilize and maintain the ZA (Knust, 2002; Knust and Bossinger, 2002). Similarly, loss of Scribble which is localized in the basolateral domain in *Drosophila* embryos results in mislocalization of apical proteins and proteins of the adherens junctions to basolateral positions, without affecting localization of basolateral proteins (Bilder and Perrimon, 2000). Scribble is co-localized with Dlg and lethal giant larvae (Lgl), and their localization mutually depends on each other. Removal of either of them in the imaginal disc epithelium leads to loss of adhesion and polarity (Bilder and Perrimon, 2000).

In vertebrate epithelial cells, overexpression of Par3 localized apically leads to mislocalization and disruption of polarity (Afonso and Henrique, 2006). Lethal giant larvae (lgl) mutant mice also show disruption of cell polarity and tissue architecture (Klezovitch et al., 2004). In the developing *Drosophila* notum, the loss or inhibition of apical membrane proteins such as Cdc42, aPKC or PAR6 leads to discontinous junctional structures and the apical constriction of affected cells (Georgiou et al., 2008). Apical constriction is thought to be one of the major driving forces of cell shape change and tissue reorganization (Sawyer

et al., 2009). These results suggest that the protein complexes localized at apical or basolateral domains are essential for the establishment of a polarized phenotype and the maintenance of tissue architecture in *Drosophila* and vertebrate cells. In addition, the apicobasal polarity pathway could regulate cell shape change by inducing apical constriction, however, which mechanism is not well understood so far.

1.3.2 Cell shape changes associated with cell-cell adhesion

How different cadherin proteins regulate cell shape changes has been well studied in *Drosophila* eye. Cadherins are adhesion molecules localized in the adherens junction, which typically interact with other cadherins in a homophilic manner through their extracellular domains (Carthew, 2005). Cytoplasmic domains of cadherins interact with the actin cytoskeleton and signaling molecules. Studies have shown that when E- and N-cadherins are missing in cone cells in *Drosophila*, the cells lose their contacts with their neighbors, and cell shape is changed (Hayashi and Carthew, 2004). Conversely, expression of both cadherins in one of the surrounding pigment cells causes disruption of the cone cell pattern by intercalation (Hayashi and Carthew, 2004). These observations suggest that cadherins are necessary and sufficient to drive changes in cell shape in epithelia. Only cone cells express N-cadherin, but surrounding pigment cells do not (Hayashi and Carthew, 2004). This specific expression of N-cadherin is important to ensure the shapes of cone cells since loss of N-cadherin changes cone-cell shape. E-cadherin is also expressed in

cone cells but it is not essential for shaping these cells (Hayashi and Carthew, 2004). One possible reason why N-cadherin affects cell shape but E-cadherin cannot is that only N-cadherin provides differential adhesion. This model is based on differential adhesion hypothesis (DAH) proposed fifty years ago (Townes and Holtfreter, 1955). According to DAH, cells are sorted on the basis of their relative adhesiveness (Steinberg, 2007; Townes and Holtfreter, 1955). It is possible that differential cell affinities of different kinds of cadherins might control cell shape in the developing *Drosophila* eye (Carthew, 2005).

Another possibility is that specific location of N-cadherin expression in cone cells might shape them correctly. N-cadherin is specifically localized to membranes that are in direct contact with other cone cell membranes, whereas E-cadherin is uniformly distributed around each cone cell membrane. It is possible that localized cadherin regulates cytoskeleton remodeling or adhesion property to specific sides of a cell which might generate asymmetric changes in adherens junction. In this explanation, the type of cadherin is not important but its non-uniform localization is crucial to ensure proper cell shape. Actually, when E-cadherin is expressed non-uniformly around a cone cell adherens junction, the cell is altered in shape (Hayashi and Carthew, 2004). It has been also suggested in vertebrates that N-cadherin is required for the polarized cell shape change critical to the cell intercalation during neurulation (Hong and Brewster, 2006).

To summarize, in *Drosophila* and in vertebrate the regulation of cell-cell

adhesion by cadherins is essential for maintaining proper cell shape and epithelial formation in the developing embryo. However, the precise molecular mechanisms underlying how cadherins shape cells are not well known. It is important to know the relationship between adhesion and apicobasal polarity pathway with regard to cell shape changes to understand dynamic morphogenetic regulation during development.

1.3.3 Signaling implications for cell shape change during development

As mentioned above, disruption of cell-cell adhesion or cell polarity lead to changes in cell shape. Epithelial cell integrity through proper expression and localization of adhesion proteins and polarity proteins is essential for inducing and maintaining correct cell and tissue shape. However, it is not well understood what extracellular signaling mechanisms are involved in this process. The Wnt signaling pathway has been raised as a possible candidate because β-catenin is not only a component of the adherens junction that links cadherin and α-catenin, but also a transcriptional activator of the canonical Wnt signaling pathway (Nelson and Nusse, 2004). Indeed, one study has shown that Wnt and BMP signaling regulate hair follicle morphogenesis in mammalian epithelia (Jamora et al., 2003). Wnt protein stabilizes β-catenin and BMP inhibitor Noggin induces Lef1. β-catenin binds to the Lef1 transcriptional complexes which in turn down-regulates E-cadherin gene. Downregulation of E-cadherin and simultaneous upregulation of P-cadherin at local areas leads to changes in cell shape during hair follicle formation (Jamora et al., 2003).

Another study has shown that Dishevelled, an important mediator of Wnt signaling pathway, regulates localization of Lgl. This suggests the Wnt signaling pathway is required for normal apicobasal polarity in *Xenopus* ectoderm (Dollar et al., 2005). Unexpectedly, individual cell shape changes were not detected. One possibility is that the levels of Lgl misexpression were too low to lead to cell shape change. Another possibility is that a redundant mechanism might exist in *Xenopus* ectoderm. This result is also very interesting because Dishevelled is a well known regulator of planar cell polarity (PCP) pathway in *Drosophila* and vertebrates (Wallingford, 2005; Wallingford, 2010). Further studies are needed to be carried to shed light on the relationship between apicobasal polarity and planar cell polarity.

It has been reported that loss of Dpp signaling causes disruption of epithelium integrity in *Drosophila* wing imaginal disc (Gibson and Perrimon, 2005; Shen and Dahmann, 2005). This suggests that BMP signaling pathway is required for morphogenetic processes including changes in cell shape, cell migration and tissue architecture. Recent studies have shown that Dpp signaling is required to achieve correct cell-cell contacts, cell positions and cell shape during *Drosophila* eye by regulating E-Cadherin (Cordero et al., 2007). In vertebrates, the BMP gradient guides dorsal migration of lateral mesoderm by regulating N-cadherin without affecting dorsal-ventral patterning during zebrafish gastrulation (von der Hardt et al., 2007). Also, it has been recently suggested that BMP signaling mediated cell adhesion is modulated via cadherin

endocytosis (Ogata et al., 2007).

To summarize, Wnt and BMP signaling are involved in cell-cell adhesion via regulating cadherin proteins which in turn leads to morphogenetic processes during development. Adhesion proteins and apicobasal polarity complex proteins are important for regulating cell shape during development and the molecular machinery is conserved in both *Drosophila* and vertebrates. Although it has been suggested that Wnt and BMP signaling are involved, precise mechanisms of how and why are not well understood.

Interestingly, recent studies suggest a profound link between cell architecture and proliferation. For example, disruption of cell architecture causes uncontrolled cell proliferation (Bilder, 2004). Indeed, several cadherin mutants (Hong and Brewster, 2006) and loss-of or gain-of-function studies of apicobasal complex protein members show ectopic cell proliferation and tumor-like cell clusters (Afonso and Henrique, 2006; Klezovitch et al., 2004). Loss of adhesion and polarity are found to occur in many cancer cells (Feigin and Muthuswamy, 2009). These studies suggest that the regulation of cell adhesion and apicobasal polarity is tightly associated with cell cycle progression. Thus, it is possible that cell and/or tissue architecture is regulated in a cell cycle dependent manner. We tested this idea in Chapter 3.

1.4 Interkinetic nuclear migration (INM)

The nuclei of dividing neural progenitors undergo a cell-cycle-dependent change in position along the apical-basal axis known as interkinetic nuclear

migration (INM) (Sauer, 1935). During cell-cycle progression, neuroepithelial progenitor cells have a radial glia-like morphology with an apical and a basal attachment, but their nuclei undergo systematic changes in position along the apical-basal axis (Baye and Link, 2007; Bayly et al., 2007; Sauer, 1935). After undergoing mitosis at the apical surface of neuroepithelium, the nuclei of neural progenitors progress to G1 phase by translocating basally, away from the apical surface, and undergo DNA replication (S phase) at the basal part of the ventricular zone. Finally, the nuclei migrate apically through G2 phase to undergo M phase in apical position along the ventriclular surface (Baye and Link, 2007; Guerrier and Polleux, 2007).

It is believed that interkinetic nuclear migration is coordinated with the cell cycle (Sauer, 1935). However, this relationship seems not simple. When cell cycle progression is inhibited by pharmacological treatment (5-azacytidine and cyclophosphamide), interkinetic nuclear migration is inhibited in neuroepithelium (Ueno et al., 2002). Interestingly, blockade of interkinetic nuclear migration does not inhibit cell cycle progression but mitosis occurs at ectopic locations in the neuroepithelium (Gambello et al., 2003; Murciano et al., 2002). This suggests that nuclear migration is not essential for cell cycle progression. However, several studies have shown that a well known cell cycle regulator Cdk1 (cyclin-dependent kinase 1) might regulate nuclear migration via the interaction through kinesin motor protein (Miki et al., 2005). Thus, the precise molecular mechanisms of the relationship between interkinetic nuclear migration and cell

cycle progression need to be further explored.

The functions of INM in development are not well characterized. However, it is proposed that INM is required for the invagination of neuroepithelium during neurulation (Langman et al., 1966; Messier, 1978). Additionally, it is relatively well known that the apicobasal polarity is required for normal INM (Cappello et al., 2006; Cui et al., 2007). INM may help maintain apicobasal polarity during cell proliferation (Baye and Link, 2007). Most interestingly, INM may be required for establishing heterogeneity among progenitors since cells can respond to extrinsic cues depending on the nucleus and cell body position and change their pattern of proliferation and differentiation (Baye and Link, 2007).

INM is an evolutionarily conserved mechanism that underlies cell cycle progression in neuronal development. Though, it is not mentioned in this section, it is known to play a role in cell fate determination (Schenk et al., 2009; Tabler et al., 2010). It is a highly complex and coordinated process that affects several aspects of neuronal development. Especially, in neuroepithelium where cells undergo INM, it is highly possible that cell and tissue morphogenesis, cell cycle progression and cell fate determination are tightly associated with each other. However, the relationships between these are not well understood during vertebrate development.

CHAPTER 2 : BONE MORPHOGENETIC PROTEINS (BMPs) REGULATE NEURAL TUBE CLOSURE VIA THE APICOBASAL POLARITY PATHWAY

2.1 Introduction

During neurulation, a flat neural plate becomes a tubular structure called neural tube. This process involves a diverse set of cell behaviors which are beautifully described in classic studies (Davidson and Keller, 1999; Jacobson et al., 1986; Smith and Schoenwolf, 1997). Early neurulation events shape the ventral midline which is called median hinge point (MHP) by characteristic cell movements including apical constriction and basal nuclear migration of neuroepithelial cells. In association with the notochord, these cell shape changes bend the ventral midline, causing the neural folds on either side of the MHP to elevate. Later, two dorsolateral hinge points (DLHPs) form which are associated with the adjacent surface ectoderm and push the neural folds together as a result they fuse across the dorsal midline. Although the relative importance of the MHP and the DLHPs differs across axial levels of the folding neural tube, together they play an important role in neurulation (Smith and Schoenwolf, 1997; Stottmann et al., 2006; Ybot-Gonzalez et al., 2002).

Recent studies implicate the active regulation of apical constriction in bending and shaping epithelial sheets, including the neural plate (Copp et al., 2003; Haigo et al., 2003; Nagele et al., 1989; Nishimura and Takeichi, 2008; Smith and Schoenwolf, 1997; van Straaten et al., 2002). This process requires contraction of the adherens belt, which runs immediately below the apical

surface of epithelial sheets and can provide a mechanism for shaping whole tissues via its association with adherens junctions (Nishimura and Takeichi, 2008). However, despite its importance in morphogenesis, only a handful of molecules have been implicated in the regulation of apical constriction (Brouns et al., 2000; Haigo et al., 2003; Nishimura and Takeichi, 2008; Sai and Ladher, 2008).

How are apicobasal events (e.g., apical constriction, cell cycle progression, apicobasal cell thickening) implicated in neural tube closure controlled and coordinated (Copp et al., 2003; Haigo et al., 2003; Nishimura and Takeichi, 2008; Yang et al., 2009). Recently, an intriguing connection between the bending of epithelial sheets into complex organs and the dynamic regulation of apicobasal epithelial polarity has emerged (Andrew and Ewald, 2010; Bryant and Mostov, 2008). These studies suggest that epithelial cells can progressively transform themselves into complex structures, such as branched tubules, by polarized cell divisions and dynamic shunting between unpolarized, semipolarized and polarized states, each influenced by distinct signals (Bryant and Mostov, 2008). In such “morphogenetically active” epithelia, altering the polarity of a few cells at a time while retaining it in others, allows the epithelial sheet to retain its overall integrity while simultaneously possessing the flexibility to be bent and shaped (Ewald et al., 2008; Yang et al., 2009).

BMP homologs have also been implicated in the morphogenesis of many epithelial tissues and can interact with molecules (e.g., cadherins) concentrated

in apically located junctional complexes (Attisano and Wrana, 2002; Gibson and Perrimon, 2005; Shen and Dahmann, 2005; Shoval et al., 2007). Such cadherin-mediated BMP activity is essential for neural crest migration and the directional, convergent-extension movements that narrow and elongate the fish embryo during gastrulation (Shoval et al., 2007; von der Hardt et al., 2007). Recent studies also demonstrate that the disruption of apically located tight junctions by the BMP homolog, TGFß, can critically regulate epithelial to mesenchymal transformation often a key event during tissue morphogenesis (Massague, 2008; Ozdamar et al., 2005).

Perturbed BMP signaling results in neural tube closure defects (McMahon et al., 1998; Stottmann et al., 2006; Ybot-Gonzalez et al., 2007). Although the role of BMP signaling in dorsal neural cell-fate specification has been extensively examined, little is known at the cellular and molecular level about how BMPs regulate neural tube closure (Liu and Niswander, 2005). In this study, we examined the role of BMP signaling in the midbrain, a region where exencephaly occurs frequently and where closure mechanisms are distinct from those employed in the caudal neural tube (Copp et al., 2003). We show that a complex 2-dimensional BMP gradient occurs in the anterior neural plate and plays a profound role in MHP formation by regulating epithelial apicobasal polarity. Coimmunoprecipitation studies demonstrate that members of the canonical BMP signaling cascade biochemically interact with the apicobasal polarity pathway in a BMP-dependent manner. As a result, direct perturbations

of the apicobasal polarity pathway mimic the morphogenetic effects of BMP blockade. Thus, by regulating apicobasal polarity, BMP signaling plays a critical role in neural tube closure.

2.2 Results

2.2.1 Expression patterns of BMP signaling components in the developing vertebrate midbrain.

We examined BMP signaling in the neurulating chick embryo between Hamburger-Hamilton (HH) Stages 4-10 (Colas and Schoenwolf, 2001; Hamilton, 1951). *BMP7* expression was seen in the notochord by HH5 and the ventral midline/MHP by HH7, where it continued to be expressed until later (Fig. 2.1A-B, 4.1A-B; data not shown). Since BMP antagonists (*Noggin* and *Chordin*) and transcriptional targets (*MSX1*) were expressed in complex patterns in the neurulating chick, we focused our analysis on the expression of phosphorylated (p)-SMAD 1/5/8, a definitive readout of canonical BMP signaling (Fig. 4.1A-E).

pSMAD 1/5/8 expression occurred in the neural plate as early as HH4 and persisted in the neural tube throughout neurulation (Fig. 2.1C-F, H; data not shown). Interestingly, pSMAD 1/5/8 expression occurred along two intersecting gradients in the neural plate (Fig. 2.1C, D, H). A dorsoventral (DV) gradient of pSMAD 1/5/8 expression was seen with the lowest levels of expression at the MHP (Fig. 2.1C, D, H). A second pSMAD 1/5/8 gradient was seen along the apicobasal (ventricular-pial) axis of the presumptive midbrain plate, with strong,

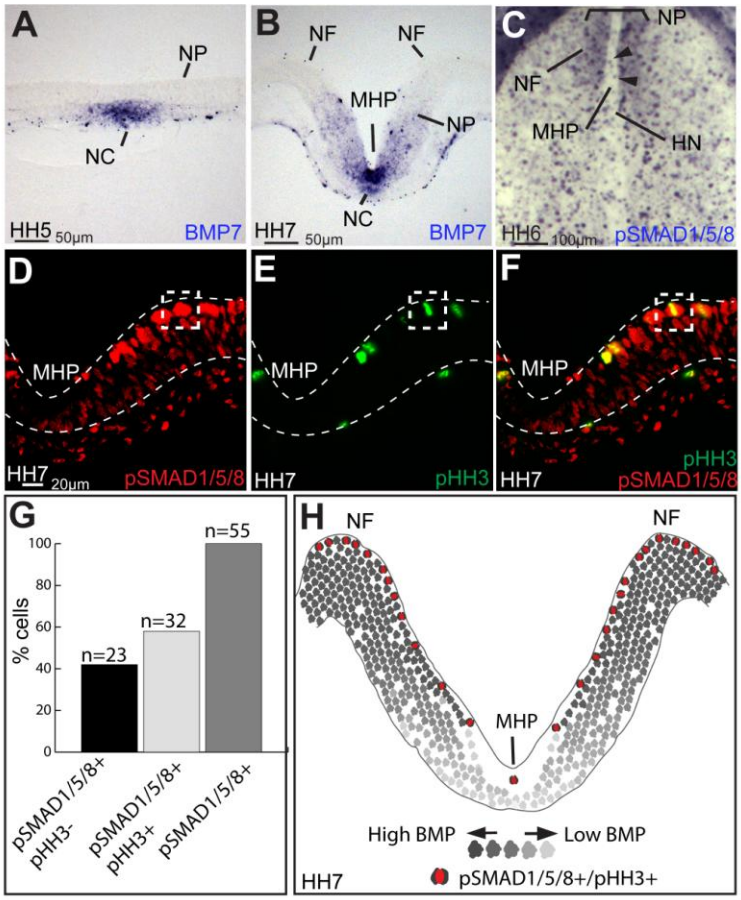

Figure 2.1 A 2-dimensional, spatiotemporally dynamic BMP gradient in the neural plate (A, B) BMP7 mRNA expression in the notochord (NC) and the presumptive midbrain neural plate (NP). Embryonic stages are noted at the bottom left of each micrograph. (C) Whole embryo (top down view, rostral to the top) demonstrating dorsoventrally graded and mosaic pSMAD 1/5/8 protein expression in the neural plate. Note that few pSMAD 1/5/8+ puncta are present in the MHP (arrowheads) compared to lateral neural plate (NP) and are difficult to visualize in the MHP in cross-sections (D-F). (D-F) Dorsoventrally and apicobasally graded pSMAD 1/5/8 expression and its colocalization with pHH3+ in apical, mitotic cells (e.g., boxed cell in F). (G) Quantitation of pSMAD 1/5/8 and pHH3 overlap in the neural plate. (H) HH7 cartoon summarizing the data in C-F. The dorsoventral and apicobasal pSMAD 1/5/8 gradients and the overlap between pSMAD 1/5/8 and pHH3+ expression are depicted. HH: Hamburger and Hamilton embryonic stages; HN: Hensen's node; MHP: median hinge point; NC: notochord; NP: neural plate; NF: neural fold.

but mosaic, expression in apical cells (Fig. 2.1C-F, H).

Neural progenitors undergo interkinetic nuclear migration as they progress through the cell cycle, with mitosis occurring apically (Sauer, 1935; Smith and Schoenwolf, 1997). Interestingly, 100% of phospho-histone H3 (pHH3)+ mitotic cells co-expressed high levels of pSMAD 1/5/8 during neurulation, while 41% of apical, pSMAD+ cells were pHH3-negative and presumably represented cells about to enter into mitosis or those that had just exited this phase (Fig. 2.1D-G; (Langman et al., 1966)). Based on previous studies, neurulation stage neural progenitors exhibit a cell cycle of 7-12 hours, with 0.5-1.3 hr. allocated to mitosis (Schoenwolf, 1985; Smith and Schoenwolf, 1987). Thus, high BMP signaling is received only transiently by apical, predominantly mitotic, progenitors during each cell cycle, with only a few such (pSMAD 1/5/8+, pHH3+) cells present at the MHP compared to the rest of the neural plate. (Fig. 2.1C-H). Therefore, we conclude that the MHP receives low levels of temporally dynamic canonical BMP signaling during neurulation (summarized in Fig. 2.1H).

2.2.2 BMPs regulate midbrain shape and size but not cell fates.

We increased [constitutively active BMP receptor 1A (caBMPR1A)] or attenuated [Noggin and dominant negative BMP receptor 1A (dnBMPR1A)] BMP signaling in the developing midbrain using *in ovo* electroporation. Since *BMP7* is co-expressed with *SHH* at the MHP during neurulation and in the floor

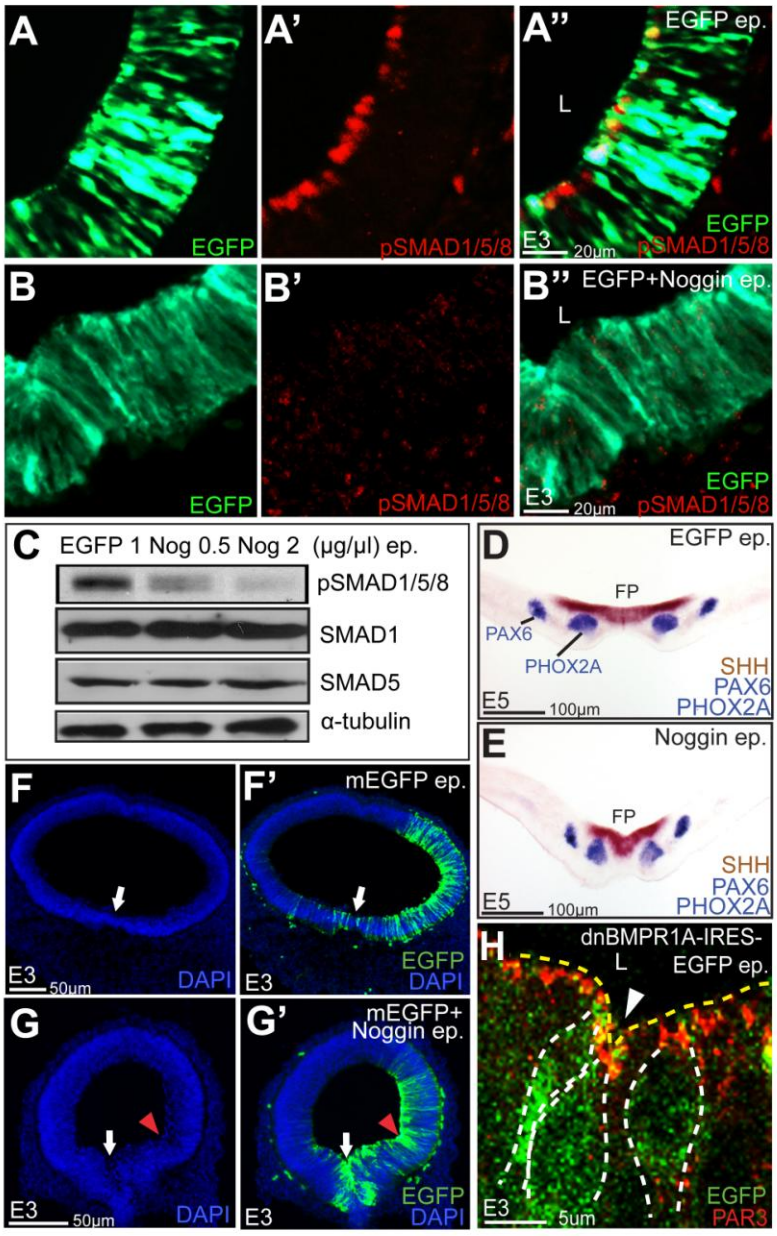
A
EGFP
A'
pSMAD1/5/8
A''
EGFP ep.
L
E3
20μm
EGFP
pSMAD1/5/8
B
EGFP
B'
pSMAD1/5/8
B''
EGFP+Noggin ep.
L
E3
20μm
EGFP
pSMAD1/5/8
C
EGFP 1 Nog 0.5 Nog 2 (μg/μl) ep.
pSMAD1/5/8
SMAD1
SMAD5
α-tubulin
D
EGFP ep.
FP
PAX6
PHOX2A
E5
100μm
SHH
PAX6
PHOX2A
E
Noggin ep.
FP
E5
100μm
SHH
PAX6
PHOX2A
F
E3
50μm
DAPI
F'
mEGFP ep.
E3
EGFP
DAPI
G
E3
50μm
DAPI
G'
mEGFP+
Noggin ep.
E3
EGFP
DAPI
H
dnBMPR1A-IRES-
EGFP ep.
L
E3
5um
EGFP
PAR3

Fig. 2.2. BMP signaling regulates midbrain shape, but not ventral cell fate specification.
(A, B) Control (A-A") and Noggin (B-B") electroporations (green cells) demonstrating severely reduced pSMAD 1/5/8 (red) expression in the latter. (C) Western blots demonstrating that Noggin reduces p-SMAD 1/5/8 levels in a dose-dependent manner, but does not change the absolute levels of SMAD1 or SMAD5 in E3 whole cell lysates. (D, E) Control (D) and Noggin-electroporated midbrains (E) demonstrating that ventral cell fates, assayed by SHH, PHOX2A and PAX6, are not perturbed by BMP blockade although midbrain shape is altered. (F-G') DAPI and EGFP (F', G') staining of controls (F, F') and Noggin-electroporated brains (G, G') demonstrating ectopic hinge-like invaginations (red arrowhead) in lateral midbrain and exaggerated ventral midline grooving (white arrow) in G compared to F. Note that the magnification in G and G' is 1.5x the magnification in F and F' for ease of viewing the invaginations. (H) High power micrograph demonstrating that like Noggin, dnBMPR1A overexpression (green) can also induce hinge-like invaginations of the PAR3+ (red) apical surface (arrowhead). EP: electroporation; L: lumen; FP: floor plate.

plate (FP) later, we first asked whether BMP perturbations affect ventral midbrain cell fate specification by modulating SHH (Fig. 4.1A; (Arkell and Beddington, 1997; Liem et al., 1997)). Western blot analyses following Noggin electroporations (0.2- 2 µg/µl) between HH7-11 resulted in a non-autonomous, dose dependent reduction of pSMAD 1/5/8 levels, but not in the levels of total SMAD1 or SMAD5 proteins in the midbrain (Fig. 2.2A-C). Despite significant pSMAD 1/5/8 reduction, BMP blockade did not alter ventral midbrain cell fate specification (Fig. 2.2D, E). However, Noggin and dnBMPR1 manipulations had a profound effect on midbrain shape, including the induction of hinge-like invaginations at multiple locations in the midbrain (Fig. 2.2F-H). The similarity of shape changes produced by dnBMPR1 and Noggin manipulations suggested that these effects were BMP-dependent and not due to non-specific effects of Noggin manipulations (see also Fig. 2.10).

2.2.3 BMPs regulate hinge point formation during neural tube closure

Given the ability of BMP blockade to induce hinge-like invaginations and the low levels of pSMAD 1/5/8 expression at the MHP, we asked whether BMP signaling could regulate endogenous MHP formation (Fig. 2.1C-H; 2.2F-H). For this purpose, we developed a focal, *in vivo* microelectroporation paradigm for manipulating early neurulation stage (HH4-6) embryos. Early EGFP electroporations resulted in a morphologically normal midbrain neural plate with proper MHP formation at HH7 and neural tube closure at HH 10-11 (Fig. 2.3A-

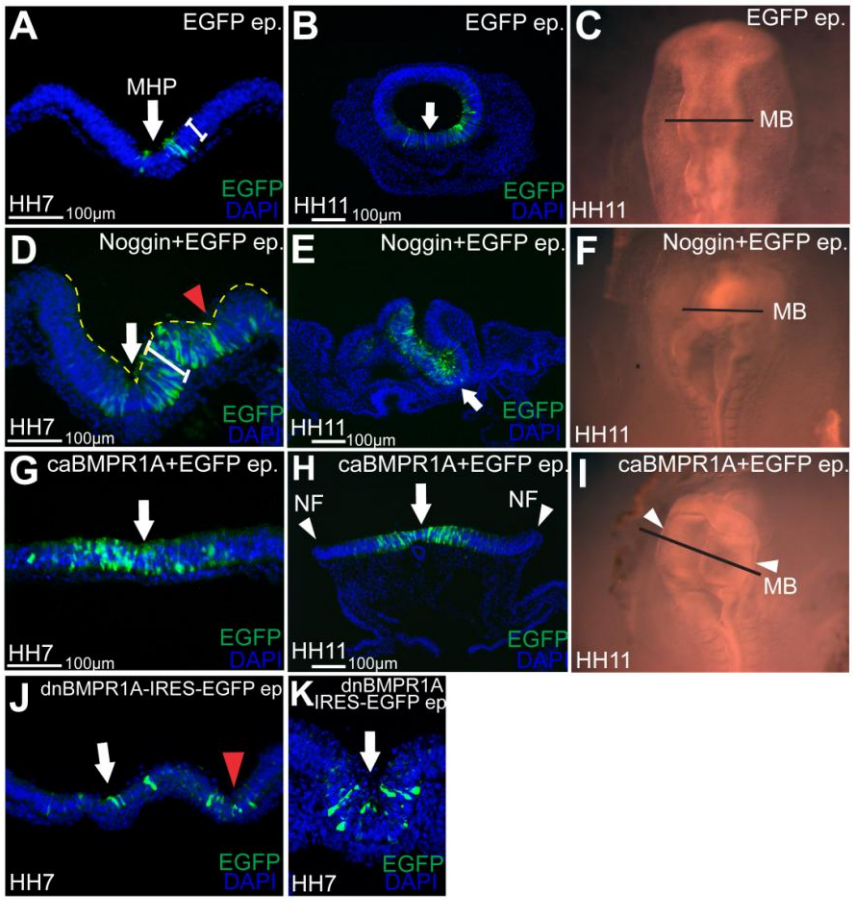

Fig. 2.3 BMP blockade is necessary and sufficient for MHP formation
Columns 1, 2:cross-sections, Column 3: Top down view of whole embryos, whose cross-sections are shown in column 2. Black lines in C, F and I indicate the level of cross-sections shown in B, E and H. (A-C) A normally contoured MHP at HH7 and HH11 (arrows, A, B) and a correctly closed neural tube at HH11 (B, C) following EGFP-electroporations at HH5. (D-F) Noggin overexpression at HH5 exaggerates the endogenous MHP (arrow in D, E) and/or induces ectopic HPs in lateral neural plate (red arrowhead, D). Note that the neural tube in E, F does not close, most likely due to the increased thickness of the neurectoderm (compare white I- bars in A and B {Fraser, 1954 #160}). (G-I) Targeted midline caBMPR1A overexpression at HH5 abolishes the MHP (arrow, G) at HH 7, and prevents the neural folds (NF, arrowheads, H, I) from coming together to close the neural tube at HH11. For quantitative details see Table 1. (J) DAPI-stained section demonstrating that dnBMPR1A overexpression (green) at HH5 induces ectopic HP formation (red arrowhead) at HH7 (3 hours after electroporation). White arrow: endogenous MHP. (K) DAPI-stained section demonstrating that focal dnBMPR1A misexpression (green) at the MHP at HH5 can also exaggerate the endogenous MHP by HH7 (Arrow, B). Note that not all cells participating in HP formation are electroporated. EP: electroporation; HH: Hamburger and Hamilton stages; MHP: median hinge point; NF: neural fold; MB: midbrain.

C; Table 2.1). By contrast, both Noggin and dnBMPR1 electroporations resulted in a dramatic exaggeration of the endogenous MHP and in the ectopic induction of HPs in lateral midbrain (Fig 2.3D-F, J-K). The neural tube failed to close in BMP blockade experiments (n=9/11 embryos), most likely due to the increased apicobasal thickening of the neural epithelium (Compare Fig. 2.3A, D; Table 2.1; (Fraser, 1954)).

Considerable controversy exists with regard to the requirement for MHP formation in neural tube closure (Copp et al., 2003; Smith and Schoenwolf, 1997). Strikingly, overexpression of caBMPR1A at the ventral midline during neural plate stages prevented MHP formation, flattening the ventral midline (Fig. 2.3G, H). Compared to controls (n=1/8 embryos), early midline electroporations of caBMPR1A, which prevented MHP formation, also consistently prevented the neural folds from elevating and drawing together so that they could not fuse across the dorsal midline (n=8/12, arrowheads, Fig. 2.3H, I; Table 2.1). Together, these results suggest that MHP formation is required for midbrain neural plate closure and that BMP blockade is both necessary and sufficient for MHP induction.

We asked whether MHP formation is a cell-autonomous effect of BMP blockade. The determination of cell-autonomy is difficult when manipulating gene expression with electroporations, since inheritance of the transgene-bearing plasmid during cell division is idiosyncratic and gene expression can shut down in a cell *after* a clear phenotype has been produced. To determine

BMPs regulate neural tube closure

	unaffected	NTD	Total
EGFP	7	1	8
Noggin	2	9	11
caBMPR1A	4	8	12

* NTD : neural tube closure defects

Table 2.1. The effects of BMP signaling on Neural tube closure.
Phenotypes of EGFP, Noggin and caBMPR1A misexpressing midbrains electroporated at HH5 and examined at HH11 for neural tube closure defects (NTDs). Unaffected embryos were determined by comparing tissue morphology with wildtype unelectroporated embryos.

whether the effects of BMP blockade were cell autonomous, we therefore directed our analyses to those embryos focally electroporated with dnBMPR1-IRES-EGFP and collected within 4 hours of electroporation. At this time, strong EGFP expression is detected and cell cycle duration (~12 hours in lateral midbrain neural plate) is not a significant confound (Fig. 2.3J, K; data not shown; (Schoenwolf, 1985; Smith and Schoenwolf, 1987)). These dnBMPR1 manipulations clearly demonstrate that HP formation is a short-range, non-autonomous event, typically involving BMP attenuation in some but not all cells participating in the HP. As we will see below, similar non-autonomous HP induction is also elicited by early apicobasal polarity manipulations followed by short-term survivals.

2.2.4 BMPs regulate hinge point formation by directing apical constriction and basal nuclear migration.

MHP formation is associated with characteristic cell behaviors such as the basal migration of nuclei, apical constriction and apicobasal shortening (Colas and Schoenwolf, 2001) (Fig. 2.4A, B). We therefore asked whether such cell behaviors were induced by BMP blockade at ectopic hinge points.

Midbrain wholemounts electroporated with either membrane-targeted EGFP (m-EGFP) alone, or in conjunction with Noggin were stained with PAR3 to distinguish the apical (PAR3+) surface from the basolateral (mEGFP+/PAR3-negative) surface. When such midbrain wholemounts were flattened so that

their apical surface could be viewed, severe apical constriction was noted in Noggin-electroporated cells and in all cells (Noggin-electroporated cells + unelectroporated neighbors) within the sampling box (respectively 68% and 67% of controls; Fig 2.4C-F).

While the above data provide a measure of total apical constriction, they do not distinguish between apical constriction and a reduction in total cell size. Therefore, we stained brains with PAR3 as before and compared ratios of apical width (aw) to the cell width at its widest point (ww) in control (mEGFP-electroporated) and Noggin+mEGFP-electroporated cells according to established protocols (Lee et al., 2007). Compared to controls, Noggin-electroporated cells displayed a 55.5% reduction in the aw:ww ratio, suggesting that the apical constriction noted in wholemounts did not simply represent altered cell sizes (Fig. 2.4G-I).

The mitotic duration in MHP cells is less than half that seen in lateral neural plate, as a result of which MHP cell nuclei spend more time at basal locations than lateral neural plate cells, possibly facilitating apical constriction (Fig. 2.4A, B; (Smith and Schoenwolf, 1997)). We therefore asked whether BMP signaling played a role in inducing basal nuclear migration at the MHP. Compared to DAPI and PAR3-stained controls, Noggin-electroporated nuclei seen at more basal locations (5.01µm vs.15.2 µm from the apical surface), reproducing the phenotype seen at the endogenous MHP (Fig. 2.4A,B; J-L and Fig. 2.2F, G (red arrowhead)).

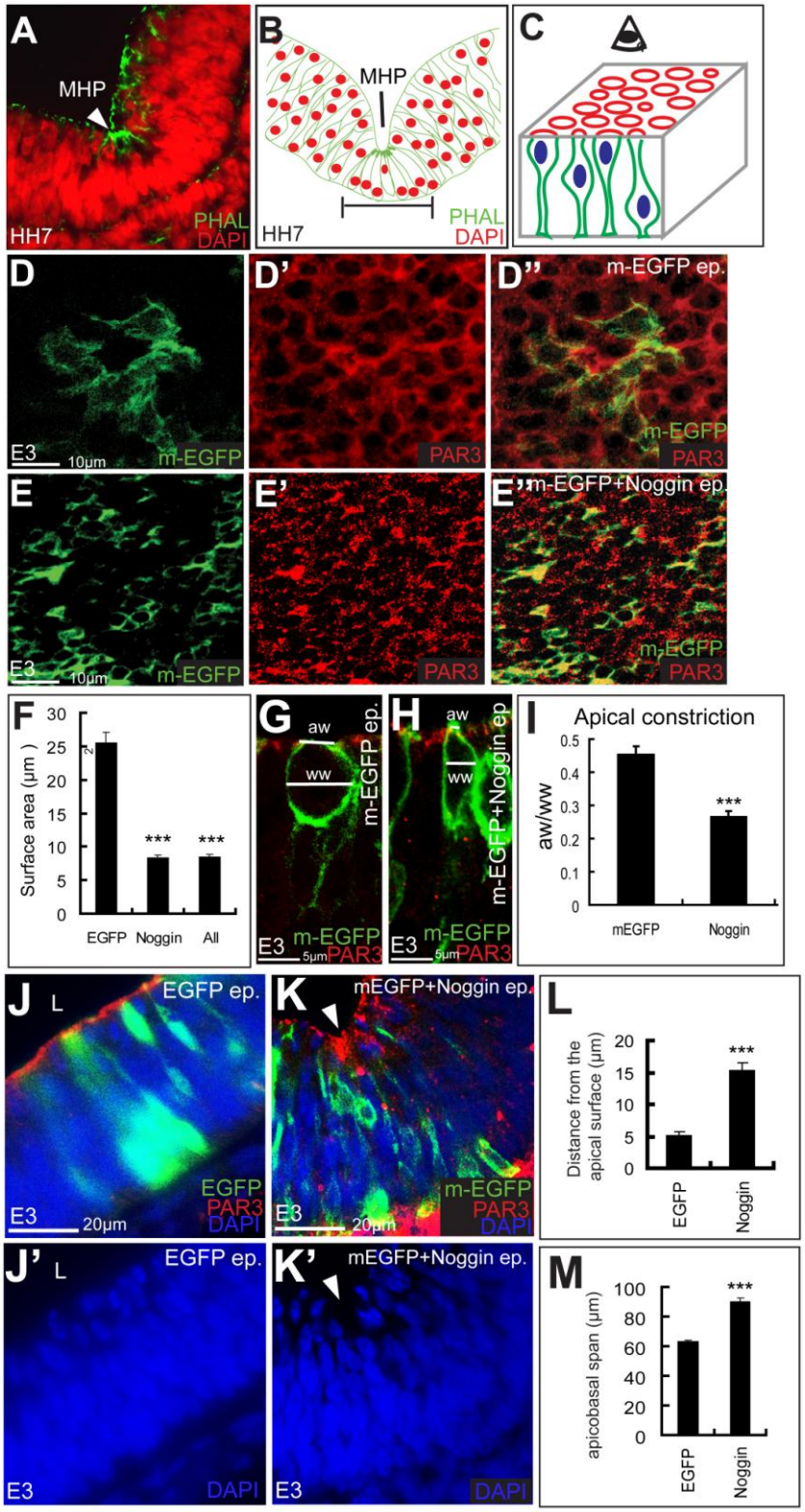
A
MHP
HH7
PHAL
DAPI
B
MHP
HH7
PHAL
DAPI
C
D
E3
10μm
m-EGFP
D'
PAR3
D''
m-EGFP ep.
m-EGFP
PAR3
E
E3
10μm
m-EGFP
E'
PAR3
E''m-EGFP+Noggin ep.
m-EGFP
PAR3
F
Surface area (μm)
30
25
20
15
10
5
0
***
***
EGFP
Noggin
All
G
aw
ww
m-EGFP ep.
E3
m-EGFP
5μm
PAR3
H
aw
ww
m-EGFP+Noggin ep.
E3
m-EGFP
5μm
PAR3
I
Apical constriction
aw/ww
0.5
0.4
0.3
0.2
0.1
0
***
mEGFP
Noggin
J
L
EGFP ep.
EGFP
PAR3
DAPI
E3
20μm
K
mEGFP+Noggin ep.
m-EGFP
PAR3
DAPI
E3
20μm
L
Distance from the apical surface (μm)
20
15
10
5
0
***
EGFP
Noggin
J'
L
EGFP ep.
E3
DAPI
K'
mEGFP+Noggin ep.
E3
DAPI
M
apicobasal span (μm)
100
80
60
40
20
0
***
EGFP
Noggin

Figure 2.4. BMP signaling regulates apicobasal cell behaviors associated with MHP formation.

(A) DAPI (pseudo-colored red) and Phalloidin (green) stained section through an HH7 neural plate demonstrating apical constriction and basal nuclear migration in most, but not all cells at the MHP. Note the condensed apical phalloidin in apically constricted MHP cells. (B) Schematic of A. (C-E) Apical constriction demonstrated by the reduced ratio of apical width:widest width in Noggin-electroporated cells (D) compared to controls (C). White lines in C and D depict where measurements were taken. E. Quantitation of C, D (aw:ww ratio in control cells: 0.45; n=43cells / 9 brains. Noggin electroporated cells: 0.27, n=87cells/12 brains p=2.034x10-10). (F-G') F, F': EGFP electroporations displaying the smooth apical (PAR3+) contour of lateral midbrain and the normal distribution of DAPI stained nuclei. Note that the density of DAPI staining is lower apically than elsewhere (see also Fig. 2.4A). G, G': Noggin-induced ectopic hinge in lateral midbrain (arrowhead) is accompanied by apical constriction (condensed PAR3, arrowhead) and basally migrated nuclei. Note the fewer number of apical Noggin+ cells (green, G) compared to those in EGFP-electroporated controls (F). F, F' and G, G' show the same micrographs with the green and red channel removed in F' and G' for clarity. (H) Quantitation of basal migration. Distance from the apical surface: control cells: 5.01µm; n=164 cells/5brains; Noggin treated cells=15.2µm; n=202cells/7brains; p=1.23x10-7 (I) Compared to controls, Noggin-electroporated cells display increased apicobasal spans (compare Fig. 2.3A and D or Fig. 2.5A and B). Apicobasal spans, EGFP electroporated cells: 63.22 µm, n=20 cells/5 brains, Noggin-electroporated cells: 90.31 um, 52 cells/8 brains; p=1.02x10-15.

During neurulation, apicobasal shortening occurs at the MHP, while the neurectoderm lateral to the MHP undergoes apicobasal thickening (Colas and Schoenwolf, 2001). However, Noggin-electroporated midbrain progenitors rapidly (within 6 hours) increased their length by 42% compared to controls (Fig. 2.4M; Compare the apicobasal thickness of sections in 2.4F' and G' and Fig. 2.3A and D; see Fig. 2.5A, B for micrographs of individual cell spans). Together, these data suggest that BMP blockade is sufficient for apical constriction and basal nuclear migration, but not for apicobasal shortening. Interestingly, despite Noggin's inability to induce apicobasal shortening, it is sufficient to elicit ectopic HPs in the midbrain.

2.2.5 BMPs regulate epithelial apicobasal polarity.

The above data show that BMP signaling regulates apicobasal cell behaviors associated with MHP formation. We therefore asked whether BMP signaling might affect MHP formation by interacting with the apicobasal polarity pathway. The apicobasal polarization of epithelial cells depends on antagonistic interactions between basolateral protein complexes (e.g. LGL-Scribble-Disks Large) and apically located protein complexes (e.g. PAR3-PAR6-aPKC complex) associated with tight and adherens junctions (Margolis and Borg, 2005). As a result, apical and baslolateral proteins exhibit no overlap in mature epithelia, although their expression can overlap in "morphogenetically active" or immature epithelia (Margolis and Borg, 2005; Suzuki et al., 2009).

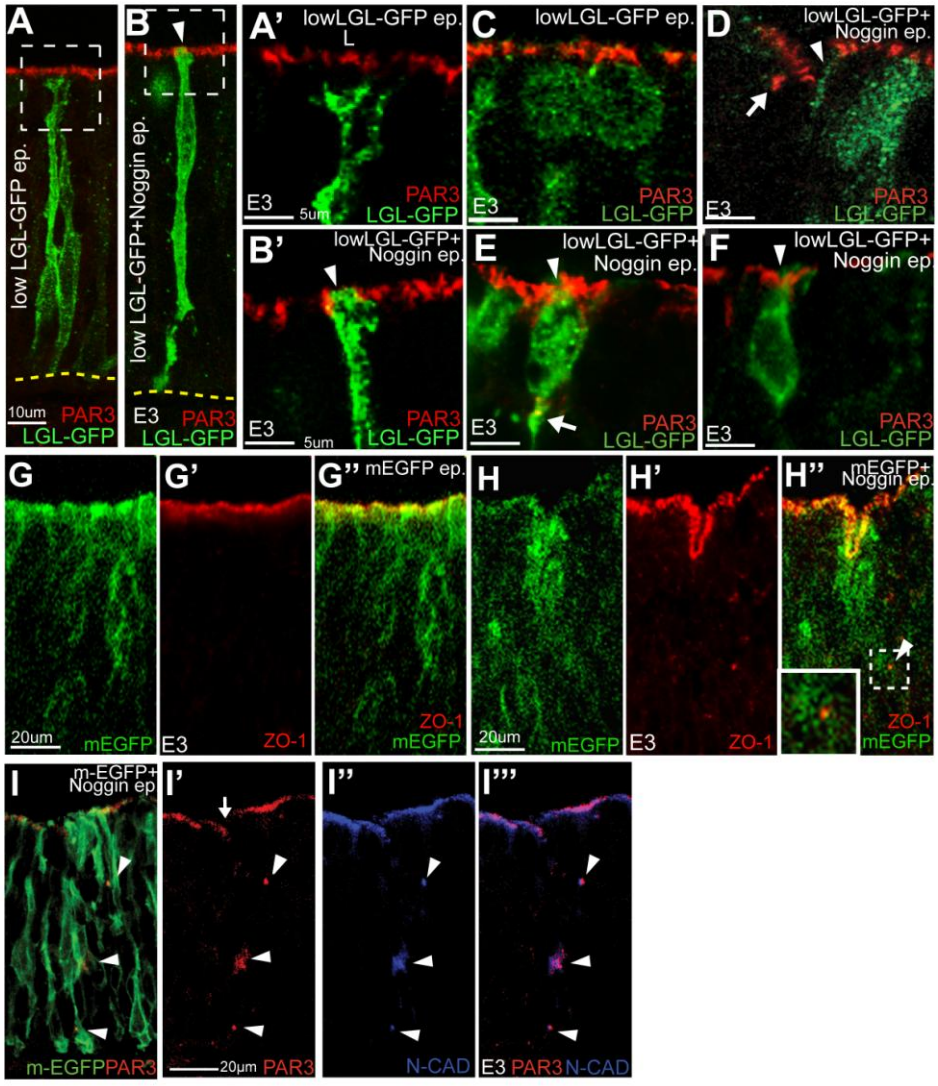
A
low LGL-GFP ep.
10um PAR3
LGL-GFP
B
low LGL-GFP+Noggin ep.
E3 PAR3
LGL-GFP
A' lowLGL-GFP ep.
L
E3 5um PAR3
LGL-GFP
C lowLGL-GFP ep.
E3 PAR3
LGL-GFP
D lowLGL-GFP+
Noggin ep.
E3 PAR3
LGL-GFP
B' lowLGL-GFP+
Noggin ep.
E3 5um PAR3
LGL-GFP
E lowLGL-GFP+
Noggin ep.
E3 PAR3
LGL-GFP
F lowLGL-GFP+
Noggin ep
E3 PAR3
LGL-GFP
G
20um mEGFP
G'
E3 ZO-1
G'' mEGFP ep.
ZO-1
mEGFP
H
20um mEGFP
H'
E3 ZO-1
H'' mEGFP+
Noggin ep.
ZO-1
mEGFP
I m-EGFP+
Noggin ep
m-EGFPPAR3
I'
20μm PAR3
I''
N-CAD
I'''
E3 PAR3 N-CAD

Figure 5. BMP signaling regulates epithelial apicobasal polarity.
(A, A') Control, low LGL-GFP electroporation showing complete segregation between the apical (PAR3+) and basolateral (LGL-GFP+) cell compartments. A' is a magnified view of the boxed area in A. (B, B') Noggin+ low LGL-GFP electroporated cells showing ectopic apical LGL-GFP expression (arrowheads in B and B'). B' is a high magnification view of the boxed area in B. A, B: Maximum intensity projections; A', B': 0.8μm optical sections. (C-F) C: Control LGL-GFP electroporations showing complete segregation of the apical and basolateral compartments in apical cells in lateral midbrain. D-F: Due to the temporally dynamic nature of HP formation, Noggin+ low LGL-GFP electroporations display variable combinations of ectopic apical LGL-GFP (arrowheads, D-F), reduced apical PAR3 (D-F), cytoplasmic PAR3 (arrows D, E; see also Fig. 4G; 5L-L"), apical constriction (E, F) and ectopic HP formation (D, F). (G-G'') Confocal images showing the exclusively apical expression of ZO1 in tight junctions in control brains. A: EGFP (green); A': ZO-1 (red); A" merge of A, A'. (H-H'') Noggin-electroporated brains showing increased cytoplasmic ZO1+ puncta (arrowhead, H'). Inset in H" shows a magnified view of the boxed area. H: EGFP (green channel), H' ZO1 (red channel), H" merge of B, B'. (I-I"') Confocal images of Noggin-electroporated cells (green, I) displaying reduced apical PAR3 and N-CAD (arrow, I') and ectopic PAR3 and N-CAD in the cytoplasm (arrowheads I-I"'). I"': merge of I', I". Note that the ectopic, basolateral expression of N-CAD (arrowheads, I'') coincides with ectopic PAR3 (arrowheads, I-I"'). Control electroporations can be seen in Fig. 2.6A-A".

Since no antibodies for basolateral proteins are available for the chick, we simultaneously visualized the apical (PAR3/N-CAD/ZO1+) and the basolateral (LGL+) compartments using immunohistochemistry combined with low-level misexpression of the LGL-GFP (1 µg/µl) fusion protein (Dollar et al., 2005). A complete segregation between apical and basolateral compartments was noted in these experiments with no overlap between PAR3/ZO1/N-CAD and LGL-GFP, suggesting that at these levels, LGL-GFP did not affect epithelial polarity (Fig. 2.5A, C, data not shown (Betschinger et al., 2003)). As expected, LGL-GFP was also seen in the cytoplasm, although this did not interfere with our ability to distinguish between the membrane-associated PAR3 and LGL proteins in the apical and basolateral compartments (Fig. 2.5A, C). In contrast to control (low) LGL-GFP electroporations, co-electroporations of Noggin with low LGL-GFP resulted in a reduction of apical PAR3 and the ectopic apical expression of LGL-GFP (Fig. 2.5A-B'). Since the process of HP formation is temporally dynamic, Noggin-electroporated cells variably displayed combinations of apical constriction, ectopic apical LGL, reduced apical junctional proteins and increased cytoplasmic PAR3, ZO1 and N-Cad puncta (Fig. 2.5C-F; 2.5G-I'").

2.2.6 BMP blockade increases PAR3 endocytosis.

We noted that Noggin-electroporated cells frequently displayed PAR3+, ZO1+, N-CAD+ cytoplasmic puncta not seen in controls (arrows, Fig. 2.5D, E, H', H", I-I'"). Western blot analysis revealed no changes in PAR3 protein level in

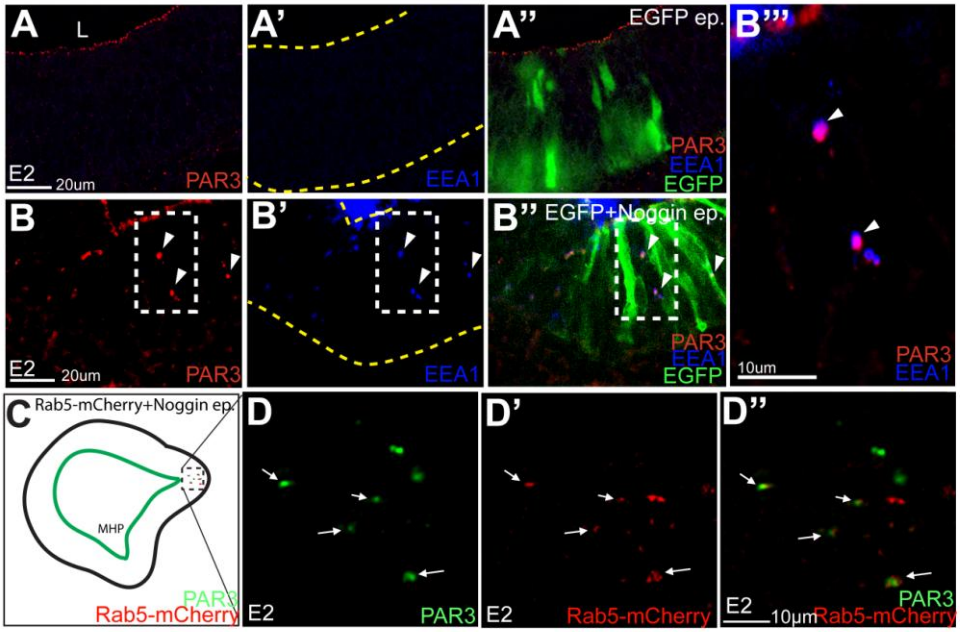

Fig. 2.6. BMP-blockade increases PAR3 endocytosis.
(A-B''') Low (A-B'') and high power (B''') images demonstrating that compared to controls (A-A''), Noggin electroporated embryos display increased PAR3+ cytoplasmic puncta which colocalize with EEA1+ endosomes (arrowheads, B-B'''). Note that the EGFP channel has been omitted in B''' for clarity. (C-D'') Noggin+low level Rab5-cherry electroporations demonstrating PAR3 and Rab5 colocalization in endosomes. C: Low power cartoon view of a Noggin (green), Rab5-cherry co-electroporated brain. The boxed area is magnified in D-D''. E: PAR3 (green channel); D': Rab5-m-cherry (red channel). D'': merge, D, D'. EP: electroporation; L: lumen.

Noggin electroporated embryos as compared to the controls (Fig. 2.7C). We therefore hypothesized that the apical loss of PAR3 noted above was due to the endocytosis-mediated removal of apical membranes leading to apical constriction, as observed during *Xenopus* gastrulation (Lee and Harland, 2010). As in the *Xenopus* study, control EGFP+ midbrain cells displayed little or no expression of the early endosomal markers EEA1 or Rab5, suggesting that these organelles turn over rapidly (Fig. 2.6A-A"; data not shown) (Lee and Harland, 2010). However, an increase in PAR3+, EEA1+ puncta in Noggin-electroporated brains demonstrated that a proportion of apical PAR3 had been shunted into endocytotic vesicles (Fig 2.6B-B"'). These results were confirmed by co-electroporations of Noggin with Rab5-cherry, which also demonstrated increased numbers of PAR3+, Rab5-cherry+ cytoplasmic puncta (Fig. 2.6C-D"). Thus, these results implicate BMP blockade-mediated endocytosis of apical proteins as a potential mechanism for apical constriction.

2.2.7 BMP signaling cascade biochemically interacts with PAR3

We next asked whether the BMP signaling cascade biochemically interacted with members of the apicobasal polarity pathway. Strikingly, immunoprecipitation of HH 9-11 brain lysates with pSMAD 1/5/8 antibody (specific for the phosphorylated forms of SMAD1/5/8) followed by immunoblotting with PAR3 or vice versa, demonstrated a biochemical interaction between the effectors of canonical BMP signaling and the apicobasal

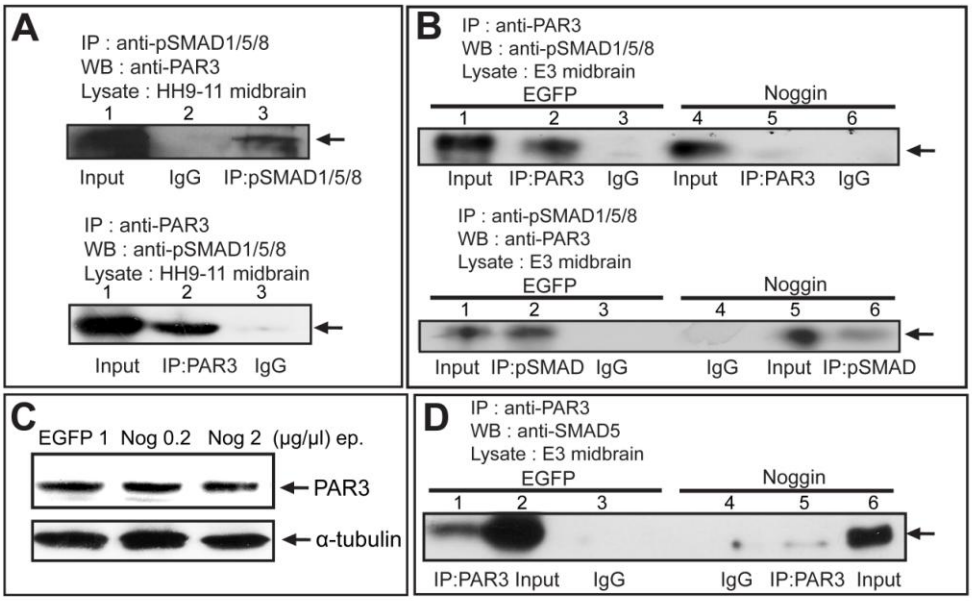

Fig. 2.7. BMP signaling cascade biochemically interacted with PAR3.
(A) Top: Biochemical interactions between pSMAD 1/5/8 and PAR3 in whole cell lysates immunoprecipitated with PAR3 and immunoblotted with pSMAD1/5/8 antibody (lane 3). Bottom: p-SMAD 1/5/8 and PAR3 interactions demonstrated by reversing pSMAD 1/5/8 and PAR3 antibodies (lane 2). (B) Compared to EGFP controls, biochemical interactions between pSMAD 1/5/8 and PAR3 are greatly reduced in Noggin-electroporated whole cell lysates. Top Row: IP-PAR3, WB: pSMAD 1/5/8. Bottom row: IP: pSMAD1/5/8 antibody WB: PAR3. (C) Top Row: Western blot experiments showing that PAR3 protein levels are not different in E3 whole cell lysates prepared from EGFP- or brains electroporated with varying doses of Noggin. Bottom Row: loading controls.
(D) Immunoprecipitation with PAR3 and Western blotting with a SMAD5 antibody (which recognizes both phosphorylated and non-phosphorylated SMAD 5). Note that the interactions between PAR3 and SMAD5 seen in EGFP-electroporated embryos (lane 1) are significantly decreased by Noggin electroporations (lane 5).

polarity pathway (Fig. 2.7A). Interestingly, while PAR3-pSMAD 1/5/8 interactions were preserved in EGFP-electroporated lysates, they were severely reduced in Noggin-electroporated lysates (Fig. 2.7B).

Reduced interactions could occur if the total protein levels of PAR3, SMAD 1, 5 or 8 proteins themselves were reduced. However, Noggin electroporations at multiple concentrations followed by immunoblotting did not show in a net loss of PAR3, SMAD1 or SMAD5 proteins (Fig. 2.7C; Fig. 2.2C). Since no interactions were noted between SMAD1 and PAR3 in wild-type tissue lysates, we eliminated SMAD1 from our analyses (data not shown) and focused on PAR3-SMAD5 interactions, since the SMAD8 antibody did not work in our hands. Despite their unchanged levels, interactions between PAR3 and SMAD5 (using antibodies that recognize both its phosphorylated and non-phosphorylated forms) were severely reduced in Noggin, but not in EGFP-electroporated cell lysates (Fig. 2.7D; Fig. 2.2C). Together with the reduced pSMAD 1/5/8 and PAR3 interactions in Noggin-electroporated brains, these results suggest that PAR3-pSMAD 5/8 interact with each other in a BMP-dependent manner.

2.2.8 Partially polarized cells at the wild type MHP.

The formation of epithelial tissues (e.g., branched tubules) frequently involves the dynamic modulation of cell polarity, giving such developing tissues the flexibility to undergo complex shape changes while retaining overall

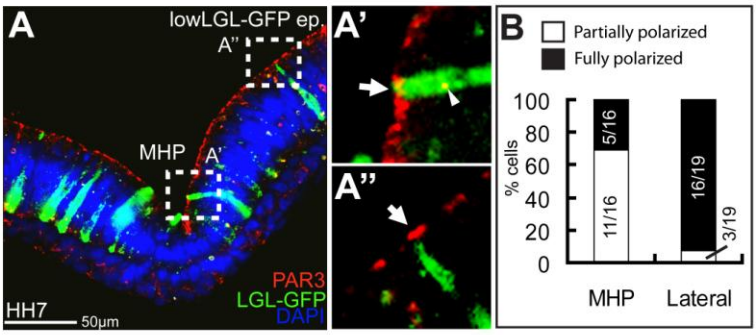

Fig. 2.8. Partially polarized cells at the wild type MHP.
(A-A") Embryo electroporated at HH5 with low LGL-GFP displays semi-polarized cells at the MHP (Box A'), but not in lateral neural plate at HH7 (Box A"). Note that the electroporated cell in A' (arrow) displays apical LGL-GFP and reduced apical PAR3 (arrow, A') unlike the cell in A" (arrow), which displays a clear segregation between apical (PAR3+) and basolateral (LGL+) compartments. (B) Greater frequency of partially polarized cells at the MHP (63% of those electroporated) where BMP signaling is weak compared to the lateral neural plate (7%) where it is strong.

epithelial organization (Bryant and Mostov, 2008; Ewald et al., 2008; Suzuki et al., 2009). Our findings that BMP blockade altered apicobasal polarity and resulted in the apical LGL expression, led us to ask whether such cells existed in the wild-type MHP where low BMP signaling occur. Combined low-level LGL-GFP electroporations and PAR3 immunohistochemistry demonstrated that such partially polarized cells (with apical LGL or LGL-PAR3 overlap) occurred in the neural plate (Fig. 2.8A-B; data not shown; see Materials and Methods for details on LGL-GFP concentrations and effects on cell polarity). Interestingly, their frequency was inversely correlated with the level of BMP signaling with the greatest numbers (n=11/16 electroporated) present at the wild-type MHP compared to lateral midbrain (n=3/19 electroporated; Fig. 2.8A-B).

2.2.9 Apical LGL is sufficient to induce MHP formation.

We next asked to what extent would apical LGL misexpression account for the hinge point-associated effects of BMP blockade. Unlike low LGL-GFP misexpression, early (HH4-6) high-level LGL-GFP (3-5 µg/µl) electroporations resulted in aberrant apical LGL-GFP expression and in ectopic hinge point induction in the lateral neural plate (Fig. 2.9C-F; a control for C is shown in Fig. 2.3A). Such ectopic hinge points, like those induced by BMP blockade, also displayed apical constriction, basal nuclear migration and increased PAR3 endocytosis into EEA1+ endosomes (Fig. 2.9D-F). As with dnBMPR1 manipulations, LGL-GFP electroporations followed by short-term survivals (3

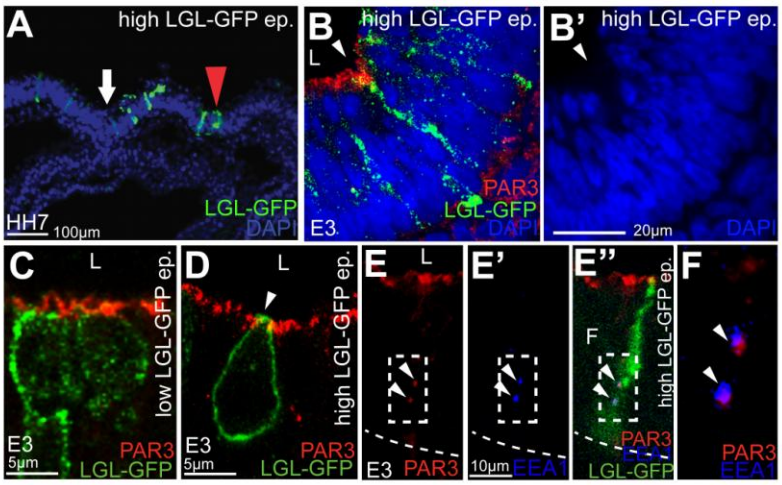

Fig. 2.9. Apical LGL is sufficient to induce MHP formation.
(C) DAPI stained sections demonstrating that high level (3µg/µl) LGL-GFP misexpression at HH5 is sufficient to induce ectopic HPs by HH7 (red arrowhead, C). White arrow (C) marks the endogenous MHP. (D, D') PAR3 and DAPI stained brains demonstrating basal nuclear migration at ectopic hinge points (arrowheads) induced by high LGL-GFP electroporations. D and D' represent the same micrograph, with the green and red channel removed in D' for clarity. (E, F) Control (low LGL-GFP, E) and high LGL-GFP (F) electroporations demonstrating apical LGL-GFP and apical constriction in F (arrowhead). (G-H) Ectopic cytoplasmic PAR3+/EEA1+ puncta in cells electroporated with high levels of LGL-GFP. G, G': single channels, G'':merge of G-G' and LGL-GFP, H: Merge of G-G' showing the boxed area in G-G'. Control (EGFP) electroporations are shown in Fig. 5K-K''. EP: electroporation; MHP: median hinge point; L: lumen.

hours) also induced HP formation in a short range, non-autonomous manner, possibly via apical junction mediated cell-cell communications. We conclude that BMP blockade targets LGL to the apical compartment. Apical LGL in turn is sufficient to account for the cellular and morphogenetic effects of BMP blockade on MHP formation.

2.2.10 MHP formation is mediated by blockade of canonical BMP signaling.

In mammary gland epithelial cells, TGFß signaling interacts with apical junctional complexes via non-canonical, transcription-independent mechanisms (Ozdamar et al., 2005). The rapid onset of BMP-mediated epithelial effects described above (Fig. 2.3) argued for the involvement of Smad-independent, non-canonical mechanisms in hinge point formation. However, the graded SMAD 1/5/8 expression and the ability of dnBMPR1A misexpression to elicit ectopic hinge points and pSMAD5/8 interactions with PAR3 (Fig. 2.1D; 2.2H; 2.7A) argued for the involvement of Smad-dependent mechanisms. To resolve this issue, we misexpressed an inhibitory Smad, Smad6, which interferes with the ability of BMPR1 to phosphorylate receptor-activated Smads (SMAD 1, 5, 8) and/or with the formation of SMAD 1/5/8-coSmad (SMAD4) complexes (Hata et al., 1998; Imamura et al., 1997). Interestingly, Smad6 overexpression mimicked the phenotypes produced by Noggin, dnBMPR1 and LGL misexpression. These phenotypes included ectopic hinge point formation, the removal of apical PAR3, basal migration of nuclei and apical constriction (Fig.

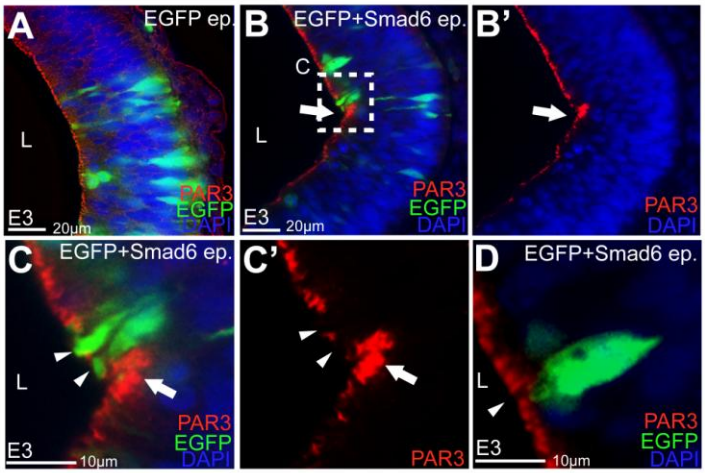

Fig. 2.10. MHP formation is mediated by blockade of canonical BMP signaling (A-B') A: The apical (PAR3+) contour of lateral midbrain at E3 in EGFP-electroporated controls. B, B': Smad6 overexpression induces ectopic HPs (arrows, B, B') with basal nuclear migration. B' shows the same micrograph as B with the green channel omitted for clarity. (C, C') High magnification image of boxed area in B demonstrating apical constriction (condensed PAR3 expression at the HP, arrow in C, C') and the loss of apical PAR3 (arrowheads in C, C'). (D) Smad6 overexpression resulting in an apically constricted lateral midbrain cell (arrowhead). L: lumen.

2.10A-D; data not shown). These results suggest that BMP blockade-regulates MHP formation in the midbrain by canonical, Smad-dependent mechanisms.

2.3 DISCUSSION

2.3.1 The cellular role of BMP signaling in regulating apicobasal polarity.

We have shown in chapter 2, BMP signaling is highest when cells are located at the apical surface where cells normally undergo mitosis. We also have shown that PAR3 and SMAD1/5/8 biochemically interact each other in the presence of BMP signaling. In the absence of BMP signaling by overexpressing BMP antagonist Noggin, we observed an increase of endocytosis of PAR3. Taken together data we have shown, we hypothesize that BMP signaling plays an important role to maintain midbrain neuroepithelial apicobasal polarity. BMP attenuation reduces the phosphorylation of SMAD5 which leads to removal of apical junctional components including PAR3 or ZO-1 into Rab5+/EEA1+ endosomes. This causes the reduction of apical membrane area leading to apical constriction, disruption of junctional structures and the apical mislocalization of basolateral protein LGL (Fig. 2.11). In the MHP where normally BMP signaling is low, cells partially lose their interaction between PAR3 and canonical BMP signaling components which in turn induce apical constriction, generating partially polarized epithelial phenotypes as we have observed in Fig. 2.8. According to recent studies, actomyosin contractility can

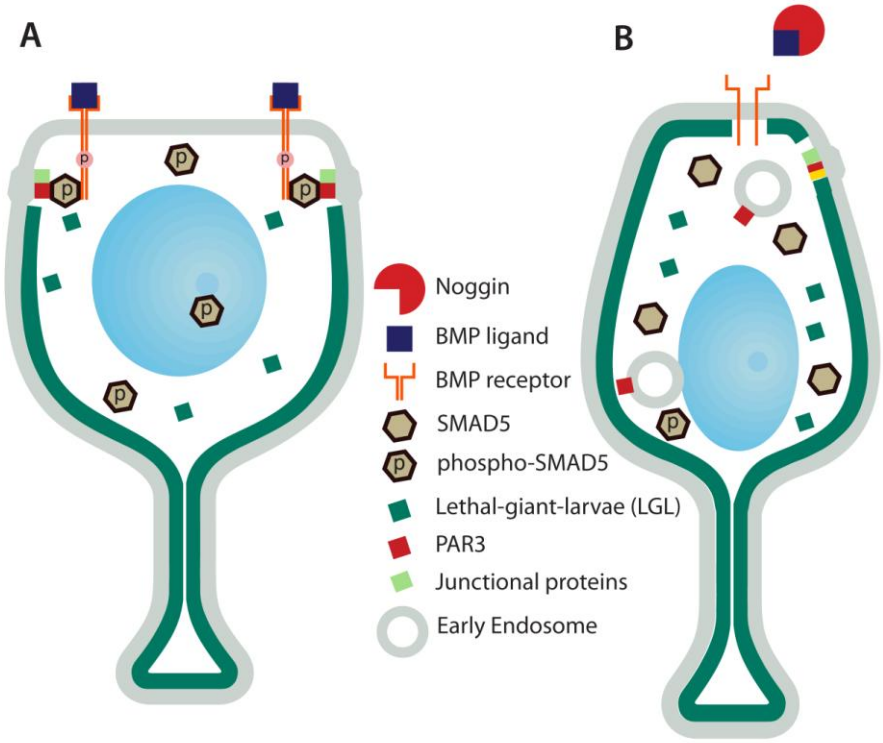

Fig. 2.11. The cellular role of BMP signaling in regulating apicobasal polarity. A. Depicts a neural plate cell receiving BMP signaling. BMP binding to its receptors phosphorylates pSMAD 1/5/8, which bind to the PAR3-PKC-PAR6 complex at the tight junction via its interactions with PAR3. The PAR complex is stabilized and LGL is restricted to the basolateral compartment and cytoplasm. B. A cell experiencing BMP attenuation. Due to reduced SMAD 1/5/8 phosphorylation, the PAR complex becomes unstable and disrupts the tight junction. This permits the apical incursion of LGL, PAR3 endocytosis and apical constriction. Note that the same cell can shuttle between states A and B in a cell cycle- dependent manner. Note also that in addition to cell-autonomous effects, non-autonomous inclusion of cells in the HP is expected, possibly by intercellular communication via the apical actin/adherens belt (not shown).

induce nuclear migration (Martini and Valdeolmillos, 2010; Schenk et al., 2009). Thus, apical constriction induced by the removal of apical components at the ventral midline in turn causes basal nuclear migration, culminating in the formation of median hinge point formation.

2.3.2 BMPs regulate MHP-induction independent of ventral cell fate specification

Although BMP and SHH activity overlap at the MHP/Floor plate, BMP blockade can regulate MHP formation, but cannot alter midbrain cell fates. Conversely, the ectopic HPs induced by BMP manipulations do not display rFP specific markers (*SHH*, *LMX1B*, *FOXA2*, Notch-Delta pathway members, Wnts, Fig. S1B; data not shown). Thus, while BMP blockade can elicit cell behaviors required for HP formation, it is not sufficient to induce rFP-specific markers and cell fates. By contrast, *SHH* misexpression induces ventral midline cell fates, but is not sufficient for inducing a morphogenetic MHP (Agarwala et al., 2001), data not shown), although it can prevent DLHP formation by blocking dorsally expressed Noggin (Ybot-Gonzalez et al., 2007). Thus, MHP induction and cell fate specification in the ventral midbrain are likely to be regulated via independent mechanisms.

2.3.3 Smad-dependent BMP signaling regulates MHP formation

TGFß-mediated regulation of the apicobasal polarity or cellular

cytoskeleton in multiple systems has been shown to occur in a BMPRII-dependent, Smad-independent manner (Eaton and Davis, 2005; Foletta et al., 2003; Ozdamar et al., 2005). *In vitro* studies in mammary gland epithelial cells have established direct interactions between TGFß signaling and Par6, an apical protein of the Par6-aPKC-Cdc42 complex (Bryant and Mostov, 2008; Ozdamar et al., 2005). TGFß receptor-mediated phosphorylation of Par6 activates the E3 ubiquitin ligase, Smurf1, degrading RhoA GTPases and disrupting tight junctions (Ozdamar et al., 2005).

Many of the changes in cell behaviors caused by BMP blockade in the midbrain (HP formation, interkinetic nuclear migration, epithelial disruption, rosette formation) were evident at < 6 hours of electroporation of Noggin-ires-EGFP and within 2 hours of the detection of EGFP fluorescence. Although the rapidity of BMP action suggests non-transcriptional (Smad-independent) mechanisms in BMP-mediated regulation of apicobasal polarity, the presence of an *MSX1* and a pSmad1/5/8 DV gradient in the neurulating midbrain support the involvement of canonical BMP signaling in regulating the cell behaviors involved in neural tube closure (Attisano and Wrana, 2002; Derynck and Zhang, 2003; Ozdamar et al., 2005). Moreover, overexpression of Smad6, which intereferes with the Smad 1/5/8-Smad 4 Smad complex formation and/or with the phosphorylation of R-Smads by BMPR1, strongly suggests that canonical BMP signaling might be involved in MHP induction in the midbrain (Hata et al., 1998; Imamura et al., 1997). Furthermore, our co-immunoprecipitation

experiments indicate a biochemical interaction between the R-Smads 1/5/8 and PAR3 in the ventral midbrain and suggests that TGFß mediated regulation of apicobasal cell polarity can occur in a Smad-dependent or Smad-independent manner (Ozdamar et al., 2005; Warner et al., 2003).

2.3.4 The non-autonomy of BMP function during MHP formation.

Only a small number of cells at the neurulating ventral midline at any given time are p-Smad1/5/8+. How do such few cells bring about a complex, non-autonomous event like HP formation? While the answer to this is not yet known, we noted that a few cells electroporated with Noggin, dnBMPR1A or Smad6 are sufficient to cause large-scale epithelial reorganization such as the formation of a hinge point (e.g., Fig. 2.3; 2.10). Similar effects have been noted in the fly embryo where cells with altered polarity can direct the polarity of their neighbors in a non-autonomous fashion (Zallen and Wieschaus, 2004).

Recent studies have also shown that an initially unpolarized cell can transform itself into a complex structure such as a cyst and then a branched tubule over time by simultaneously dividing and alternating between unpolarized, semipolarized and polarized states, each influenced by distinct sets of signals (Mostov et al., 2003). A handful of progenitors at the apical surface of the ventral midline of the midbrain that are transiently responsive to BMP signaling (pSmad 1/5/8+) could similarly alternate between different polarized states as they progress through the cell cycle while undergoing interkinetic nuclear

migration along the apicobasal axis of the midbrain (Bayly et al., 2007), data not shown). Such alterations in polarity in an affected cell could in turn influence the polarity of its neighbors via apical junctional complexes, producing the multicellular non-autonomous effects observed by us.

2.3.5 The interaction between PAR3 and pSMADs.

We have demonstrated that BMP signaling could regulate apicobasal polarity pathway by biochemical interaction between SMAD5 (or SMAD8) and PAR3 (Fig. 2.7). Studies of this interaction are incomplete so far. However, in the developing mouse orofacial tissue, it has been suggested that SMAD3 can interact with apicobasal polarity proteins on the basis of a yeast-two hybrid screen (Warner et al., 2003). Recently, it has been suggested that SMAD3 directly interacts with a serine/threonine kinase (PKB/Akt) and this interaction modulates TGF-beta signaling (Conery et al., 2004; Remy et al., 2004). These studies suggest that SMADs have roles not only as transcriptional regulator but also regulate other signaling pathway through protein-protein interaction.

CHAPTER 3 : 4D-IMAGING REVEALS THAT BMPS REGULATE CELL BEHAVIORS IN A CELL-CYCLE DEPENDENT MANNER.

3.1 Introduction

During neural tube closure, cells at the hinge points (median hinge point (MHP) and dorsolateral hinge points (DLHP)) undergo dynamic and polarized cell shape changes. Classic studies have described cell behaviors at hinge points such as apical constriction and basal migration. However, their precise temporal sequence, the causal relationship between the events and their molecular control are not well understood (Jacobson et al., 1986; Smith and Schoenwolf, 1987; Smith and Schoenwolf, 1997).

Cell cycle progression is thought to be involved in apicobasal shape changes at the MHP (Smith and Schoenwolf, 1987; Smith and Schoenwolf, 1997). As neural progenitors divide, they exhibit interkinetic (apicobasal) nuclear migration, undergoing mitosis apically, then moving basally through G1 and S phases, and apically again via G2 to the mitotic phase (Baye and Link, 2007; Sauer, 1935). This has led to the idea that basal expansion and apical constriction at the MHP can be achieved simply by altering cell cycle progression to induce basal nuclear migration. This can be achieved by reducing mitotic duration and/or increasing the duration of the other phases of the cell cycle (Bayly et al., 2007; Sauer, 1935). As I have described in Chapter 2, neural progenitors have high BMP signaling apically as they enter the mitotic (M) phase and then turn down the BMP signal as they move from the apical

surface to the basal surface (G1-S, S phases) and migrate back to the apical surface during the G2-M phase through the cell cycle (Fig. 2.1; (Baye and Link, 2007; Sauer, 1935)). Along the dorsoventral axis, BMP signaling is lowest at the MHP (Fig. 2.1). It has been suggested that cell cycle duration is significantly longer at the MHP than cells at the lateral neural plate (Smith and Schoenwolf, 1987; Smith and Schoenwolf, 1997). Thus the low BMP signaling could control MHP-associated cell behaviors by regulating cell cycle, more specifically by inducing cells to stay at the basal location. Here we tested this idea by asking how BMP signaling affects cell cycle progression in the midbrain neuroepithelium using 3D time-lapse-imaging methods.

3.2 Results

3.2.1 4D-imaging set up for chick midbrain

We developed a time-lapse imaging method for studying the dynamic cell behaviors in the developing chick midbrain. We electroporate the gene of interest at HH8-9 and collect embryos 6 hours later to allow time for the cells to express the trangene. Embryos were collected in L-15 tissue culture media and dissected as indicated along the dotted lines in Fig. 3.1A-B. The advantage of this type of dissection is that it retains all of the major signaling centers of the midbrain (roof plate, floor plate and notochord). Dissected embryos were placed in a glass bottom dish where the rostral cross-sectional face is toward the glass surface. This allows us to visualize apicobasal cell behaviors under a spinning

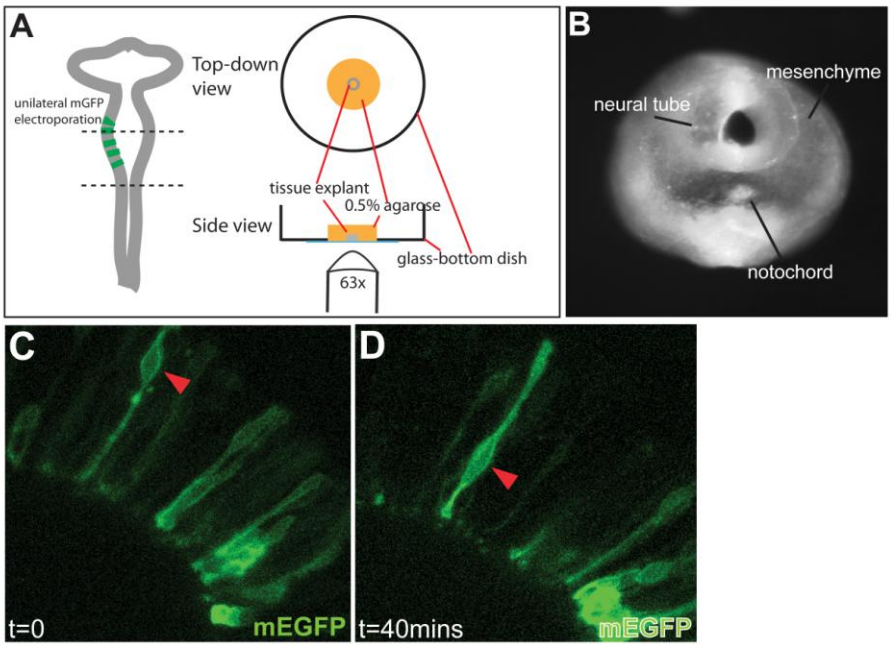

Fig. 3.1. 4D-maging method for chick midbrain.
(A) 4-6 hours after electroporation, embryos were collected and dissected as indicated with dotted lines in A, then placed a in 0.5% agarose block. The cross-sectioned neural tube faces down to the glass bottom dish (B) allowing imaging of cell movements along the apicobasal axis of midbrain neuroepithelium. (C, D) Time lapse images from two different time points showing the movement of one nucleus is marked with red arrowhead. Note that mEGFP expressing cells undergoing interkinetic nuclear migration.

disc confocal microscope (Fig. 3.1A-B).

We determined that the midbrain neuroepithelial cells undergo typical interkinetic nuclear migration as described in the introduction (Sauer, 1935). The zebrafish retina epithelium shows nuclei in G1, G2 and S phase distributed across the entire apicobasal axis, except for the M phase which occurs exclusively at the apical surface (Baye and Link, 2007; Baye and Link, 2008). Our preliminary experiments of tracking cell nuclei undergoing INM at various time intervals (Fig. 3.1C-D) combined with a 30min BrdU pulse suggest that, unlike the zebrafish retina epithelium, S-phase occurs near the basal membrane : the majority of BrdU positive cells localized at the basal surface of the midbrain neuroepithelium (Fig. 3.4D). In radial glial cells, the basally directed INM does not extend all the way to the basal surface, but is confined to the portion of the cell between the apical surface and the basal boundary of the ventricular zone or the subventricular zone (Gotz and Huttner, 2005). However, in the HH10-13 chick midbrain explants, INM spans the entire apicobasal axis of the cell (Fig. 3.2; 3.3; 3.5; 3.6).

3.2.2 Mitotic duration is not affected by BMP blockade

It is a well documented fact, conserved over various species, that mitosis occurs only at the apical surface in the neuroepithelium (Baye and Link, 2007; Gotz and Huttner, 2005; Sauer, 1935). However, the localization of nuclei can not be used as the only indicator of M-phase since the transitions from late

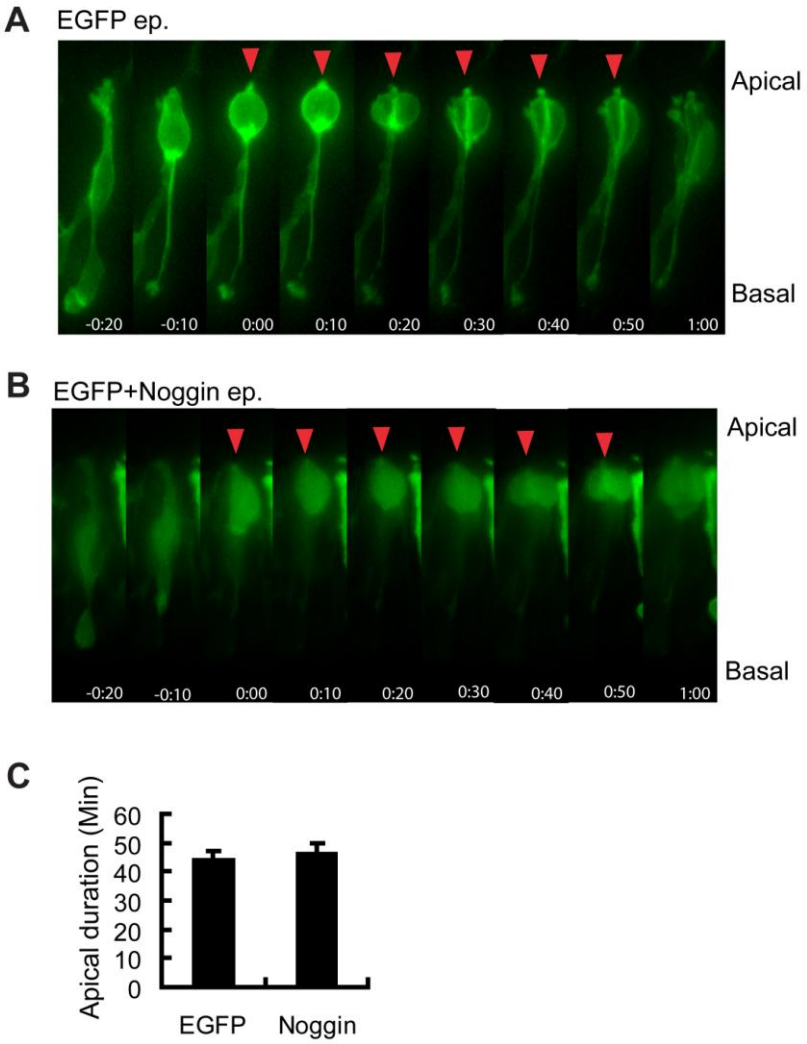

Figure 3.2. Mitotic duration is not affected by BMP blockade.
(A, B) Time-lapse images of EGFP(A) or EGFP+Noggin (B) electroporated neuroepithelial cells in lateral region of E3 midbrain with 10mins interval. Note that length of M-phase is measured from where cell nuclei positions at the most apical location (0:00) till two daughter cells are seen (0:40). (C) Quantitation data showing no significant difference between control and Noggin electroporated cells with respect to the duration of M-phase.

G2 and M or M to early G1 can also take place at or very close to the apical surface. However, the majority of time spent at the apical surface will be in M phase (Baye and Link, 2007; Sauer, 1935). We visually determined the mitotic duration for which cells stayed at the apical surface following BMP blockade with controls. The time spent at the apical surface was not significantly different between Noggin overexpressing cells and EGFP controls (Fig 3.2). It takes average 45mins in both EGFP and Noggin electroporated cells (EGFP cells: n=6 / 3 explants; Noggin electroporated cells : n=6 / 3 explants). Hence, we concluded that BMP blockade does not affect mitotic duration at the apical surface.

3.2.3 Apical to basal migration was perturbed by BMP blockade

Next, we analyzed apical to basal migration equivalent to the M-G1-S transition but mainly the G1 phase between EGFP and Noggin electroporated cells (Baye and Link, 2007; Sauer, 1935). Interestingly, apical to basal nuclear migration takes longer in Noggin electroporated cells as compared to the EGFP electroporated control cells (Fig. 3.3B, D). Noggin electroporated cells not only move slower (5.2µm/hr for control : n=9 / 4 explants versus 12.1µm/hr for Noggin : n=10 / 4 explants; $p< 1.02x10^{-12}$) but also migrate irregularly. Some cells start to move basally after mitosis but migrate back to apical direction without reaching the basal surface (Fig. 3.3D, #2 red line). This impaired basal migration is presumably due to the disruption of the apicobasal polarity pathway

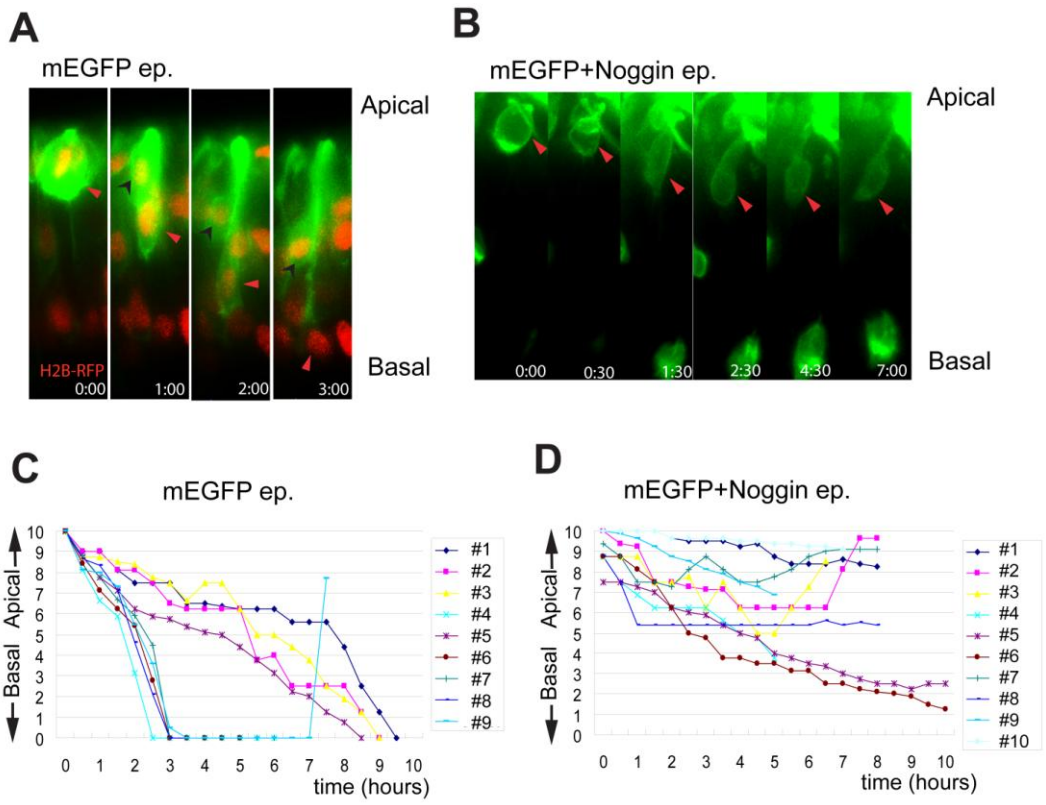

Figure 3.3. BMP blockade perturbs apical to basal nuclear migration (M-G1-S transition). (A, B) mEGFP (A) or mEGFP+Noggin (B) electroporated cells were imaged at various interval as indicated. Noggin electroporated cells showed slower apical to basal movement (red arrowheads in A and B). (C, D) Graphs showing the traces of nuclear movement imaged at 1 hour interval. Note that Noggin electroporated cells show slower and irregular migration (D) as compared to the controls (C).

(Costa et al., 2008). Apical to basal migration takes 7.8 hours on an average in EGFP control cells (n=9 / 4 explants) (Fig. 3.3A, C). However, within 10 hours of imaging, none of the Noggin electroporated cells had reached the basal surface (Fig. 3.3D). Despite the fact that we couldn't get images of the entire apical to basal traverse of the Noggin electroporated cells, they did reach the basal surface at a later time points (Fig. 3.5). Thus, it is clear that it takes a longer time for Noggin electroporated cells to reach the basal surface than controls.

3.2.4 BMP blockade abolished differential migration of daughter cells post cell division

We also observed that, depending on the mitotic spindle orientation, the two daughter cells behave differently. In the EGFP electroporated cells, the two daughter cells migrate basally at similar velocities when the spindle orientation is perpendicular to the apical surface (Fig. 3.3C, cell traces 1-3, 5, Fig. 3.4A). Interestingly, when the spindle orientation is parallel to the apical surface, the more basally located daughter cell moves faster than the other (Fig. 3.3C, cell trace 4, 6-9, Fig. 3.4B). The apically situated daughter cells behave in a similar manner as the cells where the spindle is oriented perpendicularly. In contrast, we did not observe the faster cell migration in Noggin electroporated cells that underwent cell division in a perpendicular cleavage plane to the apical surface (Fig. 3.3D). Although, spindle orientation is not a predictor of cell fate (Alexandre et al., 2010; Wilcock et al., 2007), it is possible that it could have as

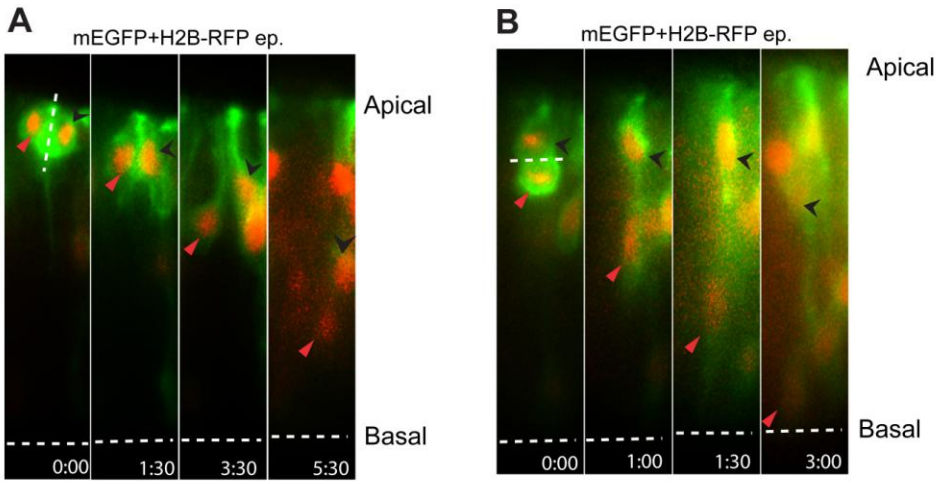

Figure 3.4. Daughter cells behave differently depending on the division plane.
(A) A metaphase cell with a division plane perpendicular to the apical surface shows that the two daughter cells migrate basally. (B) A cell that undergoes mitosis in a plane parallel to the apical surface has one of the daughter cells which the one is more basally located migrates 3 times faster than the other. Note that two cells in A (perpendicular plane of division) and the more apically divided cell show similar behaviors (takes abour 9hours to reach the basal most surface. See Fig. 3.3C, n=5), however, basally located cells with parallel division migrate basally faster (red arrowhead in B, n=5). See Fig. 3.3C blue graph (#4).

yet an unknown role and would be a open for future investigation.

3.2.5 BMP blockade increases the duration of basal pause of cell nuclei

Next, we compared the time spent by the cell nuclei at the basal location where cells are mainly in S-phase between EGFP and Noggin electroporated cells (Sauer, 1935). Schoenwolf and colleagues have suggested that cells at the MHP stay longer at the basal location as compared to the cells at lateral region. It is proposed that this longer time spent at the basal location leads to the basal expansion which eventually culminates into a hinge point (Schoenwolf and Smith, 2000b). As I have shown in Chapter 2, BMP signaling is low at the MHP and this low expression can be mimicked by Noggin overexpression. Therefore, we expected to see more cells at the basal position in Noggin overexpressing cells at any given time. Indeed, our time-lapse imaging experiments show that BMP inhibition increases the time spent by the cells at the basal location by about three fold over EGFP electroporated cells (EGFP control : 4.6hours, n=5 / 3 explants versus Noggin : 12.06 hours, n=8 / 4 explants; $p< 1.81x10^{-4}$) (Fig. 3.5). A 30min pulse labeling with BrdU showed that more cells are BrdU positive in Noggin expressed brains (46% of cells are BrdU positive) as compared to the control (31.4%, $p<4.1x10^{-4}$) (Fig. 3.5D-E). We also observed that the apicobasal extent of BrdU positive cells is larger than the controls (Fig. 3.5D-E, compare BrdU channel). This might suggest that BMP blockade accelerates basal to apical migration. However, Noggin electroporation thickens the neuroepithelium

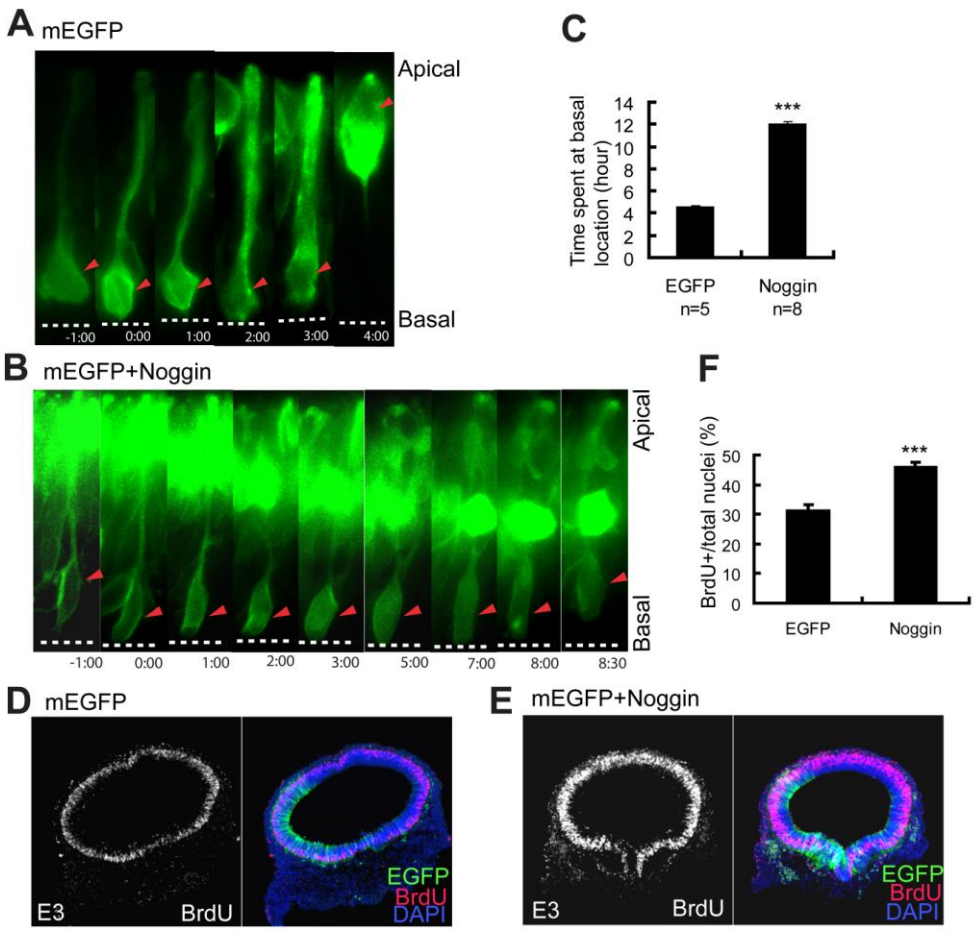

Figure 3.5. BMP blockade increases the duration of S-phase.
(A, B) Single mEGFP (arrowhead in A) or mEGFP+Noggin (arrowhead in B) electroporated cell was imaged at various time intervals as indicated. (C) Cell nuclei of Noggin electroporated cells stay longer at basal locations as compared to the controls (A, B and C). The length of S-phase was measured when cell nucleus reached the most basal position till it starts to move apically. (D, E) 30min-BrdU labelling reveals that there are more BrdU positive cells in the Noggin electroporated embryos (E) as compared to the control (D).

(Fig. 2.3A, D; 2.5A,B) and the apicobasal extent of BrdU staining was proportional to the increase of neuroepithelium thickness (data not shown). In summary, Noggin electroporated cells showed delayed apical to basal movement and longer basal pause of cell nuclei. We propose that, at any given time, cell nuclei stay longer at basal locations following BMP blockade as compared to the controls.

3.2.6 BMP blockade does not affect basal to apical migration (S-G2-M transition)

Finally, we analyzed basal to apical nuclear migration (S-G2-M transition) between EGFP and Noggin electroporated cell nuclei. We found that there is no difference in time required for basal to apical migration between EGFP and Noggin electroporated cells during basal to apical migration (EGFP electroporated cells: 58mins, n=10 / 3 explants; Noggin electroporated cells : 71mins, n=5 / 3 explants; $p<0.24$) (Fig. 3.5). Quantitative data shows slightly longer time spent in Noggin electroporated cells. However, we couldn't notice the statistical difference (Fig. 3.5C). Presumably, BMP blockade does not affect dynein mediated basal to apical nuclear migration (Schenk et al., 2009). Interestingly, in the Noggin electroporated cells, apical constriction is apparent (Fig. 3.5B, t=1:00) which further confirms that BMP blockade induces apical constriction (Fig. 2.4).

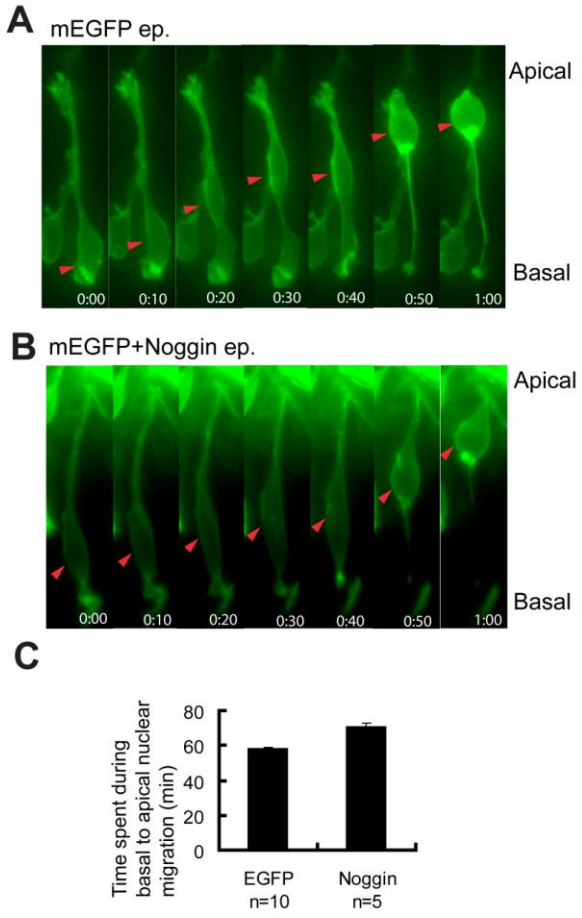

Figure 3.6. BMP blockade does not affect basal to apical nuclear migration (S-G2-M transition).

(A, B) Single mEGFP (arrowhead in A) or mEGFP+Noggin (arrowhead in B) electroporated cells were imaged at 10min interval. (C) Mesurements of time spent during nuclei migation from the basal to apical show no significant difference between control and Noggin electroporated cells.

A

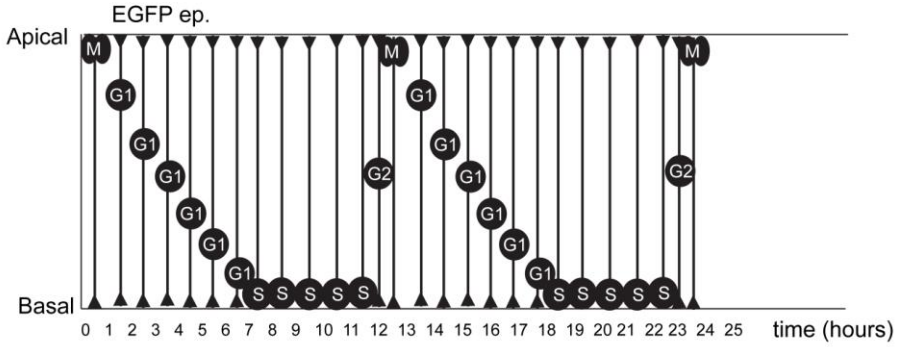

M phase : 0.75 hours
M-G1-S transition : 7.8 hours
S phase : 4.6 hours
S-G2-M transition : 0.97 hours
total cell cycle length : 14.12 hours

B

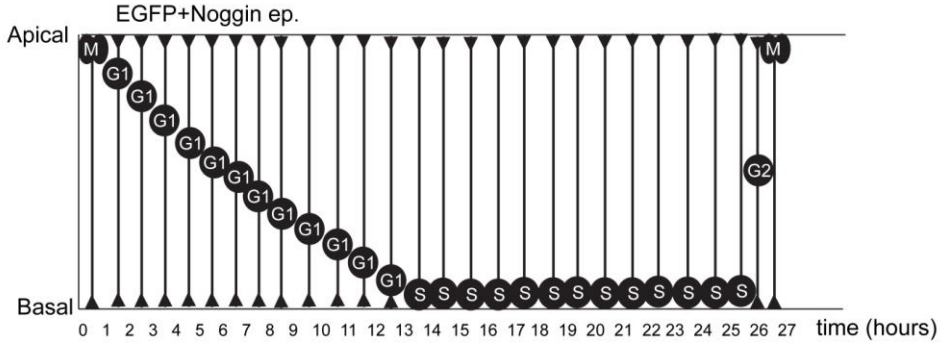

M phase : 0.75 hours
M-G1-S transition : >10.0 hours
S phase : 12.06 hours
S-G2-M transition : 1.18 hours
total cell cycle length : >23.99 hours

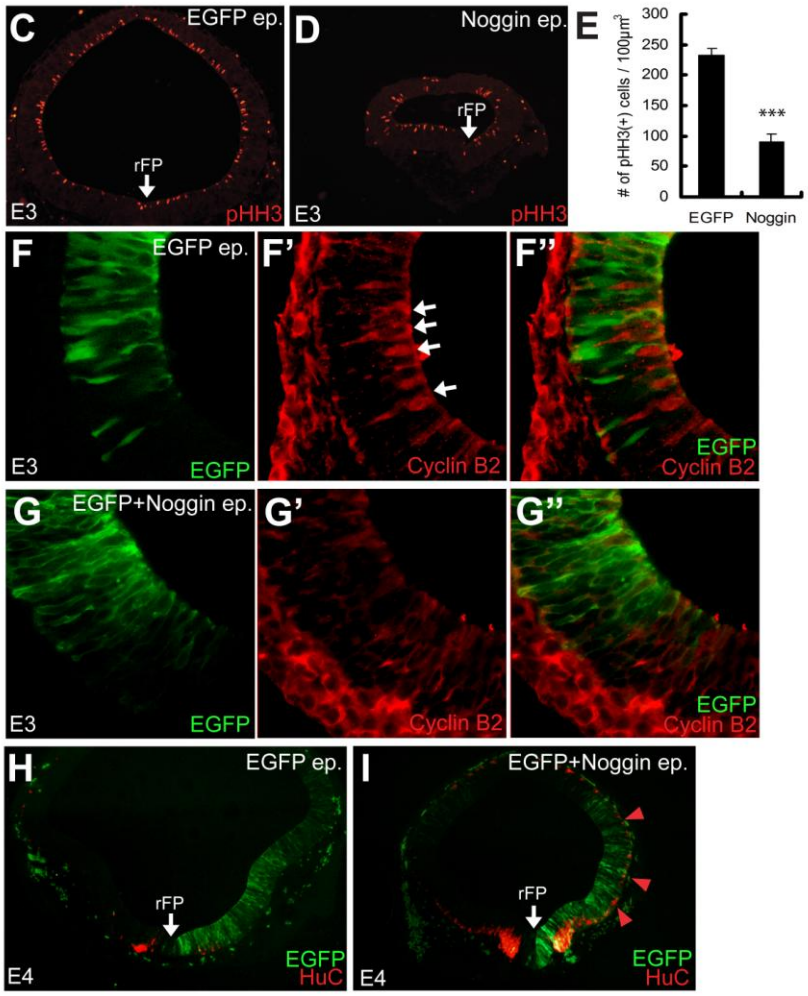

Figure 3.7. BMP blockade slows down cell proliferation by increasing the length of G1-S and S phase.

(A) Figure summarizing one cell cycle in EGFP cells (14.12hrs) and (B) in Noggin electroporated 23.99 hours. Note that this time is an underestimate for Noggin electroporated cells since we couldn't track apical to basal movement entirely. (C-E) Numbers of mitotic cells (pHH3+) are fewer in Noggin electroporated brains (D, E) than the controls (C, E). (F-G'') Reduced Cyclin B2 immunostaining in the Noggin electroporated cells (G-G'') as compared to the control cells (F-F'', arrows). (H-I) Prematurely differentiated cells (HuC+) are more in Noggin electroporated brains (I) as compared to the control (H). rFP : rostral floor plate.

3.2.7 BMP blockade increases the duration of the cell cycle

Fig. 3.7A and B summarize the data described above. We calculated the entire cell cycle length by pooling the average time duration of individual phases of cell cycle progression. The total cell cycle length is increased in response to the BMP blockade mainly due to the elongation of the time spent during apical to basal migration and the basal pause of nuclei (Fig. 3.3; 3.5). However, the time spent by cell nuclei at the apical surface and in basal to apical migration is not affected by BMP blockade (Fig. 3.2; 3.6). These data suggest that BMP blockade increases overall cell division time by increasing the G1-S and S phases. This could result the reduction of the number of mitotic cells. Indeed, in Noggin electroporated brains, pHH3 positive cells are 66% fewer than controls (Fig. 3.7C-E). We also found that the protein level of Cyclin B2, a G2-M transition marker was significantly reduced in Noggin electroporated cells, suggesting that cell cycle progression to M phase is inhibited by BMP blockade (Fig. 3.7F-G”). As a result of slower cell division and fewer mitotic cells, the size of the embryos is smaller and the total number of midbrain cells reduced (data not shown). Additionally, we found that cells prematurely undergo differentiation in Noggin electroporated embryos (Fig. 3.7F-G). Presumably, BMP blockade affects progenitor vs. neuron fate determination via the regulation of cell cycle (See Discussion).

3.2.8 Basal nuclear migration is associated with ectopic hinge formation

Frequently, we could recapitulate the formation of ectopic hinge point following Noggin electroporation, in lateral midbrain of tissue explants where a hinge point is not normally formed (Fig. 3.8). We analyzed cell behaviors at the ectopic hinge points and compared them with control EGFP electroporated cells. EGFP electroporated cells show normal interkinetic nuclear migration and at any given time, cell nuclei are distributed all along the apicobasal axis (Fig. 3.8A-B). Also, no ectopic hinge points were produced in any of our EGFP electroporations (Fig. 3.8A).

Interestingly, we found that basal nuclear migration is apparent where an ectopic hinge point is produced in Noggin electroporated explants (Fig. 3.9A-B). Especially, between 0 and 4 hours, all cell nuclei in these cases of Noggin electroporated cells were largely basally localized (Fig. 3.9B). The hinging events occurred during this time interval (0-4hours) (Fig. 3.9A-B).

Taken together the data in Chapter 2 and 3, suggest that it is highly likely that BMP blockade induces hinge point formation by altering cell cycle progression, increasing the duration of G1-S and/or S phase and maintaining the cell nuclei at the basal position.

3.3 Discussion

3.3.1 Disruption of interkinetic nuclear migration due to apicobasal polarity defects

We observed that Noggin electroporated cells show abnormal

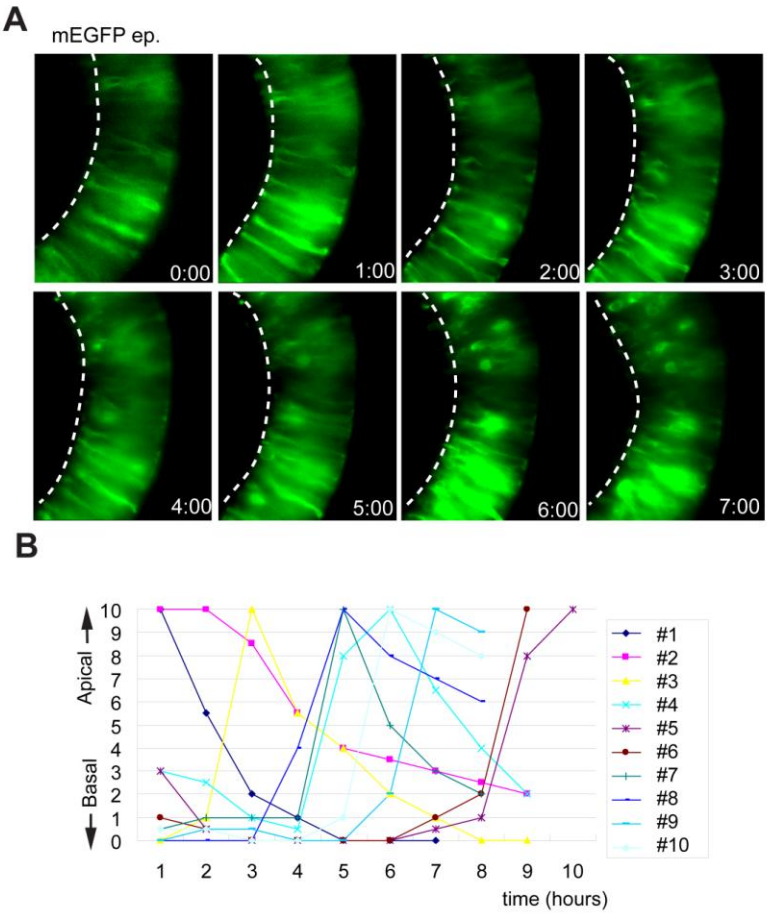

Figure. 3.8. Cell nuclei are evenly distributed along apicobasal axis in the EGFP electroporated lateral midbrain.

(A) EGFP electroporated cells undergo interkinetic nuclear migration that spans the entire apicobasal axis. Note that no ectopic invagination occurs. Images were taken with 1 hour intervals. Dashed lines indicate apical surface. (B) Tracking cell nuclei reveals that EGFP electroporated cell nuclei are distributed along apicobasal axis. 5 EGFP electroporated embryos were analyzed.

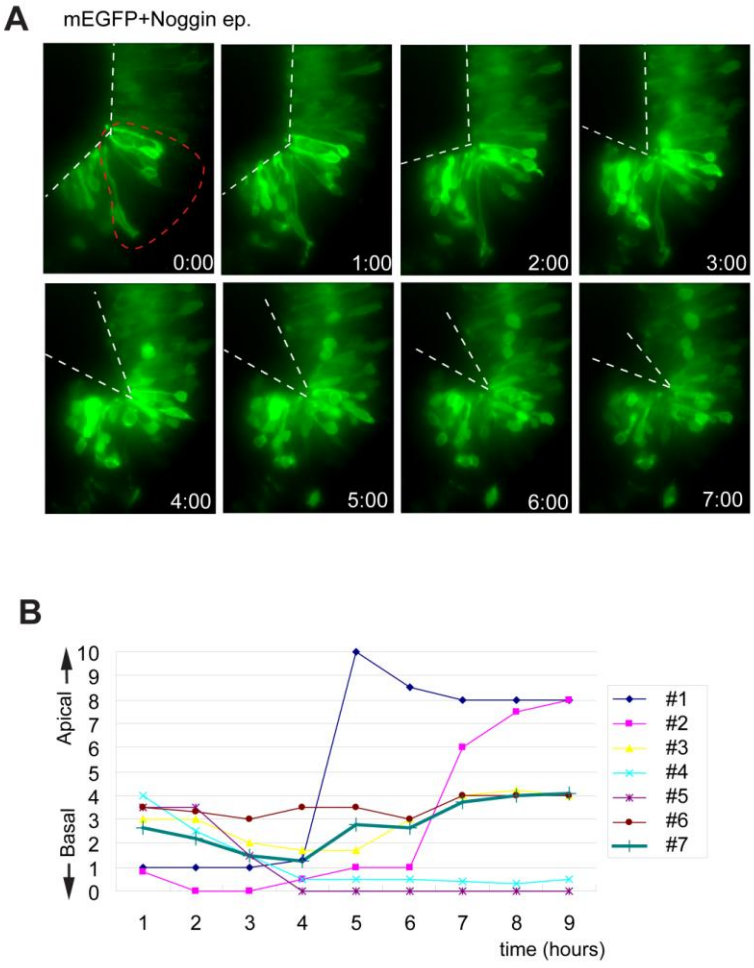

Figure. 3.9. Basal nuclear migration is associated with an ectopic hinge point in the lateral midbrain in response to BMP blockade.
(A) Analysis of cell nuclei movement show basal nuclear migration is evident where ectopic invagination occurs in lateral midbrain region of an Noggin electroporated explant. Images were taken with at 1 hour intervals. White dashed lines indicate apical surface.
(B) Cell nuclei are basally positioned when ectopic invagination is formed (0 - 4 hours). Cells in the ectopic hinge point were analyzed (red dashed line).

interkinetic nuclear migration with slower apical to basal migration than normal. Moreover 20% of Noggin electroporated cells we observed in the process of moving back to the apical surface had never reached the basal surface (Fig. 3.3). As discussed in Chapter 2, BMP blockade disrupts normal apicobasal polarity by misregulating the endocytosis of apical proteins (Fig. 2.11). In many tissues and species, disruption of apicobasal polarity is known to cause abnormal interkinetic nuclear migration (Costa et al., 2008; Klezovitch et al., 2004). We assayed for disrupted interkinetic nuclear migration by performing pHH3 immunostaining, a marker for mitotic cells. Under normal circumstances, expression of pHH3 should be confined to the apical surface. However, in the Noggin electroporated embryos, we observed subapical pHH3 positive cells (data not shown, Fig. 3.3D). Despite a lack of understanding of the precise mechanisms by which apicobasal polarity controls interkinetic nuclear migration, studies suggest that apicobasal polarity is required for interkinetic nulear migration (Costa et al., 2008; Klezovitch et al., 2004). Thus, it is possible that abnormal interkinetic nuclear migration observed in Noggin electroporated cells was due to the disruption of apicobasal polarity pathway. On the other hand, several other biological processes are also known to be associated with interkinetic nuclear migration. For example, Kinesin or Dynein motor proteins regulate nuclear migration. Hence, it is possible that BMP signaling regulates interkinetic nuclear migration by controlling mictotubule-based motor proteins (Morris, 2003; Wilhelmsen et al., 2006). Another possibility is that BMPs might

regulate interkinetic nuclear migration via Notch signaling pathway. Notch signaling is predominantly activated on the apical side of retinal cells in zebrafish and by regulating a motor protein Dynactin-1, controls INM (Del Bene et al., 2008). It is well documented that BMP signaling could regulate Notch signaling (Liu and Niswander, 2005) and we also observed that BMP blockade increases Notch1 and Notch ligand Serrate in the midbrain (data not shown).

3.3.2 Basal nuclear migration at the MHP

The cells at the MHP have longer cell cycle time as compared to the lateral non-MHP cells and specifically cell nuclei stay longer at basal locations where the majority of cells are in the S-phase (Smith and Schoenwolf, 1987; Smith and Schoenwolf, 1997). However, these studies were based on thymidine incorporation and cell cycle length determination by mathematical calculations (Wilcock et al., 2007). Our data further confirm that cell cycle length is increased in areas where BMP signaling is low with a specific increase in time required for apical to basal traverse and basal stay. These cells are mainly in the G1-S phase. This suggests that the MHP cells normally have low BMP signaling relative to the lateral cells and have longer cell cycle time by staying at the basal position longer duration. Hence, in general, cell nuclei experiencing low BMP signaling (such as at MHP) tend to stay longer at the basal location at any given time than do cells with high BMP signaling (such as non-MHP). We do not understand how many cells need to be basally migrated to induce a

hinge point. However, we assume that accumulation of such behaviors needs to reach a threshold in order to induce tissue shape changes and form the hinge point (Fig. 3.8).

3.3.3 Apical constriction and asymmetric cell division

We have shown that BMP blockade increased premature cell differentiation (Fig. 3.7F-G) and induced apical constriction (Fig. 2.4 and Fig. 3.6). In the cortex, asymmetric distribution of apical determinants dictates the binary decisions of whether a cell will become a neuron or a proliferating progenitor (Alexandre et al., 2010). Thus, it is possible that reduced apical surface size due to apical constriction forces cells toward asymmetric division which can potentially result in two daughter cells having an unequal share of proteins which are thought to be the apical determinants during mitosis (eg., PAR3, PAR6, aPKC). One of the consequences of increased asymmetric cell division would be an increase in prematurely differentiated neurons (Tabler et al., 2010). This could explain the decrease in the number of progenitor population (pHH3+ cells) and an increase in the prematurely differentiated cells (HuC+ cells) in response to BMP blockade (Fig. 3.7).

CHAPTER 4 : BONE MORPHOGENETIC PROTEINS (BMPs) REGULATE DORSAL CELL FATE SPECIFICATION IN THE VERTEBRATE MIDBRAIN

4.1 Introduction

The dorsal midbrain gives rise to the tectum or superior colliculus, a cortex like structure involved in multimodal integration (Agarwala and Ragsdale, 2002; Vachon-Presseau and Henry, 2008). Multiple BMP pathway members are expressed in and along the dorsal midline (roof plate) in the midbrain and BMP/TGFβ knockouts result in frequently exencephaly of this region (McMahon, 1997, Castriano Mishina, 2009). Early in development, graded BMP signaling either alone or in combination with other signals establishes the epidermal ectoderm, neural crest and neural plate (Liu and Niswander, 2005). In the spinal cord, multiple dorsal sources of BMP family members are thought to set up a graded BMP signal resulting in the specification of the dorsal midline signaling center (the roof plate) and 6 classes of dorsal interneurons (dI1-6) with higher levels of BMPs pushing naïve dorsal progenitors to acquire more dorsal cell fates (Liu and Niswander, 2005). In support of this idea, mouse mutants where both BMPR1A and R1B receptors are knocked out, undergo a severe loss of dI-1 and dI-2 interneurons and a corresponding increase in dI 3 and 4 subtypes (Wine-Lee et al., 2004). However, overexpression of a constitutively active activin receptor in the chick produces a selective induction of dI3 internuerons with no effect on other dorsal interneuron fates (Timmer et al., 2005). The

ablation of the roof plate (RP) in the mouse results in the selective loss of the dorsal most (dI1) interneurons, with no effects on the other cell types (Lee et al., 2000). These results suggest targeted effects on dorsal cell fate specification by TGFβ pathway members and have been explained by the redundancy of BMP expression and function on one hand and the functional specificity of some dorsally expressed family members on the other.

However, it is not fully explored whether BMPs regulate dorsal cell fate specification and whether the ventral BMP source is relevant in the midbrain neural tube. Also, a controversy exists that BMP signaling is not involved in dorsal midbrain cell fate specification (Bobak et al., 2009). Here we studied the role of BMP signaling in the developing midbrain. Study of BMP or TGFβ deletion mutants is frequently not informative since the frequent exencephaly makes analysis problematic. This prevents the proper analysis of dorsal cell fate specification since the roof plate is a major signaling source of BMPs. Electroporation of various concentrations of BMP expression constructs at a stage when the chick neural tube has closed provides us with the advantage of studying dorsal cell fate specification without the association of morphological defects.

4.2 RESULTS

4.2.1 Expression of BMP signaling components in the midbrain

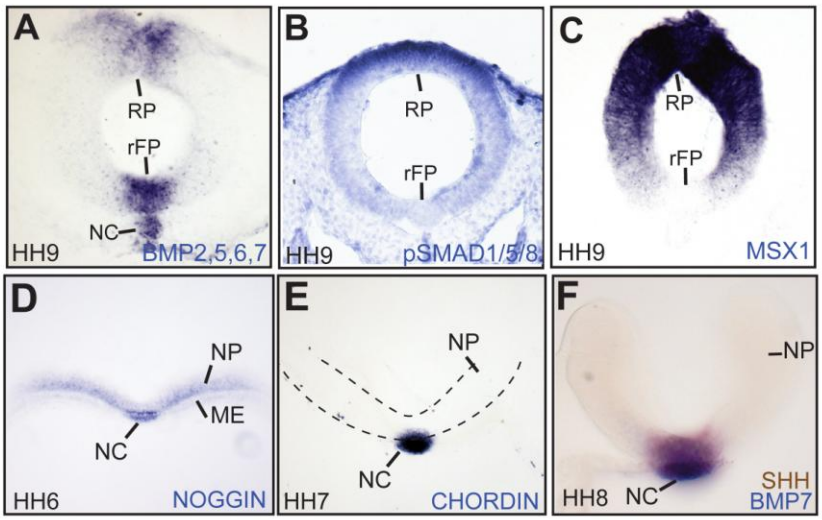

Figure 4.1. Expression of BMP signaling in the developing midbrain
Midbrain cross-sections at developmental stages shown on the bottom left of this and all subsequent micrographs. (A) Combined BMP2, 5, 6, 7 expression in the midbrain rostral floor plate (rFP) and notochord (NC). (B) Dorsoventral pSMAD1/5/8 gradient in the midbrain. Note that high BMP signaling at the roof plate and lower at the rFP. (C) Dorsoventral (DV) MSX1 gradient in the midbrain. (D-E) BMP antagonists are expressed at the notochord. (F) BMP7 expression at the floor plate and notochord where coincide with SHH.
Abbriviation : HH, Hamburger-Hamilton developmental stages; NC, notochord; rFP, rostral floor plate; RP, roof plate.

A complex expression pattern of BMPs, their antagonists (Noggin, Chordin), effectors (phosphorylated-Smad 1/5/8) and transcriptional targets (*MSX1*) was seen in the chick midbrain and notochord during development (Fig. 4.1). Several BMPs (BMP 2,5,6,7) are expressed at the dorsal and ventral midline (Fig. 4.1A). Immunostaining with phosphorylated-SMAD 1/5/8 revealed that there is a BMP gradient along the dorsoventral (DV) axis, high at the dorsal and low at the ventral midbrain as previously known in spinal cord (Liu and Niswander, 2005) (Fig. 4.1B). Also, the expression of MSX1 which is a transcriptional target of BMP activation shows a DV gradient (Furuta et al., 1997) (Fig. 4.1C). However, BMP antagonists, Noggin and Chordin are expressed in the notochord and ventral midbrain (Fig. 4.1D-E). Interestingly, the expression of BMP signaling components occurred in the ventral midline/floor plate of the midbrain and the notochord coinciding with the expression of Sonic Hedgehog (*SHH*; Fig. 4.1F). Although multiple BMPs are also expressed in the ventral midbrain, low levels of canonical BMP signaling at the ventral midbrain could be a consequence of the strong expression of Noggin and Chordin.

4.2.2 BMPs are not involved in ventral cell fate specification in the midbrain

As described in chapter 2 and Fig. 4.1B, the overall BMP signaling is lower at the ventral than dorsal midbrain, despite the fact that several BMPs are expressed there. This led us to investigate whether BMP signaling is involved in

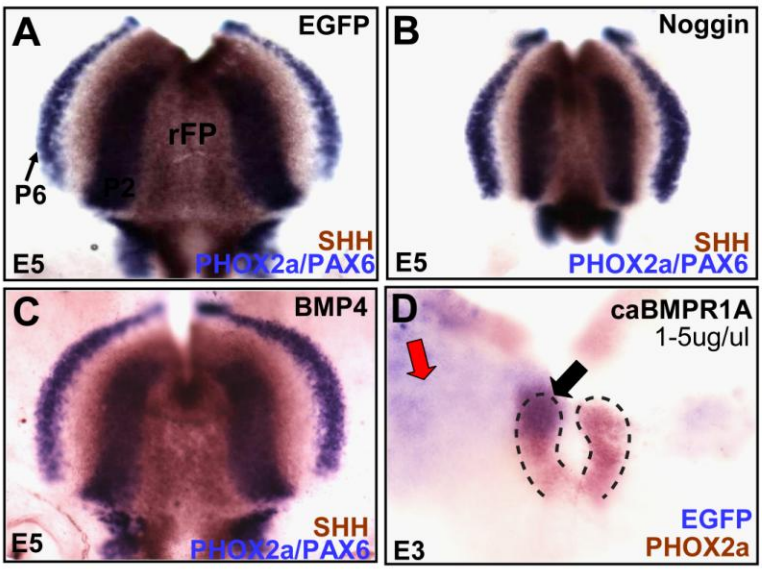

Figure 4.2. BMPs are not involved in ventral cell fate specification in the midbrain. Control (A) and Noggin (B) or BMP4 electroporated brains (C) demonstrating that ventral cell fates [assayed by SHH (brown) and PHOX2A and PAX6 (blue) in the ventral midbrain] are not perturbed by BMP loss of function or gain of function manipulation, although tissue size and shape are altered in Noggin electroporated brains. (D) Ventral electroporation of various concentration of constitutively active BMPR1A did not expand ventral cell fate (PHOX2A, black arrow) or ectopically induce (red arrow). rFP: rostral floor plate ; P6: PAX6

ventral midbrain cell fate specification. We compared the expression pattern of ventral cell fate markers SHH, PHOX2a and PAX6 following ventral BMP signal manipulations. We attenuated BMP signaling with Noggin and did not alter ventral cell fates (Fig. 4.2B) as compared to the EGFP controls (Fig 4.2A). However, midbrain shape was altered (see Chapter 2). BMP gain of function manipulations with BMP4 or a constitutively active form of BMPR1A (caBMPR1A) also did not show any alteration of ventral cell fates (Fig. 4.2C-D). We electroporated various concentration (1-5ug/ul) of caBMPR1A together with EGFP at the ventral midbrain to exclude the possibility that our manipulations were not strong enough to induce changes in ventral cell fates. Even at a high concentration of caBMPR1A (5ug/ul), ventral cell fates were not affected (Fig 4.2D). We conclude that BMP signaling is not involved in ventral cell fate specification in the developing chick midbrain.

4.2.3 BMP signaling is necessary for dorsal cell fate specification in the midbrain

As we described earlier, a DV gradient of BMP signal occurs in the midbrain. We asked whether BMPs are involved in dorsal cell fate specification in the midbrain (Fig. 4.1B-C). Interestingly, dorsal cell fates (PAX7, WNT1, ZIC1) were significantly reduced in the Noggin electroporated embryos as compared to the controls (Fig. 4.3A-D). To determine whether BMPs affected intermediate cell fates in the midbrain, we examined the DV extent of GLI3

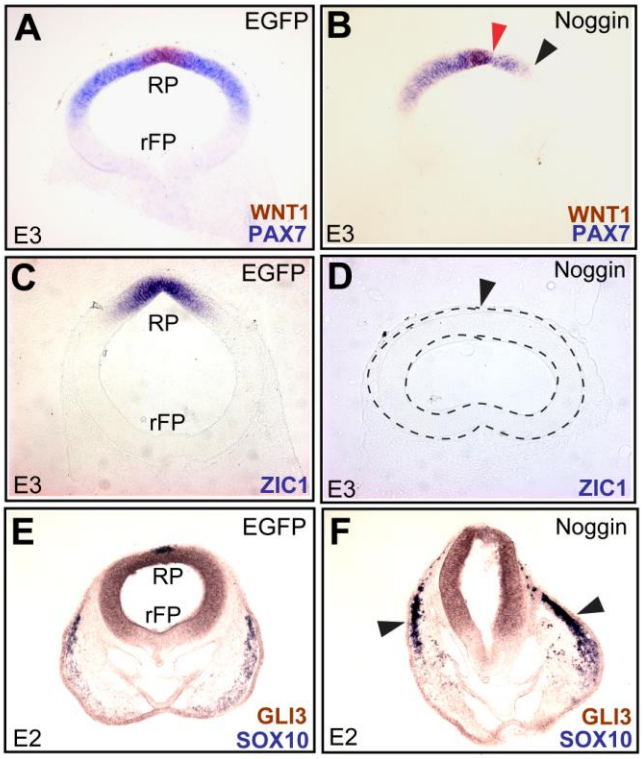

Figure 4.3. BMP signaling is necessary for the dorsal cell fate specification in the midbrain. (A-D) Reduced dorsal cell fates in Noggin electroporated sides (right half) (red arrowhead for WNT1 and black for PAX7 in B and arrowhead in E for ZIC1). A and C are controls.
(E-F) Increased neural crest cell fate (SOX10, blue) in Noggin electroporated embryos (F) as compared to controls (E). No changes noted in GLI3 (brown) cell fate (E, F).
RP: roof plate; rFP : rostral floor plate.

expression since it is more ventral to the expression of PAX7 cell fate (data not shown). GLI3 fate was not affected in the same Noggin manipulation (Fig. 4.3E-F, brown). This suggests that Noggin electroporation used for PAX7, WNT1 or ZIC1 might not be enough to affect GLI3 fate or it might be not regulated by BMP signaling. However, SOX10 positive neural crest fate was significantly increased by Noggin electroporation (Fig. 4.3E-F, blue). Thus, these data suggest that BMP signaling is necessary for the dorsal cell fate specification in a dose-dependent manner and effects of BMP manipulations are not non-specific.

4.2.4 BMP signaling is sufficient for dorsal cell fate specification in the midbrain but limited

BMP gain of function manipulations with caBMPR1A expanded WNT1, PAX7 and ZIC1 dorsal cell fates on the electroporated side (Fig. 4.4A-B). These data suggest that BMP signaling is sufficient for dorsal cell fate specification.

We asked caBMPR1A electroporation could induce dorsal cell fates at the ventral midbrain. We overexpressed caBMPR1A on the right hand side of the midbrain spanning dorsal and ventral midbrain as marked by EGFP probe (Fig. 4.4D, blue). We observed that WNT1 is ectopically induced only in the dorsal midbrain (Fig. 4.4D, brown, arrow). This suggests that there is a regional competence for BMP-mediated induction of dorsal cell fates. However, unlike WNT1, we found that PAX7 cell fate could be expanded into the ventral

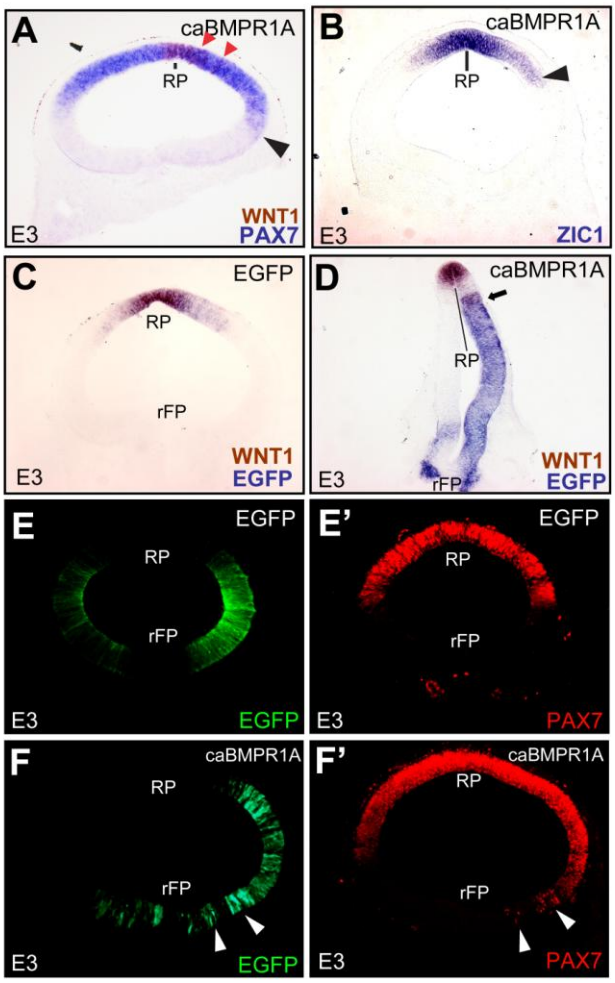

Figure 4.4 BMP signaling is sufficient for the dorsal cell fates in the midbrain but limited. (A-B) Expansion of dorsal cell fates in caBMPR1A electroporated sides (red arrowheads for WNT1 and a black for PAX7 in A and arrowhead in B for ZIC1). (C) EGFP electroporation (blue) does not induce WNT1 dorsal cell fate. (D) caBMPR1A+EGFP electroporation (blue) ectopically induced WNT1 dorsal cell fate (arrow) only in dorsal midbrain. (E-F') PAX7 immunostaining reveals that caBMPR1A electroporation can ectopically induce PAX7 at the ventral midbrain (F-F'; Arrowheads). Controls (E-E'). RP : roof plate; rFP : rostral floor plate.

midbrain following caBMPR1A overexpression (Fig. 4.4E-F'). Presumably, the regional competence for the PAX7 is wider than that for WNT1 as we could expect from their normal gene expression pattern (Fig. 4.3A). However, we observed that ectopic PAX7 positive cells in the ventral midbrain overlap with high levels of caBMPR1A electroporated cells (Fig. 4.4F-F', arrowheads) suggesting another possibility that higher concentration of BMP signaling might be required for the induction of dorsal cell fates in the ventral midbrain. Thus, further experiments with different concentrations of caBMPR1A in the ventral midbrain would be required to rule of this possibility.

4.2.5 Both ventral and dorsal BMP sources are involved in dorsal cell fate specification

Since BMP signaling is present in the ventral midbrain (Fig. 4.1A), we asked whether the ventral BMP source could affect dorsal cell fate specification. Unlike mouse, WNT1 is not expressed in the ventral midbrain in the avian embryo ((Fogel et al., 2008), Fig. 4.3A). Thus, we could still use WNT1 as a dorsal cell fate marker in the experiments with ventral BMP manipulations. Control EGFP electroporation had no effect on dorsal cell fates (Fig. 4.5A, C). To our surprise, ventral Noggin+EGFP electroporation resulted in a reduction of WNT1 or PAX7 dorsal cell fates (Fig. 4.5B, D). This suggests that Noggin acts as a long-range signaling molecule and/or a ventral BMP source is involved in dorsal cell fate specification in the chick midbrain. However, due to Noggin

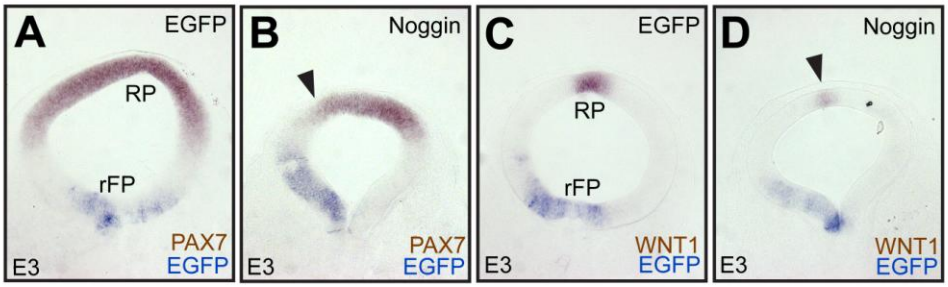

Figure 4.5 Both ventral and dorsal BMP source are involved in dorsal cell fate specification. (A-D) Dorsal cell fates (PAX7, WNT1) are reduced by ventrally electroporated Noggin (arrowheads in B and D) as compared to the controls (A, C).
rFP: rostral floor plate; RP: roof plate.

protein being a secreted molecule, dominant negative BMPR1 electroporation experiments would be required to secure the results.

4.2.6 BMP-mediated dorsal cell fate specification is Smad-dependent

In Chapter 2, we have shown that BMPs regulate epithelial polarity in a Smad-dependent manner. This observation led us to ask if BMPs regulate dorsal cell fates in a Smad-dependent manner. To test this, we selectively inhibited Smad-dependent BMP signaling by electroporating inhibitory Smad, Smad6. Smad6 is known to hinder the interaction between R-Smads and Co-Smads or inhibits phosphorylation of R-Smads (Hata et al., 1998; Imamura et al., 1997). Dorsal cell fate as monitored by WNT1 was reduced on the Smad6 overexpressing side (Fig. 4.6A-A'). Another dorsal cell fate marker PAX7, was also reduced where Smad6 was expressed (Fig. 4.6B-B'', arrow). Thus, we conclude that BMP-mediated dorsal cell fate specification is Smad-dependent. How Smad-dependent BMP signaling could regulate both cell fate specification and epithelial organization is a topic for further investigation (See Discussion).

4.3 DISCUSSION

4.3.1 BMP signaling works differently in the ventral vs. dorsal midbrain

It should be noted that pSMAD1/5/8 expression pattern is quite different along the apicobasal axis. In the ventral midbrain, stronger pSMAD1/5/8 signal is seen at the apical surface (Fig. 2.1C-H). However, in the dorsal midbrain,

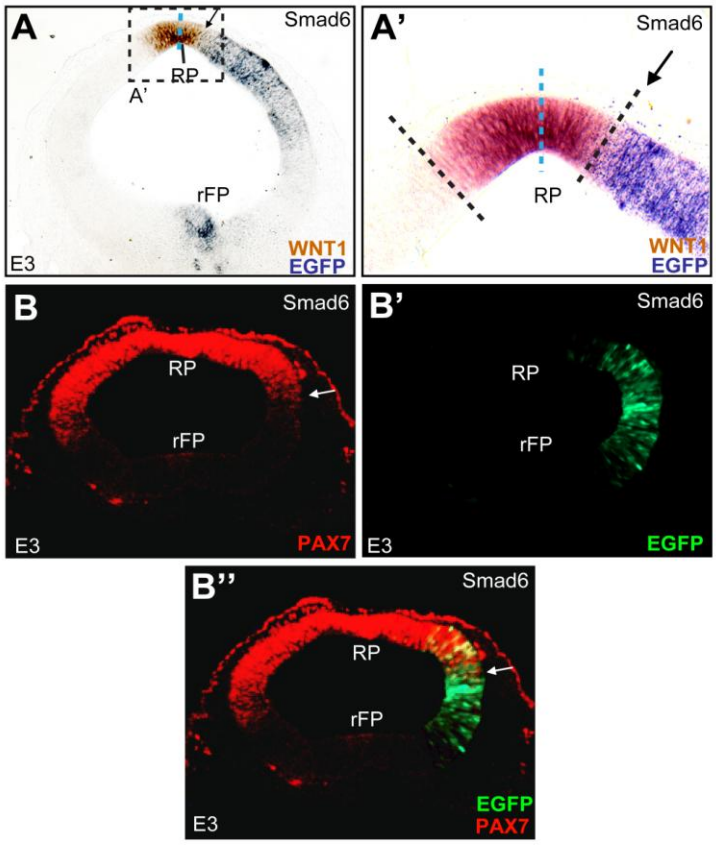

Figure 4.6. BMP-mediated dorsal cell fate specification is Smad-dependent.
(A-A') WNT1 dorsal cell fate is reduced in Smad6 (blue, arrows) electroporated side (arrow) as compared to the control side. Blue dotted line indicates dorsal midline. (B-B'') PAX7 immunostaining reveals that SMAD6 inhibits PAX7 fate (white arrow).
RP : roof plate; rFP : rostral floor plate.

pSMAD1/5/8 is high regardless of the apicobasal axis level (Fig. 4.1B). This might produce distinct readouts in the dorsal and ventral midbrain. In the ventral midbrain, as proposed in our model, BMP signaling is required for the maintenance of apicobasal junctional complex via interaction with PAR3 (Fig. 2.11). Thus, its main role in the ventral midbrain is to maintain epithelial organization of the midline. However, as mentioned earlier, in the dorsal midbrain, BMPs signaling is high even when cell nuclei are at basal location, suggesting BMP signaling has a distinct role in the dorsal midbrain. Its expression is seen in the nucleus as well as in the cytoplasm suggesting a role for transcriptional regulation.

4.3.2 BMP regulates dorsal cell fate specification in a Smad dependent manner

As we suggested in Chapter 2 and this chapter, BMP signaling regulates both epithelial organization and dorsal cell fate specification in a Smad dependent manner. In Chapter 2, protein-protein interactions between pSMAD5 and PAR3 data and Smad6 data suggested a possible involvement of Smads in the BMP-mediated regulation of apicobasal polarity pathway. However, it is not clear if this was transcription dependent. We can not rule out the possibility of involvement of transcriptional regulation in BMP-mediated regulation of apicobasal polarity pathway. However, even if it is dependent on Smad activity, it does not necessarily imply transcriptional regulation. As we discussed in

Chapter 2, Smads can interact with other members of signaling components. In this case, Smad dependent transcriptional regulation is not required.

It is well documented that BMP-mediated dorsal cell fate specification is transcriptionally regulated in the spinal cord, though we have no evidence whether it is the case in the midbrain (Liu and Niswander, 2005). Together with the ideas described above, we hypothesize that BMP signaling regulates both cell fate specification and epithelial polarity in a Smad-dependent manner. However, the former could be involved in Smad-dependent transcriptional regulation and latter could be Smad-dependent non-transcriptional manner. This needs further study.

4.3.3 A ventral BMP source might compensate for the changes of BMP signaling in the dorsal midbrain following BMP manipulation.

BMP manipulation experiments in the spinal cord often result in affects on only a certain type of interneuron fate (Lee et al., 2000; Timmer et al., 2005). This does not support a gradient model. One possible explaination of this observation is the cell delamination or epithelial to mesenchymal transition (EMT) at the dorsal midline in response to BMP blockade. Dorsal midbrain is the region where neural crest cells are born and this is also regulated by the BMP signaling pathway (Krispin et al., 2010; Raible, 2006). We observed that massive cell delamination occurs following BMP blockade. However, cell delamination does not affect PAX7 dorsal cell fate specification (data not

shown). Another possibility is that ventral BMP source can stabilize the effect of BMP manipulations in the dorsal region. Indeed, a ventral BMP source could affect dorsal cell fate specification (Fig. 4.5). Presumably, a ventral BMP source can compensate for the loss of BMP signaling from dorsal part of the brain following BMP manipulations. This could explain why other groups observed a loss of only certain types of dorsal cell fate, but not all fates following various BMP manipulations in the spinal cord. Alternatively, it is possible that there might be different mechanisms at play in neural tube patterning. For example, multiple BMPs are expressed in the midbrain including BMP7 (Fig. 4.1A). BMP7 could regulate TGFβ signaling more effectively than BMP (Heinecke et al., 2009). Also it has been shown that nodal related signaling is involved in DV patterning in the spinal cord (Liu and Niswander, 2005). This raises the possibility that an interplay between BMP and TGFβ signaling might play a role in the cell fate specification in the midbrain (Liem et al., 1997; Liu and Niswander, 2005).

CHAPTER 5. CONCLUSION

In this study, we have shown that low level, temporally dynamic BMP signaling occurs at the ventral midline hinge point (MHP). BMP attenuation is necessary and sufficient for MHP formation and neural tube closure by inducing apical constriction and basal nuclear migration. Also, these cell behaviors are regulated by the protein-protein interaction between BMP-target receptor Smads and the polarity protein PAR3. These interactions play a key role in maintaining epithelial polarity in the neural tube. Attenuated BMP signaling at the MHP prevents these interactions, resulting in perturbed polarity and the endocytosis of apical proteins, thereby leading to apical constriction and hinge point formation.

In addition, we uncovered that BMP-mediated cell behaviors are regulated in a cell-cycle dependent manner. BMP blockade perturbed apical to basal nuclear movement (M-G1-S transition) and elongated the duration of basal stay (S-phase) of nuclei of the midbrain neuroepithelial cells undergoing interkinetic nuclear migration. Longer duration of the S-phase makes more cell nuclei stay at the basal position at any given time in response to BMP attenuation. We also found that basal shifting of cell nuclei is associated with ectopic hinge point formation. Taken together, we conclude that BMP attenuation induces hinge point by inducing basal nuclear migration by altering cell cycle progression by increasing the duration of S phase which maintains the

cell nuclei at the basal position. Thus, the basal nuclear migration at the MHP might be due to low level of BMP signaling.

BMP signaling also regulates cell fate specification in the midbrain. We found that BMP signaling is necessary and sufficient for dorsal but not ventral cell fate specification. However, BMP-mediated induction of dorsal cell fates is limited in a context dependent manner. Also, BMPs regulate dorsal cell fate specification in a Smad-dependent manner in the chick midbrain.

To summarize, BMP signaling regulates epithelial organization in the ventral midline and cell fate specification in the dorsal midbrain.

APPENDICES

Appendix A: Materials and Methods

Chick embryos

Fertilized Leghorn eggs (Ideal Poultry, Texas) were incubated at 38˚C and the embryos staged according to Hamburger and Hamilton (Hamilton, 1951).

Expression vectors

In vivo gene expression was driven by the xenopus (pXex), human (pEFX) Elongation-Factor 1∞, pMes or pCS2 promoters (Agarwala et al., 2001; Johnson and Krieg, 1994; Swartz et al., 2001). Embryos were electroporated with EGFP (Agarwala et al., 2001), membrane targeted-EGFP (m-EGFP), Noggin, dominant negative BMP receptors 1A-IRES-EGFP (dnBMPR1A), constitutively active BMP receptor 1A-IRES-EGFP (ca-BMPR1A), EFX-LGL-GFP, pXex-Smad6 and pCS2-Rab5-mCherry.

In ovo electroporation

Unless mentioned, 0.02-5µg/µl DNA was electroporated into HH stages 7-11 embryos (“late” electroporations) according to previously established protocols (Agarwala et al., 2001). For “early” (HH 4-6) electroporations, the epiblast was irrigated with Ringers solution and a glass pipette filled with DNA and fast green

was inserted through a unilateral incision in the vitelline membrane. 0.3µl of DNA was picospritzed into the lumen formed by the neural groove below and the vitelline membrane above. Embryos were microelectroporated as for late electroporations, but with the negative electrode placed in a pool of Ringer's on the vitelline membrane above the presumptive midbrain and the positive electrode positioned below the embryo (Agarwala et al., 2001; Colas and Schoenwolf, 2001). Only 1/8 early electroporated embryos displayed morphological defects and were eliminated from analyses (see Table 1). Electroporated embryos were returned to the incubator for 3 hours-4 days prior to harvesting. No differences were noted between phenotypes produced by early and late electroporations.

In situ hybridization

Embryos were harvested between HH6-E5 and immersion-fixed in 4% paraformaldehyde. DIG or FL conjugated antisense riboprobes were prepared from chick cDNAs for *BMP2, BMP5, BMP6, BMP7, SHH, CHORDIN, EGFP, GLI3, NOGGIN, PHOX2A, PAX6, PAX7, SOX10, WNT1, ZIC1 and MSX1*. One or two color whole-mount in-situ hybridizations were conducted according to previously established protocols (Agarwala et al., 2001).

Immunohistochemistry

Embryos were fixed in 4% paraformaldehyde for 15 min-2 hours. 14µm

midbrains cross-sections were stained with one or more of the following antibodies: rabbit anti-pHH3 (Upstate; 1:500), rabbit anti-PAR3 (Upstate; 1:500), rabbit anti-phosphorylated (p)-SMAD 1/5/8 (Cell signal; 1:1000), mouse anti-N-Cadherin (DSHB; 1:500), mouse anti-ZO-1 (BD biosciences; 1:1000), mouse anti-EEA1 (BD biosciences; 1:50) and mouse anti-GFP (Molecular Probes; 1:500). Alexa-conjugated secondary antibodies were used for fluorescent detection using standard protocols (Afonso and Henrique, 2006). Alexa-conjugated phallotoxins (Molecular Probes) were used for the direct detection of F (filamentous)-actin. DAPI staining was used for visualizing nuclei.

Wholemount p-Smads 1/5/8 immunohistochemistry

Wholemount pSMAD 1/5/8 immunolabeling was conducted by adapting the wholemount in situ hybridization protocol described above, by substituting the probe hybridization step with a 2 day incubation in the primary antibody at 4˚C (Agarwala and Ragsdale, 2002).

Imaging

Immunofluorescent confocal images were obtained with a Zeiss Laser Scanning Microscope (LSM5 Pascal) or an Olympus IX51 spinning disc microscope and captured with AxioVision (Zeiss) or Slide Book Pro software. For the time-lapse experiments, 100ms of exposure time for both FITC and Cy3 channel were used. Imaging interval was 10mins and optimal optical thickness was

determined by the Slide Book 5. Multiple areas of the explants were imaged by using automated X-Y stage. Data analyses were conducted using Imaris software and Adobe Photoshop. For the normal fluorescent immunostaining, unless mentioned, confocal images are presented as single 0.5-0.8 µm thick optical sections.

Immunoprecipitation and western blot analysis

For Western blotting, whole cell lysates were prepared from HH9-11 wild-type midbrains or the electroporated regions of E3 midbrains. Midbrain tissue was lysed with RIPA buffer (50mM Tris, 150mM NaCl, 0.1% SDS, 0.5% Na-deoxycholate, 1% Triton X, 1mM PMSF) and subsequently loaded on a 12% SDS-PAGE**.** 100µg of protein from chick midbrains in HKET lysis buffer (25mM HEPES pH 7.4, 150mM sodium chloride, 1mM EDTA, 1% Triton X-100, 100mM DTT, protease inhibitor cocktail, 1mM sodium fluoride and 0.1 mM sodium orthovanadate) was incubated with either 10 µg/ml of normal rabbit IgG (Alpha Diagnostic Intl. Inc) or 20 µg/ml of anti-PAR3 (Millipore), anti SMAD1 or 5 (Cell Signaling Technology) or anti-pSMAD 1/5/8 (Cell Signaling Technology). Protein complexes were immunoprecipitated using 20µl of protein A/G agarose beads, separated by SDS-PAGE, immunoblotted with PAR3 or pSMAD 1/5/8 antibodies and detected by ECL chemiluminescence (Thermoscientific; IL). The molecular weight of the PAR3, SMAD1, SMAD5 and pSMAD 1/5/8 was ascertained using the *Gallus gallus* database.

Quantitative Analyses

All quantification in this study was conducted using ImageJ software on midbrains electroporated at HH7-11 and harvested at E1-E3. Unless mentioned, quantitative data was obtained from 2-3 14µm sections/per control or Noggin-electroporated brain at the rostrocaudal midpoint of the midbrain. Data was displayed as the mean ± s.e.m. Statistical significance evaluated using an unpaired Student's *t*-test.

Overlap between pSmad 1/5/8 and pHH3 expression: The overlap between mitotic (pHH3+) and p-Smad 1/5/8+ cells was computed in HH7 midbrain cross-sections immunostained for both markers. All pHH3+ cells, pSmad 1/5/8+ cells and cells expressing both markers in 2 sections/5 embryos were tabulated and the number of cells that were pHH3+/pSMAD 1/5/8+ or just pSMAD1/5/8+ were calculated as a percentage of the total number of p-SMAD 1/5/8+ cells. No pHH3+/p-SMAD-negative cells were found in the HH7 neural plate.

Apical Constriction: Apical constriction was measured in two ways. First, cross-sections obtained from embryos electroporated with mEGFP alone or mEGFP + Noggin, were stained with the apical marker PAR3. The apical width (aw) and the cell-width at the cell's widest point (ww) were measured according to established protocols in all cells whose entire outlines (mEGFP+) could be discerned in control (n=43 cells/35 sections/10 E3 embryos) and Noggin-electroporated cells (n= 87 cells/41 sections/12 E3 embryos (Lee et al., 2007). Differences in the aw:ww ratio between controls and Noggin-electroporated

embryos were compared using a *t* test.

Second, a direct measurement of apical constriction was made in mEGFP and Noggin+mEGFP electroporated flattened wholemounts stained with PAR3 at E3. Since the effects of Noggin and dnBMPR1 were non-autonomous, a sampling box subtending 50µm x 50µm was drawn in ventrolateral midbrain and the apical surface areas of all cells and only electroporated cells within the box were separately measured using ImageJ (Control: n=48cells/3brains; Noggin-electroporated brains: Noggin+ cells: n=161cells/4brains; All cells: n=435cells/3brains). The differences between control and Noggin-treated embryos were compared using a *t*-test.

Basal Nuclear Migration*:* Basal nuclear migration was determined by centering a sampling box subtending 70µm x70µm at an ectopic hinge point and drawing a line (perpendicular to the apical surface) from the apical surface to the apical tip of each DAPI+ cell in 2-sections/E3 midbrain in control and Noggin-electroporated embryos. The differences were evaluated using a *t*-test.

Apicobasal Length*:* The apicobasal span of individual midbrain progenitors was measured in E3 brains electroporated with m-EGFP alone or in conjunction with Noggin. A sampling box subtending 70µm on each side was drawn on each of 2 sections positioned in ventrolateral midbrain. Within the box, the apicobasal span of every electroporated cell whose outline could be fully visualized in control and Noggin-electroporated brains was measured. The apicobasal lengths of controls (n=20/5 brains) and Noggin-electroporated midbrain

progenitors with visible apical and basal processes (n=52/12 brains) were measured and compared using a *t*-test.

Numbers of Partially Polarized Cells in the Neural Plate. Embryos were electroporated with low level LGL-GFP (1µg/µl) between HH 4-6 and examined at HH7 in cross-sections immunostained for GFP and PAR3. This concentration did not induce HPs in early electroporations and did not alter cell polarity in HH7-11 electroporations. By contrast 3-5 µg/µl LGL-GFP induced ectopic hinge points in early and late electroporations. Only those brains (n=9) with a low frequency of electroporated cells were analyzed. Within these embryos only those cells (n=35) with clearly discernable outlines were selected for analyses. Cells that displayed apical LGL-GFP, but maintained contact with the apical and basal surfaces, were designated as partially polarized. Those cells that displayed full segregation between apical (PAR3+) and basolateral (LGL-GFP) compartments were designated as polarized.

The basal location of nuclei and apically condensed Phalloidin identified MHP cells (Colas and Schoenwolf, 2001). Cells located 50µm away from the MHP were designated as lateral cells. This region excluded the neural folds. The number of polarized and partially polarized cells was computed as a percentage of total number of electroporated cells analyzed at each location. It should be noted that the same brains were utilized for estimating cell polarity at the MHP and in lateral neural plate. Together with the inability of the low LGL-GFP concentration paradigm to induce ectopic HPs in early electroporations or

to alter polarity in late electroporations, we are confident that the MHP-lateral neural plate differences in cell polarity are genuine and do not represent a differential loss of cell polarity due to low-level LGL-GFP manipulations.

Count BrdU positive cells*:* All BrdU positive cells were counted in a randomly selected sampling box subtending 70µm x70µm at an EGFP or EGFP+Noggin electroporated area. Also, number of DAPI positive nuclei was counted at the same time. We calculated the proportion of BrdU positive cells among all cells (DAPI positive) in a given sampling box. 31.4% of cells were BrdU positive in EGFP control embryos (n=10 / 4 embryos) and 46% of cells in Noggin electroporated embryos (n=10 / 4 embryos). $p<4.1x10^{-4}$. The differences were evaluated using a *t*-test.

BIBLIOGRAPHY

Afonso, C. and Henrique, D. (2006). PAR3 acts as a molecular organizer to define the apical domain of chick neuroepithelial cells. *J Cell Sci* **119**, 4293-304.

Agarwala, S. and Ragsdale, C. W. (2002). A role for midbrain arcs in nucleogenesis. *Development* **129**, 5779-88.

Agarwala, S., Sanders, T. A. and Ragsdale, C. W. (2001). Sonic hedgehog control of size and shape in midbrain pattern formation. *Science* **291**, 2147-50.

Alexandre, P., Reugels, A. M., Barker, D., Blanc, E. and Clarke, J. D. (2010). Neurons derive from the more apical daughter in asymmetric divisions in the zebrafish neural tube. *Nat Neurosci* **13**, 673-9.

Andrew, D. J. and Ewald, A. J. (2010). Morphogenesis of epithelial tubes: Insights into tube formation, elongation, and elaboration. *Dev Biol* **341**, 34-55.

Arkell, R. and Beddington, R. S. (1997). BMP-7 influences pattern and growth of the developing hindbrain of mouse embryos. *Development* **124**, 1-12.

Attisano, L. and Wrana, J. L. (2002). Signal transduction by the TGF-beta superfamily. *Science* **296**, 1646-7.

Baye, L. M. and Link, B. A. (2007). Interkinetic nuclear migration and the selection of neurogenic cell divisions during vertebrate retinogenesis. *J Neurosci* **27**, 10143-52.

Baye, L. M. and Link, B. A. (2008). Nuclear migration during retinal development. *Brain Res* **1192**, 29-36.

Bayly, R. D., Ngo, M., Aglyamova, G. V. and Agarwala, S. (2007). Regulation of ventral midbrain patterning by Hedgehog signaling. *Development* **134**, 2115-24.

Betschinger, J., Mechtler, K. and Knoblich, J. A. (2003). The Par complex directs asymmetric cell division by phosphorylating the cytoskeletal protein Lgl. *Nature* **422**, 326-30.

Bilder, D. (2004). Epithelial polarity and proliferation control: links from the Drosophila neoplastic tumor suppressors. *Genes Dev* **18**, 1909-25.

Bilder, D. and Perrimon, N. (2000). Localization of apical epithelial determinants by the basolateral PDZ protein Scribble. *Nature* **403**, 676-80.

Bilder, D., Schober, M. and Perrimon, N. (2003). Integrated activity of PDZ protein complexes regulates epithelial polarity. *Nat Cell Biol* **5**, 53-8.

Bobak, N., Agoston, Z. and Schulte, D. (2009). Evidence against involvement of Bmp receptor 1b signaling in fate specification of the chick mesencephalic alar plate at HH16. *Neurosci Lett* **461**, 223-8.

Brouns, M. R., Matheson, S. F., Hu, K. Q., Delalle, I., Caviness, V. S., Silver, J., Bronson, R. T. and Settleman, J. (2000). The adhesion signaling molecule p190 RhoGAP is required for morphogenetic processes in neural development. *Development* **127**, 4891-903.

Bryant, D. M. and Mostov, K. E. (2008). From cells to organs: building polarized tissue. *Nat Rev Mol Cell Biol* **9**, 887-901.

Cappello, S., Attardo, A., Wu, X., Iwasato, T., Itohara, S., Wilsch-Brauninger,

M., Eilken, H. M., Rieger, M. A., Schroeder, T. T., Huttner, W. B. et al. (2006). The Rho-GTPase cdc42 regulates neural progenitor fate at the apical surface. *Nat Neurosci* **9**, 1099-107.

Carthew, R. W. (2005). Adhesion proteins and the control of cell shape. *Curr Opin Genet Dev* **15**, 358-63.

Chalmers, A. D., Pambos, M., Mason, J., Lang, S., Wylie, C. and Papalopulu, N. (2005). aPKC, Crumbs3 and Lgl2 control apicobasal polarity in early vertebrate development. *Development* **132**, 977-86.

Colas, J. F. and Schoenwolf, G. C. (2001). Towards a cellular and molecular understanding of neurulation. *Dev Dyn* **221**, 117-45.

Conery, A. R., Cao, Y., Thompson, E. A., Townsend, C. M., Jr., Ko, T. C. and Luo, K. (2004). Akt interacts directly with Smad3 to regulate the sensitivity to TGF-beta induced apoptosis. *Nat Cell Biol* **6**, 366-72.

Copp, A. J., Greene, N. D. and Murdoch, J. N. (2003). The genetic basis of mammalian neurulation. *Nat Rev Genet* **4**, 784-93.

Cordero, J. B., Larson, D. E., Craig, C. R., Hays, R. and Cagan, R. (2007). Dynamic decapentaplegic signaling regulates patterning and adhesion in the Drosophila pupal retina. *Development* **134**, 1861-71.

Costa, M. R., Wen, G., Lepier, A., Schroeder, T. and Gotz, M. (2008). Par-complex proteins promote proliferative progenitor divisions in the developing mouse cerebral cortex. *Development* **135**, 11-22.

Cui, X. S., Li, X. Y. and Kim, N. H. (2007). Cdc42 is implicated in polarity

during meiotic resumption and blastocyst formation in the mouse. *Mol Reprod Dev* **74**, 785-94.

Davidson, L. A. and Keller, R. E. (1999). Neural tube closure in Xenopus laevis involves medial migration, directed protrusive activity, cell intercalation and convergent extension. *Development* **126**, 4547-56.

Del Bene, F., Wehman, A. M., Link, B. A. and Baier, H. (2008). Regulation of neurogenesis by interkinetic nuclear migration through an apical-basal notch gradient. *Cell* **134**, 1055-65.

Derynck, R. and Zhang, Y. E. (2003). Smad-dependent and Smad-independent pathways in TGF-beta family signalling. *Nature* **425**, 577-84.

Dollar, G. L., Weber, U., Mlodzik, M. and Sokol, S. Y. (2005). Regulation of Lethal giant larvae by Dishevelled. *Nature* **437**, 1376-80.

Doudney, K. and Stanier, P. (2005). Epithelial cell polarity genes are required for neural tube closure. *Am J Med Genet C Semin Med Genet* **135C**, 42-7.

Eaton, B. A. and Davis, G. W. (2005). LIM Kinase1 controls synaptic stability downstream of the type II BMP receptor. *Neuron* **47**, 695-708.

Ewald, A. J., Brenot, A., Duong, M., Chan, B. S. and Werb, Z. (2008). Collective epithelial migration and cell rearrangements drive mammary branching morphogenesis. *Dev Cell* **14**, 570-81.

Feigin, M. E. and Muthuswamy, S. K. (2009). Polarity proteins regulate mammalian cell-cell junctions and cancer pathogenesis. *Curr Opin Cell Biol* **21**, 694-700.

Felder, B., Stegmann, K., Schultealbert, A., Geller, F., Strehl, E., Ermert, A. and Koch, M. C. (2002). Evaluation of BMP4 and its specific inhibitor NOG as candidates in human neural tube defects (NTDs). *Eur J Hum Genet* **10**, 753-6.

Fogel, J. L., Chiang, C., Huang, X. and Agarwala, S. (2008). Ventral specification and perturbed boundary formation in the mouse midbrain in the absence of Hedgehog signaling. *Dev Dyn* **237**, 1359-72.

Foletta, V. C., Lim, M. A., Soosairajah, J., Kelly, A. P., Stanley, E. G., Shannon, M., He, W., Das, S., Massague, J. and Bernard, O. (2003). Direct signaling by the BMP type II receptor via the cytoskeletal regulator LIMK1. *J Cell Biol* **162**, 1089-98.

Fraser, R. C. (1954). Studies on the hypoblast of the young chick embryo. *J. Exp. Zool* **126**, 349-399.

Furuta, Y., Piston, D. W. and Hogan, B. L. (1997). Bone morphogenetic proteins (BMPs) as regulators of dorsal forebrain development. *Development* **124**, 2203-12.

Gambello, M. J., Darling, D. L., Yingling, J., Tanaka, T., Gleeson, J. G. and Wynshaw-Boris, A. (2003). Multiple dose-dependent effects of Lis1 on cerebral cortical development. *J Neurosci* **23**, 1719-29.

Ganzler-Odenthal, S. I. and Redies, C. (1998). Blocking N-cadherin function disrupts the epithelial structure of differentiating neural tissue in the embryonic chicken brain. *J Neurosci* **18**, 5415-25.

Georgiou, M., Marinari, E., Burden, J. and Baum, B. (2008). Cdc42, Par6,

and aPKC regulate Arp2/3-mediated endocytosis to control local adherens junction stability. *Curr Biol* **18**, 1631-8.

Ghosh, S., Marquardt, T., Thaler, J. P., Carter, N., Andrews, S. E., Pfaff, S. L. and Hunter, T. (2008). Instructive role of aPKCzeta subcellular localization in the assembly of adherens junctions in neural progenitors. *Proc Natl Acad Sci U S A* **105**, 335-40.

Gibson, M. C. and Perrimon, N. (2003). Apicobasal polarization: epithelial form and function. *Curr Opin Cell Biol* **15**, 747-52.

Gibson, M. C. and Perrimon, N. (2005). Extrusion and death of DPP/BMP-compromised epithelial cells in the developing Drosophila wing. *Science* **307**, 1785-9.

Gotz, M. and Huttner, W. B. (2005). The cell biology of neurogenesis. *Nat Rev Mol Cell Biol* **6**, 777-88.

Guerrier, S. and Polleux, F. (2007). The ups and downs of neural progenitors: Cep120 and TACCs control interkinetic nuclear migration. *Neuron* **56**, 1-3.

Haigo, S. L., Hildebrand, J. D., Harland, R. M. and Wallingford, J. B. (2003). Shroom induces apical constriction and is required for hingepoint formation during neural tube closure. *Curr Biol* **13**, 2125-37.

Hamilton, H. a. (1951). A series of normal stages in the development of the chick embryo. *J. Morph.* **88:49**

Hata, A., Lagna, G., Massague, J. and Hemmati-Brivanlou, A. (1998). Smad6 inhibits BMP/Smad1 signaling by specifically competing with the Smad4 tumor

suppressor. *Genes Dev* **12**, 186-97.

Hayashi, T. and Carthew, R. W. (2004). Surface mechanics mediate pattern formation in the developing retina. *Nature* **431**, 647-52.

Heinecke, K., Seher, A., Schmitz, W., Mueller, T. D., Sebald, W. and Nickel, J. (2009). Receptor oligomerization and beyond: a case study in bone morphogenetic proteins. *BMC Biol* **7**, 59.

Hong, E. and Brewster, R. (2006). N-cadherin is required for the polarized cell behaviors that drive neurulation in the zebrafish. *Development* **133**, 3895-905.

Hurd, T. W. and Margolis, B. (2005). Pars and polarity: taking control of Rac. *Nat Cell Biol* **7**, 205-7.

Iemura, S., Yamamoto, T. S., Takagi, C., Uchiyama, H., Natsume, T., Shimasaki, S., Sugino, H. and Ueno, N. (1998). Direct binding of follistatin to a complex of bone-morphogenetic protein and its receptor inhibits ventral and epidermal cell fates in early Xenopus embryo. *Proc Natl Acad Sci U S A* **95**, 9337-42.

Imamura, T., Takase, M., Nishihara, A., Oeda, E., Hanai, J., Kawabata, M. and Miyazono, K. (1997). Smad6 inhibits signalling by the TGF-beta superfamily. *Nature* **389**, 622-6.

Jacobson, A. G., Oster, G. F., Odell, G. M. and Cheng, L. Y. (1986). Neurulation and the cortical tractor model for epithelial folding. *J Embryol Exp Morphol* **96**, 19-49.

Jamora, C., DasGupta, R., Kocieniewski, P. and Fuchs, E. (2003). Links

between signal transduction, transcription and adhesion in epithelial bud development. *Nature* **422**, 317-22.

Johnson, A. D. and Krieg, P. A. (1994). pXeX, a vector for efficient expression of cloned sequences in Xenopus embryos. *Gene* **147**, 223-6.

Keller, R. (2002). Shaping the vertebrate body plan by polarized embryonic cell movements. *Science* **298**, 1950-4.

Klezovitch, O., Fernandez, T. E., Tapscott, S. J. and Vasioukhin, V. (2004). Loss of cell polarity causes severe brain dysplasia in Lgl1 knockout mice. *Genes Dev* **18**, 559-71.

Knust, E. (2002). Regulation of epithelial cell shape and polarity by cell-cell adhesion (Review). *Mol Membr Biol* **19**, 113-20.

Knust, E. and Bossinger, O. (2002). Composition and formation of intercellular junctions in epithelial cells. *Science* **298**, 1955-9.

Krispin, S., Nitzan, E., Kassem, Y. and Kalcheim, C. (2010). Evidence for a dynamic spatiotemporal fate map and early fate restrictions of premigratory avian neural crest. *Development* **137**, 585-95.

Langman, J., Guerrant, R. L. and Freeman, B. G. (1966). Behavior of neuro-epithelial cells during closure of the neural tube. *J Comp Neurol* **127**, 399-411.

Lee, C., Scherr, H. M. and Wallingford, J. B. (2007). Shroom family proteins regulate gamma-tubulin distribution and microtubule architecture during epithelial cell shape change. *Development* **134**, 1431-41.

Lee, J. Y. and Harland, R. M. (2007). Actomyosin contractility and microtubules

drive apical constriction in Xenopus bottle cells. *Dev Biol* **311**, 40-52.

Lee, J. Y. and Harland, R. M. (2010). Endocytosis is required for efficient apical constriction during Xenopus gastrulation. *Curr Biol* **20**, 253-8.

Lee, K. J., Dietrich, P. and Jessell, T. M. (2000). Genetic ablation reveals that the roof plate is essential for dorsal interneuron specification. *Nature* **403**, 734-40.

Liem, K. F., Jr., Tremml, G. and Jessell, T. M. (1997). A role for the roof plate and its resident TGFbeta-related proteins in neuronal patterning in the dorsal spinal cord. *Cell* **91**, 127-38.

Liu, A. and Niswander, L. A. (2005). Bone morphogenetic protein signalling and vertebrate nervous system development. *Nat Rev Neurosci* **6**, 945-54.

Lowery, L. A. and Sive, H. (2004). Strategies of vertebrate neurulation and a re-evaluation of teleost neural tube formation. *Mech Dev* **121**, 1189-97.

Margolis, B. and Borg, J. P. (2005). Apicobasal polarity complexes. *J Cell Sci* **118**, 5157-9.

Martini, F. J. and Valdeolmillos, M. (2010). Actomyosin contraction at the cell rear drives nuclear translocation in migrating cortical interneurons. *J Neurosci* **30**, 8660-70.

Massague, J. (2008). TGFbeta in Cancer. *Cell* **134**, 215-30.

McMahon, J. A., Takada, S., Zimmerman, L. B., Fan, C. M., Harland, R. M. and McMahon, A. P. (1998). Noggin-mediated antagonism of BMP signaling is required for growth and patterning of the neural tube and somite. *Genes Dev* **12**,

1438-52.

Messier, P. E. (1978). Microtubules, interkinetic nuclear migration and neurulation. *Experientia* **34**, 289-96.

Miki, H., Okada, Y. and Hirokawa, N. (2005). Analysis of the kinesin superfamily: insights into structure and function. *Trends Cell Biol* **15**, 467-76.

Morris, N. R. (2003). Nuclear positioning: the means is at the ends. *Curr Opin Cell Biol* **15**, 54-9.

Mostov, K., Su, T. and ter Beest, M. (2003). Polarized epithelial membrane traffic: conservation and plasticity. *Nat Cell Biol* **5**, 287-93.

Murciano, A., Zamora, J., Lopez-Sanchez, J. and Frade, J. M. (2002). Interkinetic nuclear movement may provide spatial clues to the regulation of neurogenesis. *Mol Cell Neurosci* **21**, 285-300.

Nagele, R. G., Bush, K. T., Kosciuk, M. C., Hunter, E. T., Steinberg, A. B. and Lee, H. Y. (1989). Intrinsic and extrinsic factors collaborate to generate driving forces for neural tube formation in the chick: a study using morphometry and computerized three-dimensional reconstruction. *Brain Res Dev Brain Res* **50**, 101-11.

Nakamura, T., Takio, K., Eto, Y., Shibai, H., Titani, K. and Sugino, H. (1990). Activin-binding protein from rat ovary is follistatin. *Science* **247**, 836-8.

Nelson, W. J. (2003). Adaptation of core mechanisms to generate cell polarity. *Nature* **422**, 766-74.

Nelson, W. J. and Nusse, R. (2004). Convergence of Wnt, beta-catenin, and

cadherin pathways. *Science* **303**, 1483-7.

Nishimura, T. and Takeichi, M. (2008). Shroom3-mediated recruitment of Rho kinases to the apical cell junctions regulates epithelial and neuroepithelial planar remodeling. *Development* **135**, 1493-502.

Ogata, S., Morokuma, J., Hayata, T., Kolle, G., Niehrs, C., Ueno, N. and Cho, K. W. (2007). TGF-beta signaling-mediated morphogenesis: modulation of cell adhesion via cadherin endocytosis. *Genes Dev* **21**, 1817-31.

Ozdamar, B., Bose, R., Barrios-Rodiles, M., Wang, H. R., Zhang, Y. and Wrana, J. L. (2005). Regulation of the polarity protein Par6 by TGFbeta receptors controls epithelial cell plasticity. *Science* **307**, 1603-9.

Raible, D. W. (2006). Development of the neural crest: achieving specificity in regulatory pathways. *Curr Opin Cell Biol* **18**, 698-703.

Remy, I., Montmarquette, A. and Michnick, S. W. (2004). PKB/Akt modulates TGF-beta signalling through a direct interaction with Smad3. *Nat Cell Biol* **6**, 358-65.

Sai, X. and Ladher, R. K. (2008). FGF signaling regulates cytoskeletal remodeling during epithelial morphogenesis. *Curr Biol* **18**, 976-81.

Sauer, L. (1935). Mitosis in the neural tube. *J. Comp. Neurol.* **62**, 377-97.

Sawyer, J. M., Harrell, J. R., Shemer, G., Sullivan-Brown, J., Roh-Johnson, M. and Goldstein, B. (2009). Apical constriction: a cell shape change that can drive morphogenesis. *Dev Biol* **341**, 5-19.

Schenk, J., Wilsch-Brauninger, M., Calegari, F. and Huttner, W. B. (2009).

Myosin II is required for interkinetic nuclear migration of neural progenitors. *Proc Natl Acad Sci U S A* **106**, 16487-92.

Schoenwolf, G. C. (1985). Shaping and bending of the avian neuroepithelium: morphometric analyses. *Dev Biol* **109**, 127-39.

Schoenwolf, G. C. and Smith, J. L. (2000a). Gastrulation and early mesodermal patterning in vertebrates. *Methods Mol Biol* **135**, 113-25.

Schoenwolf, G. C. and Smith, J. L. (2000b). Mechanisms of neurulation. *Methods Mol Biol* **136**, 125-34.

Shen, J. and Dahmann, C. (2005). Extrusion of cells with inappropriate Dpp signaling from Drosophila wing disc epithelia. *Science* **307**, 1789-90.

Shoval, I., Ludwig, A. and Kalcheim, C. (2007). Antagonistic roles of full-length N-cadherin and its soluble BMP cleavage product in neural crest delamination. *Development* **134**, 491-501.

Smith, J. L. and Schoenwolf, G. C. (1987). Cell cycle and neuroepithelial cell shape during bending of the chick neural plate. *Anat Rec* **218**, 196-206.

Smith, J. L. and Schoenwolf, G. C. (1997). Neurulation: coming to closure. *Trends Neurosci* **20**, 510-7.

Steinberg, M. S. (2007). Differential adhesion in morphogenesis: a modern view. *Curr Opin Genet Dev* **17**, 281-6.

Stottmann, R. W., Berrong, M., Matta, K., Choi, M. and Klingensmith, J. (2006). The BMP antagonist Noggin promotes cranial and spinal neurulation by distinct mechanisms. *Dev Biol* **295**, 647-63.

Suzuki, T., Elias, B. C., Seth, A., Shen, L., Turner, J. R., Giorgianni, F., Desiderio, D., Guntaka, R. and Rao, R. (2009). PKC eta regulates occludin phosphorylation and epithelial tight junction integrity. *Proc Natl Acad Sci U S A* **106**, 61-6.

Swartz, M., Eberhart, J., Mastick, G. S. and Krull, C. E. (2001). Sparking new frontiers: using in vivo electroporation for genetic manipulations. *Dev Biol* **233**, 13-21.

Tabler, J. M., Yamanaka, H. and Green, J. B. (2010). PAR-1 promotes primary neurogenesis and asymmetric cell divisions via control of spindle orientation. *Development* **137**, 2501-5.

Timmer, J., Chesnutt, C. and Niswander, L. (2005). The activin signaling pathway promotes differentiation of dI3 interneurons in the spinal neural tube. *Dev Biol* **285**, 1-10.

Timmer, J. R., Wang, C. and Niswander, L. (2002). BMP signaling patterns the dorsal and intermediate neural tube via regulation of homeobox and helix-loop-helix transcription factors. *Development* **129**, 2459-72.

Townes, P. L. and Holtfreter, J. (1955). Directed movements and selective adhesion of embryonic amphibian cells. *J. Exp. Zool* **128**, 53-120.

Tsukita, S., Furuse, M. and Itoh, M. (2001). Multifunctional strands in tight junctions. *Nat Rev Mol Cell Biol* **2**, 285-93.

Ueno, M., Nonaka, S., Yamazaki, R., Deguchi, N. and Murai, M. (2002). SN-38 induces cell cycle arrest and apoptosis in human testicular cancer. *Eur Urol*

42, 390-7.

Vachon-Presseau, E. and Henry, L. (2008). The influences of associative cortices on cross-modal integration in the superior colliculus. *J Neurosci* **28**, 1787-8.

van Straaten, H. W., Sieben, I. and Hekking, J. W. (2002). Multistep role for actin in initial closure of the mesencephalic neural groove in the chick embryo. *Dev Dyn* **224**, 103-8.

von der Hardt, S., Bakkers, J., Inbal, A., Carvalho, L., Solnica-Krezel, L., Heisenberg, C. P. and Hammerschmidt, M. (2007). The Bmp gradient of the zebrafish gastrula guides migrating lateral cells by regulating cell-cell adhesion. *Curr Biol* **17**, 475-87.

Wallingford, J. B. (2005). Vertebrate gastrulation: polarity genes control the matrix. *Curr Biol* **15**, R414-6.

Wallingford, J. B. (2010). Planar cell polarity signaling, cilia and polarized ciliary beating. *Curr Opin Cell Biol* **22**, 597-604.

Wallingford, J. B. and Harland, R. M. (2002). Neural tube closure requires Dishevelled-dependent convergent extension of the midline. *Development* **129**, 5815-25.

Warner, D. R., Pisano, M. M., Roberts, E. A. and Greene, R. M. (2003). Identification of three novel Smad binding proteins involved in cell polarity. *FEBS Lett* **539**, 167-73.

Wilcock, A. C., Swedlow, J. R. and Storey, K. G. (2007). Mitotic spindle

orientation distinguishes stem cell and terminal modes of neuron production in the early spinal cord. *Development* **134**, 1943-54.

Wilhelmsen, K., Ketema, M., Truong, H. and Sonnenberg, A. (2006). KASH-domain proteins in nuclear migration, anchorage and other processes. *J Cell Sci* **119**, 5021-9.

Wine-Lee, L., Ahn, K. J., Richardson, R. D., Mishina, Y., Lyons, K. M. and Crenshaw, E. B., 3rd. (2004). Signaling through BMP type 1 receptors is required for development of interneuron cell types in the dorsal spinal cord. *Development* **131**, 5393-403.

Yamanaka, T., Horikoshi, Y., Izumi, N., Suzuki, A., Mizuno, K. and Ohno, S. (2006). Lgl mediates apical domain disassembly by suppressing the PAR-3-aPKC-PAR-6 complex to orient apical membrane polarity. *J Cell Sci* **119**, 2107-18.

Yang, X., Zou, J., Hyde, D. R., Davidson, L. A. and Wei, X. (2009). Stepwise maturation of apicobasal polarity of the neuroepithelium is essential for vertebrate neurulation. *J Neurosci* **29**, 11426-40.

Ybot-Gonzalez, P., Cogram, P., Gerrelli, D. and Copp, A. J. (2002). Sonic hedgehog and the molecular regulation of mouse neural tube closure. *Development* **129**, 2507-17.

Ybot-Gonzalez, P., Gaston-Massuet, C., Girdler, G., Klingensmith, J., Arkell, R., Greene, N. D. and Copp, A. J. (2007). Neural plate morphogenesis during mouse neurulation is regulated by antagonism of Bmp signalling. *Development*

134, 3203-11.

Zallen, J. A. and Wieschaus, E. (2004). Patterned gene expression directs bipolar planar polarity in Drosophila. *Dev Cell* **6**, 343-55.